Geoscientific Paper GP2023-1

Metamorphic map of the Flin Flon domain, west-central Manitoba
(parts of NTS 63J, K, N, O)

Manitoba

Metamorphic map of the Flin Flon domain, west-central Manitoba (parts of NTS 63J, K, N, O)

by M. Lazzarotto, D.R.M. Pattison, S. Gagné and C.G. Couëslan
Manitoba Geological Survey
Winnipeg, 2023

External author contact information:

Manuele Lazzarotto	David R.M. Pattison	Simon Gagné
Luganiga Exploration Ltd.	Department of Geoscience, University of Calgary	Kinross Gold Corporation
Email: rattorosa@gmail.com	Email: pattison@ucalgary.ca	Email: simon.gagne@kinross.com

Front cover photo:

Massive basalt flows comprise the shoreline of Inlet arm (Schist Lake, Manitoba).

Abstract

A new comprehensive map of metamorphic mineral assemblages, mineral isograds and metamorphic zones of the Paleoproterozoic Flin Flon domain of Manitoba and Saskatchewan has been compiled. The exposed Flin Flon domain is bounded to the north by the metasedimentary gneisses of the Kisseynew domain and to the south by the unconformably overlying Phanerozoic units of the Western Canada Sedimentary Basin. The Flin Flon domain consists of an amalgamation of ocean-floor, island-arc, and derived sedimentary assemblages that were intruded by plutons. These units were deformed and metamorphosed during the Trans-Hudson orogeny (~1.86–1.69 Ga). Two phases of metamorphism are recorded and include early contact metamorphism related to the intrusion of plutons, followed by regional metamorphism. Contact metamorphic aureoles are observed extending up to two kilometres around most intrusions. A series of regional isograds and metamorphic zones have been identified for mafic metavolcanic and metasedimentary rocks. The isograds define a northward increase in metamorphic grade from the Phanerozoic cover in the south to the Kisseynew domain in the north. With increasing grade, the mineral isograds for metavolcanic rocks consist of actinolite-in, prehnite and pumpellyite-out, biotite-in, hornblende-in, oligoclase-in, actinolite-out, chlorite-out, garnet-in and epidote-out. The mineral isograds for metasedimentary rocks with increasing grade consist of garnet-in, staurolite-in, andalusite-in, sillimanite-in, staurolite-out and migmatite-in, with all these isograds occurring up-grade of the garnet-in isograd in the metabasites (i.e., within the epidote-amphibolite facies and amphibolite facies). The Flin Flon domain has been subdivided into five areas, each characterized by a different sequence of isograds. The Flin Flon area mainly contains metavolcanic rocks that increase in metamorphic grade from prehnite–pumpellyite facies to amphibolite facies. In this area, the garnet-in isograd occurs up-grade of the epidote-out isograd. The Cranberry–Iskwasum–Elbow lakes area is a large region of greenschist facies rocks in the centre of the Flin Flon domain. The File Lake–Reed Lake area contains a sequence of tectonically interleaved metavolcanic and metasedimentary rocks whose metamorphic grade increases from upper-greenschist to upper-amphibolite facies. In metavolcanic rocks, the epidote-out isograd occurs up-grade of the garnet-in isograd and down-grade of the sillimanite-in isograd for metasedimentary rocks. The Snow Lake area contains a similar sequence of isograds to the File Lake–Reed Lake area; however, the sillimanite-in isograd for metasedimentary rocks occurs down-grade of the epidote-out isograd in metavolcanic rocks. The Niblock Lake–Saw Lake area is underlain by metasedimentary rocks that define isograds for andalusite-in, sillimanite-in, staurolite-out and migmatite-in. An isograd delimiting the amphibolite facies is mapped in the sub-Phanerozoic Flin Flon domain. Under the Phanerozoic sedimentary rocks in the western part of the belt, grade increases to amphibolite facies to the south, whereas in the eastern part of the map area it increases towards the southeast. Pressure and temperature conditions of the observed mineral assemblages are estimated using thermodynamic phase-equilibria modelling. Peak metamorphic conditions of 450 °C and 3.3–4.4 kbar were calculated for the greenschist to amphibolite facies transition. Greenschist facies rocks of the Cranberry–Iskwasum–Elbow lakes area reached maximum temperatures of 470 °C. Rocks of the File Lake–Reed Lake area underwent metamorphism at conditions of 400 °C and 3 kbar below the hornblende-in isograd at the northern shore of Reed Lake, 530 °C and 4.5 kbar at the metasedimentary garnet-in isograd at the northern end of Morton Lake, and 650 °C and 5.5 kbar at the migmatite-in isograd in the northern File Lake area. Mineral assemblages and isograds in the Snow Lake area indicate conditions of 450 °C and 3.5–4 kbar at the actinolite-out isograd west of Wekusko Lake and 550–600 °C and 4.5–5.5 kbar at the sillimanite-in isograd around the town of Snow Lake. Andalusite-in followed by sillimanite-in in the Niblock Lake–Saw Lake area occurred at 550–600 °C and 3–3.5 kbar, whereas partial melting started at 650 °C and >4.5 kbar. Systematic differences in the mineralogy of metamorphosed alteration zones associated with volcanogenic massive-sulphide deposits in the Flin Flon belt is a function of regional metamorphic grade. Recognizing these unique mineral assemblages can be used as a vector for finding mineral deposits.

Résumé

Une nouvelle carte détaillée a été compilée pour illustrer les associations minéralogiques métamorphiques, les isogrades de minéraux et les zones métamorphiques du domaine paléoprotérozoïque de Flin Flon au Manitoba et en Saskatchewan. Le domaine exposé de Flin Flon est délimité au nord par les gneiss métasédimentaires du domaine de Kisseynew et au sud par les unités phanérozoïques sus-jacentes en discordance du bassin sédimentaire de l'Ouest canadien. Le domaine de Flin Flon est constitué d'un amalgame d'associations de plancher océanique, d'arcs insulaires et de dépôts sédimentaires dérivés qui ont subi l'intrusion de plutons. Ces unités ont été déformées et métamorphisées pendant l'orogène trans-hudsonien (~1,86–1,69 Ga). Deux phases de métamorphisme sont enregistrées et comprennent un métamorphisme de contact précoce lié à l'intrusion de plutons, suivi d'un métamorphisme régional. On observe des auréoles de métamorphisme de contact s'étendant jusqu'à deux kilomètres autour de la plupart des masses intrusives. Une série d'isogrades régionaux et de zones métamorphiques a été identifiée pour les roches métasédimentaires et métavolcaniques mafiques. Les isogrades définissent une augmentation vers le nord de l'intensité du métamorphisme depuis la couverture phanérozoïque au sud jusqu'au domaine de Kisseynew au nord. Parallèlement à l'accroissement de l'intensité, les isogrades de minéraux pour les roches métavolcaniques suivent la progression suivante : apparition de l'actinolite, disparition de la prehnite et de pumpellyite, apparition de la biotite, apparition de la hornblende, apparition de l'oligoclase, disparition de l'actinolite, disparition de la chlorite, apparition du grenat et disparition de l'épidote. De même, les isogrades de minéraux pour les roches métasédimentaires évoluent comme suit avec l'accroissement de l'intensité : apparition du grenat, apparition de la staurolite, apparition de l'andalousite, apparition de la sillimanite, disparition de la staurolite et apparition de la migmatite, tous ces isogrades ayant une intensité supérieure à celle de l'isograde d'apparition du grenat dans les métabasites (c.-à-d. dans le faciès des amphibolites à épidote et le faciès de type amphibolite). Le domaine de Flin Flon a été sous-divisé en cinq zones, chacune se caractérisant par une série d'isogrades différents. La zone de Flin Flon renferme principalement des roches métavolcaniques dont l'intensité du métamorphisme augmente du faciès à prehnite–pumpellyite au faciès de type amphibolite. Dans cette zone, l'isograde d'apparition du grenat est présent à une intensité supérieure à celle de l'isograde de disparition de l'épidote. La zone des lacs Cranberry, Iskwasum et Elbow est une vaste région de roches du faciès de schistes verts située au centre du domaine de Flin Flon. La zone des lacs File et Reed renferme une série de roches métasédimentaires et métavolcaniques techtoniquement intercalaires dont l'intensité

du métamorphisme s'accroît du faciès de schistes verts supérieur au faciès de type amphibolite supérieur. Dans les roches métavolcaniques, l'isograde de disparition de l'épidote se produit à une intensité supérieure à celle de l'isograde d'apparition du grenat et à une intensité inférieure à celle de l'isograde d'apparition de la sillimanite pour les roches métasédimentaires. La zone de Snow Lake renferme une série d'isogrades similaire à celle de la zone des lacs File et Reed; toutefois, l'isograde d'apparition de la sillimanite pour les roches métasédimentaires est présent à une intensité inférieure de l'isograde de disparition de l'épidote dans les roches métavolcaniques. La zone des lacs Niblock et Saw repose sur des roches métasédimentaires caractérisées par les isogrades suivants : apparition de l'andalousite, apparition de la sillimanite, disparition de la staurolite et apparition de la migmatite. Un isograde délimitant le faciès de type amphibolite est cartographié dans le domaine subphanérozoïque de Flin Flon. Sous les roches sédimentaires phanérozoïques situées dans la partie occidentale de la ceinture, l'intensité augmente pour passer au faciès de type amphibolite vers le sud, tandis que l'intensité augmente vers le sud-est dans la partie orientale de la région cartographiée. Les conditions de pression et de température des associations minéralogiques observées sont estimées au moyen de la modélisation des équilibres de phase thermodynamiques. Les conditions de 450 °C et de 3,3 à 4,4 kbar au pic du métamorphisme ont été calculées pour la transition du faciès de schistes verts au faciès de type amphibolite. Les roches du faciès de schistes verts dans la zone des lacs Cranberry, Iskwasum et Elbow ont atteint des températures maximales de 470 °C. Les roches de la zone des lacs File et Reed ont subi un métamorphisme dans des conditions de 400 °C et 3 kbar sous l'isograde d'apparition de la hornblende sur la rive nord du lac Reed, de 530 °C et 4,5 kbar à l'isograde d'apparition du grenat métasédimentaire situé à l'extrémité nord du lac Morton, et de 650 °C et 5,5 kbar à l'isograde d'apparition de la migmatite dans la partie nord de la zone du lac File. Les associations minéralogiques et les isogrades de la zone du lac Snow révèlent des conditions de 450 °C et de 3,5 à 4 kbar dans l'isograde de disparition de l'actinolite à l'ouest du lac Wekusko, ainsi que de 550 à 600 °C et de 4,5 à 5,5 kbar à l'isograde d'apparition de la sillimanite aux alentours de la ville de Snow Lake. L'isograde d'apparition de l'andalousite suivi de l'isograde d'apparition de la sillimanite dans la zone des lacs Niblock et Saw se sont produits à des conditions de 550 à 600 °C et de 3 à 3,5 kbar, alors que la fonte partielle a commencé à 650 °C et >4,5 kbar. Les différences systématiques dans la minéralogie des zones d'altération métamorphisées associées aux gisements de sulfures massifs volcanogènes dans la ceinture de Flin Flon sont liées à l'intensité du métamorphisme de chaque zone. L'observation de ces associations minéralogiques uniques peut servir de vecteur pour repérer des dépôts de minéraux.

TABLE OF CONTENTS

TABLES

FIGURES

MAP

APPENDICES

Introduction

The Flin Flon domain (FD) has been investigated and mapped at various scales by geologists over the past 100 years. Even though these mapping efforts increased the understanding of the geology and related economic potential of the FD, no comprehensive metamorphic map was ever compiled. This publication presents a new map and accompanying report of metamorphic mineral assemblages, isograds and zones compiled from samples and data collected by the authors and by Bailes and McRitchie (1978), Froese and Moore (1980), Bailes (1985), Bailes and Syme (1989), Briggs (1990), Zaleski et al. (1991), Kraus and Menard (1997), Norquay (1997), Ryan (1998), Zwanzig and Bailes (2010), Gilbert (2012), Syme and Whalen (2012), Couëslan and Martins (2014), Syme (2015), Starr (2017), Starr and Pattison (2019a, b), and Starr et al. (2020).

This report focuses on newly defined metamorphic zones, isograds and mineral assemblages, an assessment of the implied pressure-temperature conditions, and the relationship of metamorphism to the structural history, economic geology and overall tectonic evolution of the FD. Descriptions are organized by bulk composition and are presented in order of increasing metamorphic grade. Samples were collected by the first author as part of his Ph.D. thesis on the metamorphism of the FD (Lazzarotto et al., 2020), and where possible, rock samples and/or thin sections

from previous studies were re-examined (see references above). This combined approach allowed for a more uniform interpretation of the isograds and metamorphic zones within the FD. All rocks in the study attained at least prehnite–pumpelleyite facies metamorphic conditions; however, the 'meta-' prefix has been omitted to improve the legibility of the report.

Geology of the Flin Flon domain

The FD is situated in west-central Manitoba and east-central Saskatchewan, extending for 240 km from east to west, and is exposed for about 40 km south to north. It comprises polydeformed volcanic and intrusive rocks interleaved with sedimentary rocks. The exposed FD is bounded to the north by the sedimentary gneisses of the Kisseynew domain (KD) and to the south by the unconformably overlying Phanerozoic units of the Western Canada Sedimentary Basin (Figure 1). Under the Phanerozoic sedimentary rocks, units of the FD have been documented in drillcore up to 40 km south of the exposed margin.

The FD is part of the juvenile "Reindeer zone" of the Trans-Hudson orogen, a domain formed from the convergence between the Hearne, Superior and Sask cratons (Hoffmann, 1988). Circa 1.92–1.88 Ga juvenile-arc and ocean-floor rocks were juxtaposed in an accretionary collage as a consequence of arc-arc collision at about 1.88–1.87 Ga (Lucas et al., 1996). The
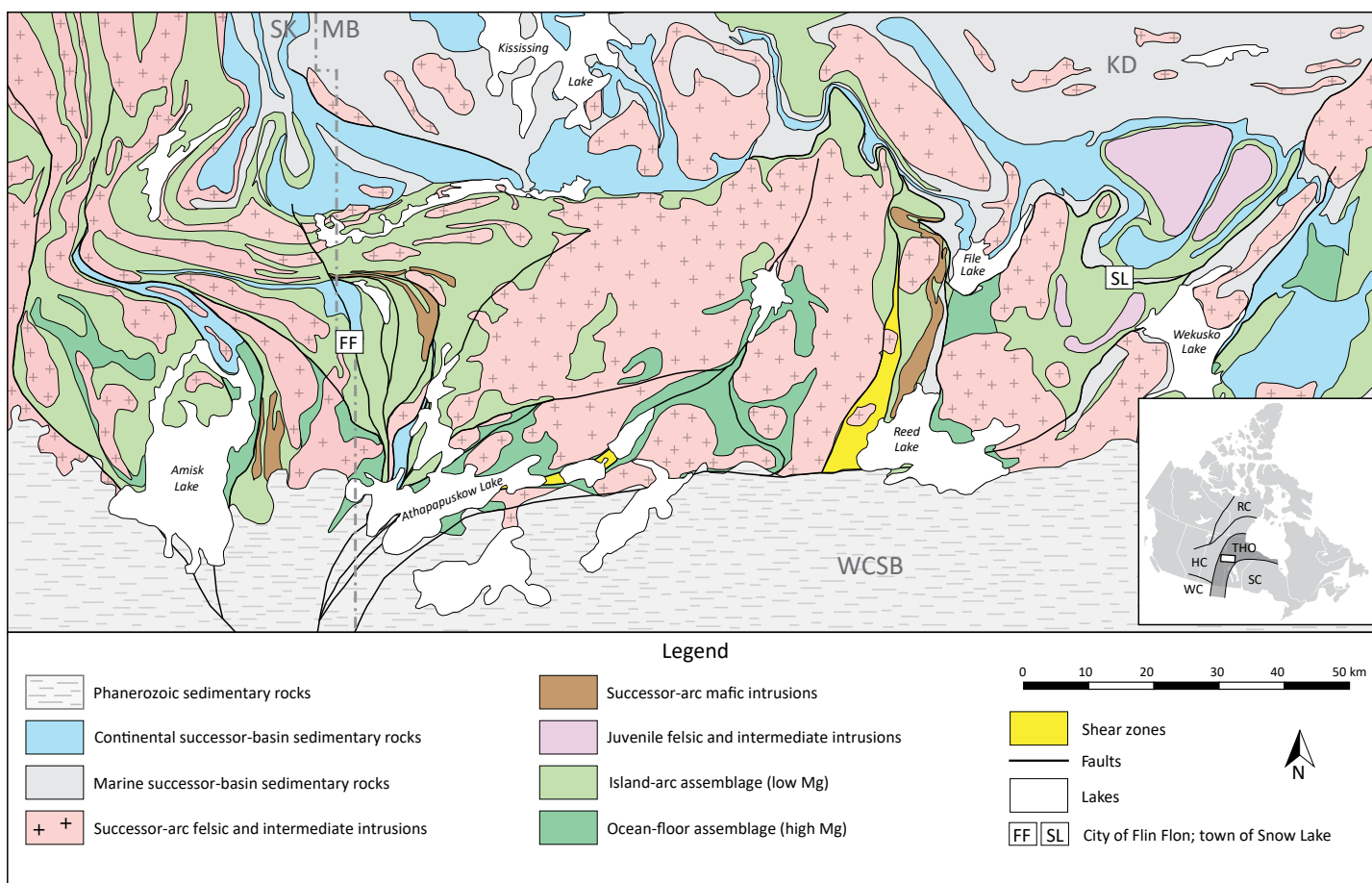

Figure 1: *Simplified geology of the Flin Flon domain (modified from NATMAP Shield Margin Project Working Group, 1998). Abbreviations: HC, Hearne craton; KD, Kisseynew domain; MB, Manitoba; RC, Rae craton; SC, Superior craton; SK, Saskatchewan; THO, Trans-Hudson orogen; WC, Wyoming craton; WCSB, Western Canada Sedimentary Basin.*

arc-related assemblages comprise a wide range of volcanic, volcaniclastic and related synvolcanic intrusive rocks, whereas the ocean-floor assemblages are mainly composed of mid-ocean–ridge-like basalt and related mafic–ultramafic complexes (Syme and Bailes, 1993; Stern et al., 1995a, b; Lucas et al., 1996). Post-accretion and successor-arc magmatism resulted in the emplacement of calcalkaline plutons ca. 1.87–1.83 Ga (Lucas et al., 1996). Sedimentary rocks consisting of thick sequences of fluvial-alluvial conglomerate and sandstone of the Missi group, and marine turbidite deposits of the Burntwood group were deposited between 1.85 and 1.83 Ga (Ansdell et al., 1995; Lucas et al., 1996; Stern et al., 1999, Syme et al., 1999). The volcanic and sedimentary rocks were imbricated and deformed along early structures (Lucas et al., 1996; Stern et al., 1999). The newly accreted terranes collided with the Sask craton at 1.84–1.83 Ga and with the Superior craton at 1.83–1.80 Ga (Bleeker, 1990; Ellis et al., 1999; Ashton et al., 2005).

The NATMAP Shield Margin Project (NATMAP Shield Margin Project Working Group, 1998) and the LITHOPROBE Trans-Hudson Orogen Transect (Lewry et al., 1994; White et al., 1994; Clowes et al., 1999) showed that the FD is part of a northeast-dipping stack of three crustal units: 1) at the lowest level are ortho- and para-gneisses of the Sask craton (3.20–2.40 Ga); 2) at the intermediate level are variably metamorphosed volcanic and plutonic units of the FD (1.99–1.85 Ga); and 3) at the highest level are Burntwood group sedimentary rocks and igneous plutons of the Kisseynew domain (1.85–1.80 Ga).

Four main episodes of deformation and associated metamorphism have been recognized in the FD (e.g., Gordon et al., 1990; Ansdell et al., 1995; Fedorowich et al., 1995; Lucas et al., 1996; David et al., 1996; Schneider et al., 2007; LaFrance et al., 2016): 1) intra-oceanic accretion of arc-, ocean-floor-, and older crustal assemblages at 1.88–1.87 Ga and associated metamorphism; 2) post-accretion magmatism, and related contact metamorphism, sedimentation and deformation at 1.87–1.84 Ga; 3) collisional shortening causing peak metamorphism at 1.84–1.80 Ga; and 4) post-collisional thrusting, folding, and strike-slip faults at 1.80–1.69 Ga.

The FD is one of the largest Paleoproterozoic volcanogenic massive-sulphide (VMS) districts in the world, with 29 past and active mines producing close to 320 million tonnes of Cu-Zn-Au ore (Pehrsson et al., 2016). All mined VMS deposits in the FD are associated with juvenile arc-affinity volcanic rocks (Syme and Bailes, 1993).

Volcanic rocks (1.92–1.87 Ga)

Apart from some younger volcanics outcropping on the east side of Wekusko Lake and throughout the Kississing–File Lake areas (Ansdell et al., 1999; Zwanzig and Bailes, 2010), volcanic rocks in the FD range in age between 1.92–1.87 Ga and can be subdivided into a series of island-arc and ocean-floor assemblages (Lucas et al., 1996; Syme et al., 1999). The units are characterized by variations in their lithological and geochemical associations.

Juvenile-arc assemblage

The FD contains seven spatially separate juvenile-arc assemblages. From west to east these are the Hanson Lake, West Amisk, Birch Lake, Flin Flon, North Star, Fourmile Island and Snow Lake assemblages (Syme et al., 1998). These are separated by major faults or intervening ocean-floor units, sedimentary rock units or plutons. In the western part of the FD, the arc assemblages are internally complex, comprising numerous fault-bounded and folded blocks of volcanic rocks (Bailes and Syme, 1989).

The juvenile-arc assemblages include a large variety of extrusive and volcaniclastic rocks. These assemblages are bimodal, mainly metamorphosed basalt/basaltic andesite and rhyolite/dacite (Syme et al., 1999). Geochemically these include tholeiitic, calcalkaline, shoshonitic and boninitic rocks. Less common are volcaniclastic sedimentary rocks. Synvolcanic intrusions vary from granitoid plutons to hypabyssal dykes and sills. The majority of the arc rocks contain primary structures, such as pillows and amygdules, that suggest that they were deposited in a subaqueous environment (Figure 2a, b). There is also evidence of rocks that were erupted in a shallow marine or subaerial setting (e.g., presence of pumice).

Ocean-floor assemblage

The FD contains four distinct ocean-floor units. From west to east these are the West Arm block, the Elbow–Athapapuskow assemblage, the Northeast Reed assemblage, and the Roberts Lake block. The ocean-floor assemblages are composed mainly of mid-ocean–ridge-like basalt, layered mafic–ultramafic intrusive complexes, and minor ocean-island and ocean-plateau basalt (Syme and Bailes, 1993; Stern et al., 1995a). Basalt and mafic–ultramafic complexes are usually separated by younger intrusions.

The ocean-floor assemblages comprise thick units of pillowed and massive basalt. Rare fragmental units include mafic volcaniclastic rocks, basaltic flow top breccias and reworked hyaloclastite. Abundant mafic synvolcanic dykes and sills intrude the units. Some basalt units containing epidosite domains suggest seafloor hydrothermal activity (Figure 2c) consistent with eruption in a mid-ocean ridge setting (Stern et al., 1995a; Ames et al., 2002). Mafic–ultramafic complexes commonly consist of gabbro interlayered with pyroxenite and lesser peridotite and anorthosite. Ocean-island and ocean-plateau basalt units are characterized by strongly vesiculated basalt and massive flows.

Pillowed flows form the best-preserved igneous structures at outcrop scale. Typically, pillow cores are light in colour, rich in epidote and contain few small amygdules; rims are dark coloured and contain more chlorite, actinolite and hornblende, and occasionally abundant and/or large amygdules. At grades below amphibolite facies, pseudomorphs after plagioclase and/or pyroxene are often aligned, preserving trachytic textures typical
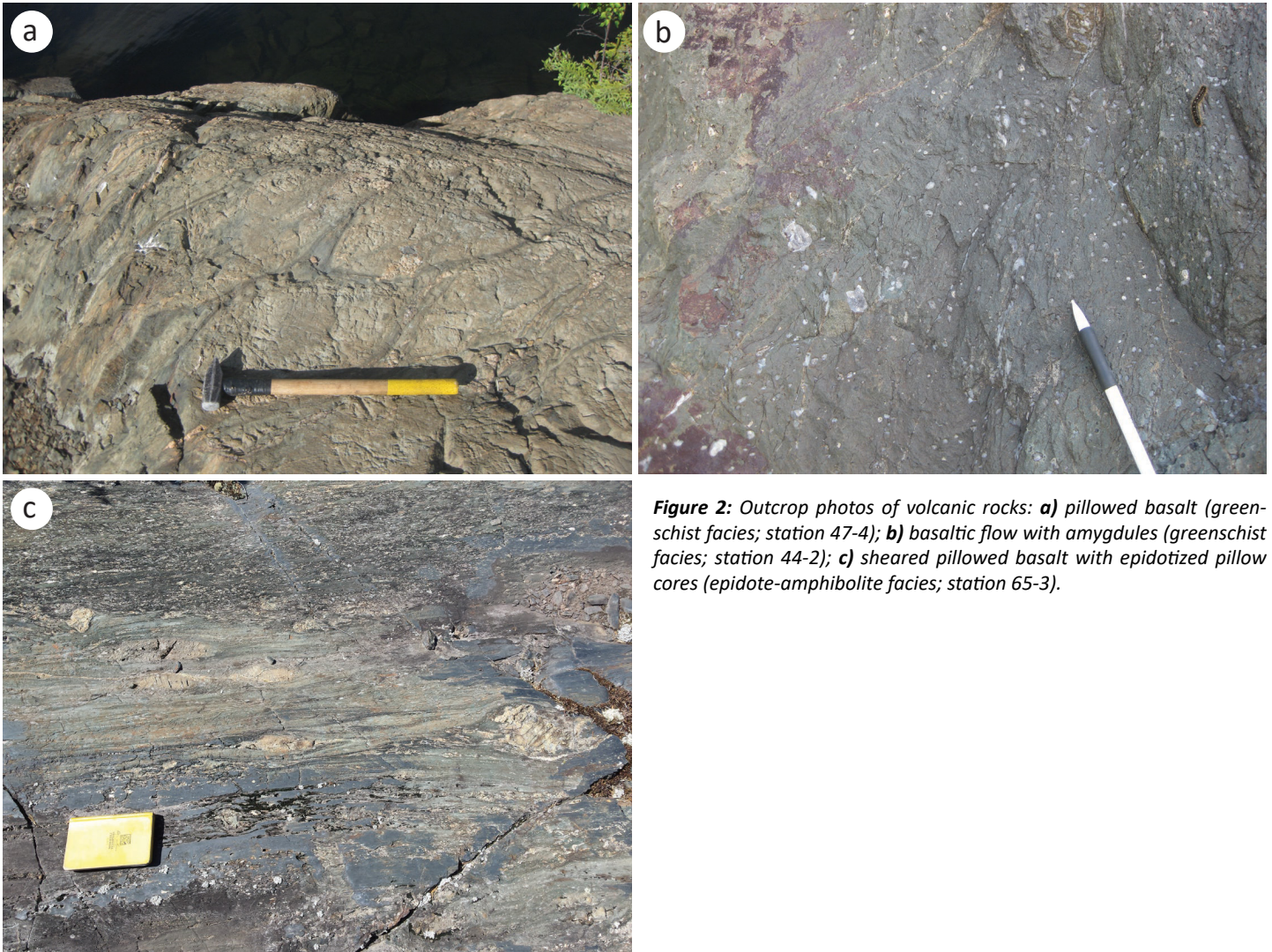
Figure 2: *Outcrop photos of volcanic rocks:* ***a)*** *pillowed basalt (greenschist facies; station 47-4);* ***b)*** *basaltic flow with amygdules (greenschist facies; station 44-2);* ***c)*** *sheared pillowed basalt with epidotized pillow cores (epidote-amphibolite facies; station 65-3).*

of magmatic flows. Igneous structures are deformed and metamorphic minerals such as amphibole, biotite or chlorite define a foliation in areas of high strain.

Sedimentary rocks (1.87–1.83 Ga)

Sedimentary rocks mostly occur in the central and eastern part of the FD and vary in age from 1.87 to 1.83 Ga (Syme et al., 1998). Units can be subdivided into continental and marine sedimentary rocks, characterized by different lithological and geochemical compositions.

Missi group

Deposition of Missi group rocks is diachronous across the FD. Deposition has been dated at 1.847–1.842 Ga in the central FD (Ansdell et al., 1992; Heaman et al., 1992; Ansdell, 1993), and at 1.832–1.826 Ga in the eastern FD (Connors and Ansdell, 1994; Ansdell et al., 1999). Rocks were sourced from the accreted complex (1.92–1.85 Ga) as well as from older crustal sources (Sask craton, 2.60–2.20 Ga; Ansdell et al., 1992; Ansdell, 1993). The Missi group rocks unconformably overlie volcanic and plutonic units of the juvenile and early successor arcs (Stauffer, 1990; Syme et al., 1998). They are characterized by thick packages of

conglomerate, pebbly sandstone and sandstone in the FD (Figure 3a, b), and are metamorphosed to quartzofeldspathic gneisses in the KD. According to Zwanzig and Bailes (2010), sandstone mainly consists of quartz with minor plagioclase (10–20%), and biotite (<12%). Missi group rocks contain abundant clasts of volcanic and sedimentary rocks derived from arc- and ocean-floor–assemblages, and successor-arc plutonic rocks. These include basalt, andesite, dacite, rhyolite, granitoid and derived orthogneisses.

The Missi group is interpreted as fluvial-alluvial rocks deposited along an uplifted and deeply incised terrain (Stauffer and Mukherjee, 1971; Bailes and Syme, 1989). Sedimentary layering and grading is preserved in most Missi group strata from the prehnite–pumpellyite to amphibolite facies. Crossbedding is observed in fine and pebbly sandstones and their recrystallized counterparts (Figure 3b). Metamorphic recrystallization of fine-grained quartz arenite to quartzite is common.

Burntwood group

According to stratigraphic relationships and geochronological data, Burntwood group assemblages were deposited at 1855–1840 Ma, 5–10 Ma prior to the deposition of the Missi group (Bailes, 1980; Zwanzig, 1990; David et al., 1996). In the
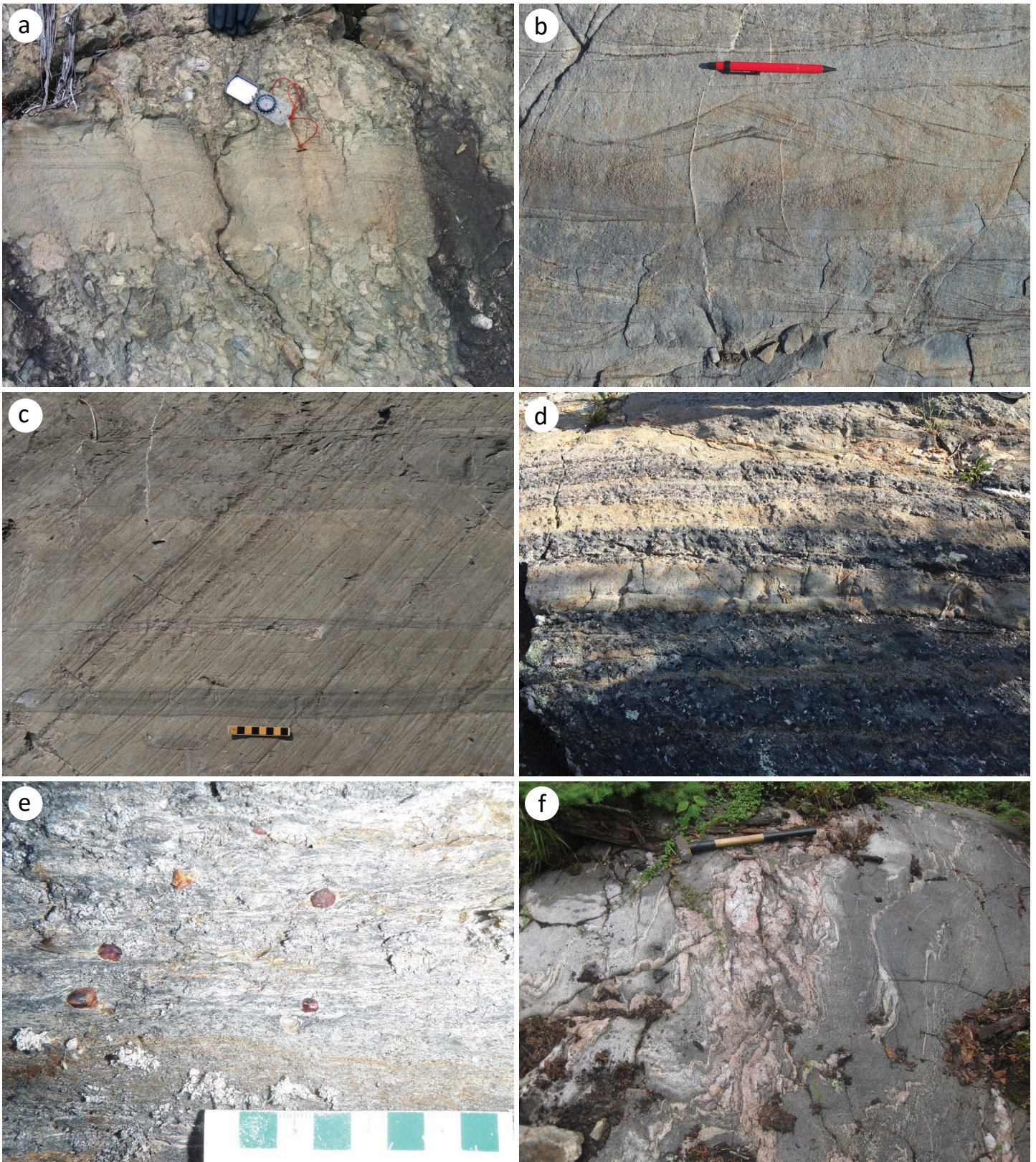
Figure 3: Outcrop photos of sedimentary rocks: *a)* interlayered conglomerate and sandstone from the Missi group (north of Flin Flon); *b)* crossbedding in Missi group sandstone (north of Snow Lake); *c)* layered siltstone and sandstone from the Burntwood group (Taylor Bay road, west shore of Wekusko Lake); *d)* Burntwood group metaturbidite with staurolite-rich layers; *e)* garnet-sillimanite schist derived from Burntwood group metaturbidite (station 2102); *f)* pods of leucosome in Burntwood group migmatite (station 60-8).

FD, the Burntwood group assemblages comprise greywacke, silt-stone, mudstone and rare conglomerate, and are commonly in fault contact with Missi group rocks (Zwanzig, 2000; Zwanzig and Bailes, 2010). A number of authors suggested that Burntwood group and Missi group sedimentary rocks were locally deposited contemporaneously (Bailes, 1980; Zwanzig and Bailes, 2010). Psammitic to pelitic gneisses and related migmatitic gneisses derived from Burntwood group rocks are the major components of the KD (Bailes and McRitchie, 1978). Abundant immature volcanic-derived detritus in the turbidites has been reported (Bailes, 1980). The rocks are interpreted as turbidity current deposits that were deposited in prograding submarine fans fed by river systems draining the adjacent successor-arc terrane.

Primary sedimentary structures are abundant and well pre-served in weakly recrystallized greywacke, siltstone and mud-stone strata of greenschist facies and lower amphibolite facies (Figure 3c). Features such as Bouma sequence zonation typical of turbidity currents (Bailes, 1980), scour marks, intraformational clasts, and soft sediment deformation are commonly observed. Within the Bouma sequence, grain gradation, parallel lamination and current ripple laminations are typical. At higher metamor-phic grade, bedding is the main sedimentary structure that is pre-served. The distribution of metamorphic-mineral assemblages is controlled by the bulk composition of the protolith. In beds of metamorphosed mudstone, porphyroblasts of garnet, silliman-ite and staurolite are common (Figure 3d, e). Metamorphosed graded sandstone/siltstone/mudstone beds contain more abun-dant porphyroblasts in the originally muddier tops of the beds (mainly garnet, staurolite, andalusite and sillimanite in the form of fibrolite knots), leading to "inverse metamorphic grading".

Intrusive rocks (1.88–1.83 Ga)

Intrusive magmatism in the FD can be broadly subdivided in three stages (Whalen et al., 1999): 1) evolved-arc (1.92 Ga) and early juvenile-arc (1.90–1.88 Ga) plutonism during intraoceanic arc-back-arc formation; 2) early (1.88–1.86 Ga) and middle (1.86–1.84 Ga) successor-arc plutonism following accretion; and 3) late (1.84–1.83 Ga) successor-arc plutonism accompanying successor basin formation and waning arc mag-matism.

Plutonic rocks in the FD are compositionally variable, vary-ing from gabbro and diorite to tonalite and granodiorite. Tex-turally they range from fine to coarse grained and equigranular to porphyritic. Homogeneous, quartz-phyric tonalite is the pre-dominant felsic rock type in early juvenile-arc and early suc-cessor-arc plutons. Zoned diorite-granodiorite intrusions with varying grain size are typical for middle successor-arc plutons. Granites, and other K-feldspar bearing granitoid intrusions, are rare and most common in late successor-arc plutons. Xenoliths of mafic intrusive and volcanic units are common in plutons of all ages. Most intrusive rocks pre-date the regional metamor-phic peak.

Structural geology

Deposition and accretion of juvenile volcanic-arc and ocean-floor rocks took place roughly between 1.92 and 1.85 Ga (Syme et al., 1998). Pre-metamorphic tilting and folding of these rocks, identified as the D_0 phase of deformation, occurred some time prior to 1.85 Ga (Gordon et al., 1990). Missi group rocks were deposited unconformably on juvenile volcanic-arc and ocean-floor rocks at ca. 1.85–1.83 Ga (Bailes et al., 1987; Gordon, 1989; Gordon et al., 1990). Two main syn-metamorphic deformation phases (D_1 and D_2) affected volcanic and sedimentary rocks throughout the region. D_1 produced a bedding-parallel foliation, isoclinal recumbent folds, and possibly some thrust nappes [D_1 in Thomas (1992); Gale et al. (1999); Ryan and Williams (1999); Zwanzig (2000); D_4 in LaFrance et al. (2016)]. It is thought to have resulted from north-south convergence of the Hearne and Supe-rior cratons beginning ca. 1.83 Ga (Gordon, 1989; Gordon et al., 1990). D_1 folds were refolded during D_2 producing upright, open to tight folds plunging gently to the northeast and generating an axial cleavage [D_2 in Thomas (1992); Kraus and Williams (1998); Gale et al. (1999); Zwanzig (2000); D_5 in Lafrance et al. (2016)]. East- to east-northeast–trending flexural folds produced by D_3 deformation have been observed in some areas [D_3 in Bailes (1980, 1985); Thomas (1992); D_4 in Gale et al. (1999)]. Post-met-amorphic brittle deformation during D_4 resulted in fractures and faults, some of which offset regional metamorphic isograds [D_4 in Bailes (1985); D_7 in LaFrance et al. (2016)].

Bulk compositions

Bulk compositional data were collected by the author for eight volcanic and five sedimentary rocks of prehnite–pumpel-lyite to amphibolite facies in the Flin Flon–Athapapuskow Lake area and in the File Lake area. In addition, major- and trace-ele-ment bulk compositions for >400 samples from all over the FD were obtained from the bulk rock chemistry datasets of Bailes (1980; 34 samples), Zwanzig and Bailes (2010; 95 samples), Gil-bert (2012; 149 samples), Syme and Whalen (2012; 28 samples), Syme (2015; 69 samples) and Starr (2017; 62 samples). For a full list of utilized bulk compositions refer to Appendix 1.

Ferric iron estimation

Mafic minerals such as amphibole, pyroxene, epidote, bio-tite and magnetite can contain a significant amount of ferric iron, therefore it is important to consider the effects of ferric iron on the composition of these minerals, particularly during phase equilibria modelling. To estimate the amount of ferric iron in the volcanic and sedimentary rocks, a combination of differ-ent methods was used: 1) determination of FeO and Fe_2O_3 using wet titration of selected samples; and for basites 2) documenta-tion of Fe^{3+}-bearing phases and their ferric iron content (epidote, amphibole, magnetite); and 3) T–XFe^{3+} (XFe^{3+} = Fe^{3+} / [Fe^{3+} + Fe^{2+}] in terms of mol. %) and pressure–temperature-equilibrium (P–T) modelling for different ferric iron contents and pressures (see thermodynamic modelling below and Starr et al., 2020).

Complete major element analyses (including chemical wet titration of FeO and Fe_2O_3) were performed on 13 newly collected rock samples from the FD. The XFe_2O_3 ($XFe_2O_3 = Fe_2O_3$ / [Fe_2O_3 + FeO] in terms of wt. % oxide) values measured for volcanic rocks vary between 0.22 and 0.31, with an average of 0.26; whereas for five sedimentary rock samples XFe_2O_3 values range from 0.04 to 0.10. In molar elements XFe^{3+} this corresponds to 0.20 to 0.29 for volcanic rocks and 0.04 to 0.09 for sedimentary rocks. The degree to which these values represent the actual ferric iron ratios during metamorphism is affected by the amount of oxidation during weathering and post-metamorphic alteration, as well as the potential for oxidation during sample preparation. These results are thus interpreted as maximum values.

Several minerals that contain ferric iron have been documented. Minor magnetite (<1 vol. %) was observed in several samples. Down-grade of the epidote-out isograd, epidote was recorded in most analysed samples, with modes up to 10%. Mineral formulae recalculation suggests that all the iron in epidote is Fe^{3+} (0.7–1.0 cations per formula unit). Amphiboles are present in most mafic rock samples throughout the study area. They account for up to 50% of the mode in amphibolite facies rocks. Determining the ferric iron content of metamorphic amphiboles is difficult due to the inability of the electron probe microanalyser (EPMA) to differentiate between valence states of elements, and the fact that a variable number of cations is involved in the recalculation of the mineral formulae. To assess the ferric iron content of amphiboles, the minimum, maximum and average recalculation factors approach delineated in Holland and Blundy (1994) and Schumacher (1997) was used. Amphibole XFe^{3+} varies between 0.03 and 0.27, with an average of 0.18. Still, this approach comes with some level of uncertainty. Combining the above mineral compositions allows for the calculation of bulk rock ferric iron contents. The calculations depend on the modes and ferric iron compositions of the ferric-iron–bearing minerals. Whole-rock compositions in wt. % were calculated by multiplying the modes of each mineral by its measured mineral composition obtained from EPMA analyses [see Starr and Pattison (2019b) and Starr et al. (2020) for detailed description of method and calculations]. The calculated whole-rock XFe_2O_3 ranges between 0.04 and 0.38, with an average of 0.17 (XFe^{3+} = 0.04 to 0.36, with an average of 0.16). For this study, bulk compositional ferric iron XFe_2O_3 is estimated at 0.16 (or XFe^{3+} of 0.15), a value that provides the best match to the observed phase relations (see below) and which is similar to the average 0.17 (or XFe^{3+} of 0.16) estimate discussed above.

Volcanic rocks

Mafic volcanic rock samples usually contain multiple compositional domains. These include the matrix, amygdules, phenocrysts, and core-rim-selvage structures in pillows. All bulk compositions used in this report were obtained from analyses that avoided or mechanically removed amygdules and vein material before processing. The investigated bulk compositional data for basaltic rocks are plotted on an ACF diagram projected from apatite and quartz, in which A = Al_2O_3 + Fe_2O_3, C = CaO − 3.33 x P_2O_5 and F = FeO + MgO (Figure 4a).

Mafic volcanic rocks are divided into two compositional groups: high-Mg and low-Mg. In the FD, high-Mg compositions are typical of ocean-floor rocks, whereas low-Mg compositions are characteristic of arc-related rocks. High-Mg basalt samples plot closer to the FeO + MgO apex in the AFC diagram (Figure 4a), reflecting their higher MgO (6–10 wt. %) and FeO (11–15 wt. %) compared to the low-Mg basalt samples (2–5 wt. % MgO, 6–12 wt. % FeO). High-Mg basalts are also higher in CaO (8–13 wt. %) and TiO_2 (1.0–1.2 wt. %), and lower in SiO_2 (46–50 wt. %) compared to low-Mg basalt (4–10 wt. % CaO, <0.8 wt. % TiO_2, 48–60 wt. % SiO_2). Observations in rocks of the FD suggest that higher CaO content correlates with slightly higher epidote (and amphibole) content in the rocks. Alumina is similar in both bulk compositions (12–18 wt. %). Low-Mg basalts plot slightly closer to the alumina apex compared to high-Mg basalts in the projected ACF diagram (Figure 4a). This is in agreement with the slightly lower modal amount of plagioclase present in the high-Mg rocks. In general, low-Mg compositions show a greater spread across the ACF diagram compared to high-Mg bulk compositions. The red stars in Figure 4a are the average bulk compositions used to calculated diagrams in the 'Phase equilibria modelling' section (raw data shown in Figure 4).

Sedimentary rocks

Bulk compositional data for sedimentary rocks are plotted on an alkalis-iron-magnesium (AFM) diagram projected from muscovite, plagioclase and quartz for muscovite-bearing samples ("normal"-K) in which A = [Al_2O_3 − (3K_2O + CaO + Na_2O)], F = FeO and M = MgO (Figure 4b); and on an AFM diagram projected from An_{30} plagioclase for muscovite-free samples ("low"-K; Figure 4c). A discussion of this projection is given by Froese (1969). The composition of plagioclase varies between samples (An_{10}–An_{45}), with a composition of An_{30} being average for these rocks. All Na_2O is assumed to reside in plagioclase, but CaO can occur in minerals other than plagioclase such as amphibole. Under this assumption, the Al_2O_3 removed from the bulk composition due to plagioclase of composition An_{30} equals 1 x Na_2O (for the albite component) and 0.3 x Na_2O / 0.7 (for the anorthite content), using the amount of Na_2O as a measure of how much plagioclase is present in the rock. This results in the following values for the apices of Figure 4c: A = Al_2O_3 − Na_2O − 0.3 x Na_2O / 0.7; F = FeO; and M = MgO. In both cases, ferric iron has been omitted from the projection for sedimentary rocks due to the rarity of magnetite, suggesting low Fe^{3+}.

In general, mudstone typical of the Burntwood group have slightly lower SiO_2 (57–65 wt. %) and are enriched in Al_2O_3 (17–21 wt. %), K_2O (2.5–4.0 wt. %) and TiO_2 (0.5–0.7 wt. %) compared to greywacke typical of the Missi group (60–80 wt. % SiO_2, 15–17 wt. % Al_2O_3, <2.5 wt. % K_2O, and <0.5 wt. % TiO_2). In the AFM diagram in Figure 4b, normal-K Burntwood group rocks show an increased Al content compared to Missi group rocks. This difference is mainly caused by the lower modal percentage of plagio-
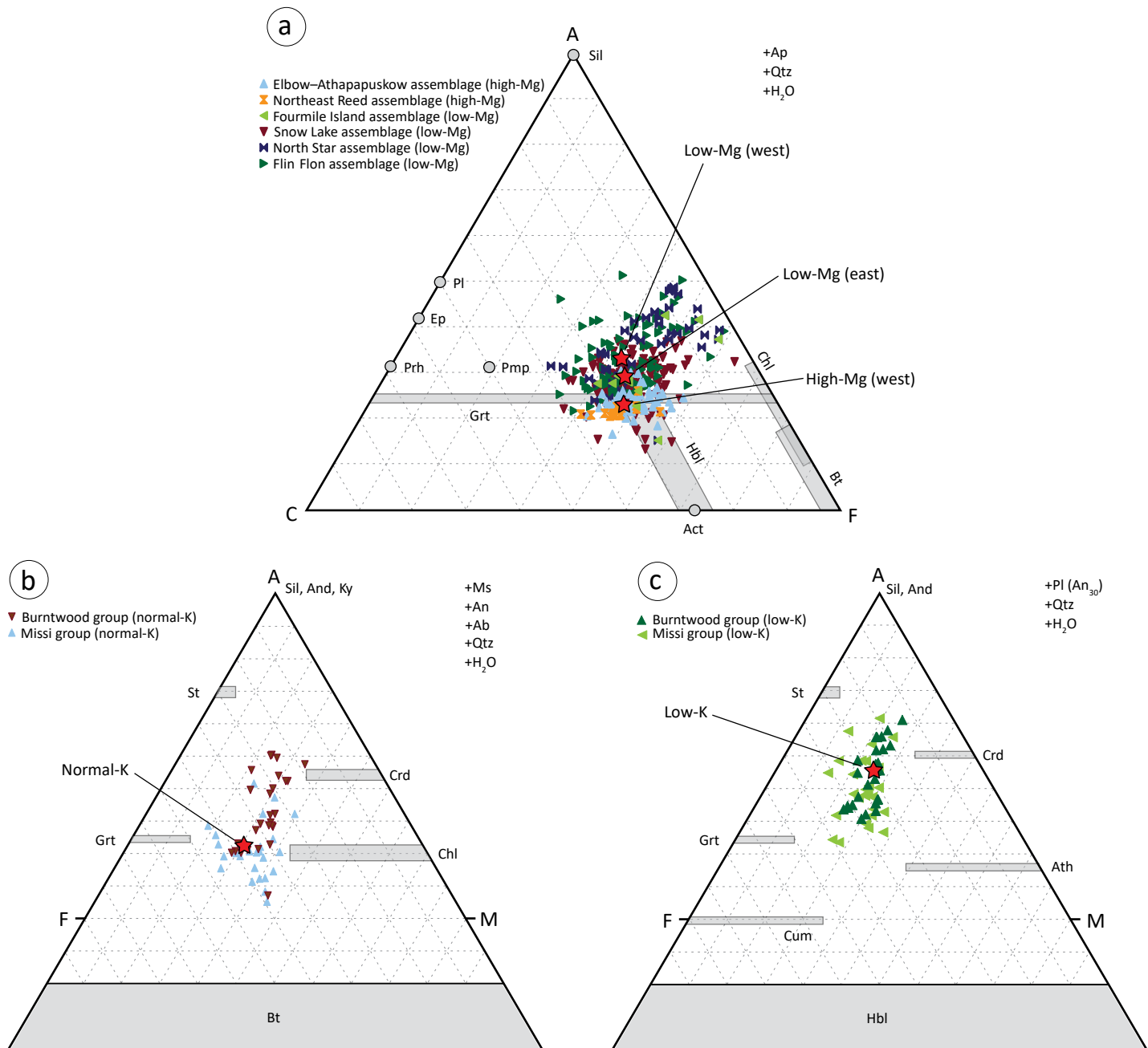
Figure 4: *Bulk compositions for rocks from the Flin Flon domain:* ***a)*** *ACF diagram with rock compositions for the high-Mg (west) and low-Mg (east and west) basaltic and andesitic rocks;* ***b)*** *AFM diagram for normal-K mudstone (east) projected from muscovite, plagioclase and quartz;* ***c)*** *AFM diagram for low-K mudstone (east) projected from plagioclase (An₃₀) and quartz. The red stars indicate average compositions used to calculate phase equilibria diagrams, see text for details. Abbreviations: Ab, albite; Act, actinolite; An, anorthite; And, andalusite; Ap, apatite; Ath, anthophyllite; Bt, biotite; Chl, chlorite; Crd, cordierite; Cum, cummingtonite; Ep, epidote; Grt, garnet; Hbl, hornblende; Ky, kyanite; Ms, muscovite; Pl, plagioclase; Pmp, pumpellyite; Prh, prehnite; Qtz, quartz; Sil, sillimanite; St, staurolite.*

clase in the Burntwood group rocks (up to 15%) compared to the Missi group rocks (up to 20%). This trend is not observed in low-K rocks. Bulk compositional MgO and FeO are lower in greywacke (0.5–4.8 wt. % MgO; 3.7–7.3 wt. % FeO) compared to mudstone (2.5–4.0 wt. % MgO; 4.1–9.5 wt. % FeO). Ferric iron has an average of 1.1 wt. % Fe_2O_3 for greywacke and 1.5 wt. % Fe_2O_3 for mudstone. Average XFe_2O_3 values are 0.18 for greywacke (XFe^{3+} = 0.17) and 0.17 for mudstone (XFe^{3+} = 0.16). Iron and magnesium ratios, calculated as X_{Mg} = Mg / (Mg + Fe^{2+}), are similar for both normal-K and low-K rocks of the Burntwood and Missi groups,

with X_{Mg} of 0.33–0.52 for Missi group greywacke (average 0.42), and 0.41–0.65 for Burntwood group mudstone (average 0.47). The red stars in Figure 4b, c are the average bulk compositions used to calculated diagrams in the 'Phase equilibria modelling' section and only consider measured iron as Fe^{2+} (Table 1; raw data in Figure 4).

The Burntwood group mudstone has relatively low potassium compared to an average metapelite, which typically contains 3.6–4.2 wt. % K_2O (Ague, 1991; Pattison and Spear, 2018). As a consequence, the most abundant metamorphic K-bearing

Table 1: Bulk compositions used to calculate phase-equilibria diagrams of Figures 9 and 10.

	High-Mg metabasalt (west)	Low-Mg metabasalt (west)	Low-Mg metabasalt (east)	Low-K metasediment (east)	Normal-K metasediment (east)
wt. % oxides					
SiO_2	48.92	53.84	56.03	58.97	59.40
Al_2O_3	14.09	14.94	15.42	17.44	20.70
TiO_2	1.19	0.62	0.84	1.12	0.55
FeO (total)	13.59	11.46	11.54	9.61	7.22
MnO	0.20	0.00	0.19	0.06	0.05
MgO	7.15	4.98	3.26	3.54	2.64
CaO	8.72	7.80	8.65	2.07	1.42
Na_2O	2.51	2.69	2.56	2.17	1.78
K_2O	0.21	0.70	0.58	2.44	3.78
P_2O_5	0.14	0.13	0.17	0.16	0.14
Total (anhydrous)	96.72	97.16	99.24	97.58	97.68
XFe_2O_3	0.16	0.16	0.16	0.16	0.16
Mole elements % (after projection described in text)					
Si	52.66	58.38	60.24	65.73	67.54
Al	17.89	19.10	19.55	22.92	27.75
Ti	0.97	0.50	0.68	0.94	0.47
Fe^{3+}	1.84	1.56	1.56	1.34	1.03
Fe^{2+}	10.40	8.84	8.82	7.61	5.84
Mn	0.18	0.17	0.17	0.06	0.05
Mg	11.47	8.05	5.22	5.88	4.47
Ca	9.85	8.87	9.69	2.22	1.51
Na	5.25	5.66	5.33	4.69	3.92
K	0.29	0.97	0.80	3.47	5.48
XFe^{3+}	0.15	0.15	0.15	0.15	0.15

mineral in the greenschist and amphibolite facies is biotite. Both muscovite-bearing (normal-K) and muscovite-free (low-K) assemblages have been reported in this study and several previous studies (e.g., Froese and Gasparrini, 1975; Bailes and McRitchie, 1978; Briggs, 1990; Briggs and Foster, 1992; Kraus and Menard, 1997; Menard and Gordon, 1997). Muscovite-free assemblages are more abundant in the File Lake–Reed Lake and Snow Lake areas, whereas muscovite-bearing assemblages occur mainly in the Niblock Lake area. Metamorphic K-feldspar has been reported in migmatites found at the transition into the Kisseynew domain (e.g., Bailes and McRitchie, 1978; Zwanzig and Bailes, 2010).

Metamorphism

With the exception of post-collisional igneous rocks, all rocks in the FD experienced regional metamorphism that post-dated earlier intrusions and associated contact metamorphism. Regional and contact metamorphism are described separately below. In this report, the focus is on regional metamorphism of volcanic and sedimentary rock units, whose mineral assemblages are most sensitive to variations in metamorphic grade. This includes basaltic and andesitic rocks of the juvenile-arc and ocean-floor assemblages, and metamorphosed mudstone of the Burntwood group.

In this report, metamorphic mineral isograds are defined by the first appearance of a mineral (mineral-in isograd) or the last occurrence of a mineral (mineral-out isograd), without taking into consideration features such as inclusions (pre-metamorphic assemblage) or fracture fills (late/retrograde assemblage). Mineral-out isograds are less likely to represent equilibrium conditions than mineral-in isograds because some minerals, such as actinolite and staurolite, may persist as metastable relicts (e.g., Starr and Pattison, 2019a). Because of the difficulty in assessing when minerals start to become unstable, we have based the mineral-out isograds on the observational criterion of physical absence of the mineral in question, recognizing that the mineral-out isograds might occur at higher grade than expected assuming equilibrium. This is discussed further in the 'Phase equilibria modelling' section.

Previous metamorphic studies in the Flin Flon belt

A number of studies have focused on metamorphism in the Flin Flon domain (e.g., Froese and Gasparrini, 1975; Bailes

and McRitchie, 1978; Froese and Moore, 1980; Gordon, 1989; Gordon et al., 1991, 1994; Zaleski et al., 1991; Briggs and Foster, 1992; Digel and Gordon, 1993, 1995; Digel and Ghent, 1994; Fedorowich et al., 1995; Norman et al., 1995; Kraus and Menard, 1997; Menard and Gordon, 1997; Ryan, 1998; Jungwirth et al., 2000; Starr and Pattison, 2019a, b; Lazzarotto et al., 2020; Starr et al., 2020). These studies show that metamorphic grade in the exposed part of the FD generally increases from south to north (Figure 5).

Digel and Gordon (1993, 1995), and Digel and Ghent (1994) mapped a series of mineral zones in basaltic rocks of the Flin Flon area ranging from prehnite–pumpellyite zone in the south to hornblende–oligoclase–albite zone in the north (Figure 5). They show isograds for prehnite + pumpellite-out + actinolite-in, hornblende-in, actinolite-out, and epidote + chlorite-out. Starr and Pattison (2019a, b) and Starr at al. (2020) expanded on these studies and showed that the sequence includes an oligoclase-in isograd and a separate isograd for actinolite-in (Figure 5). Digel and Gordon (1993) calculated a temperature and pressure of approximately 290 °C and 2.9 kbar for lower-greenschist facies rocks near Flin Flon, and 550 °C and 5.5 kbar for rocks at the greenschist to amphibolite facies transition north of Flin Flon, resulting in a metamorphic field gradient of 100 °C/kbar. Starr et al. (2020) calculated similar conditions at prehnite–pumpellyite facies (250–300 °C and 2.3–3.2 kbar) and somewhat lower temperatures at the greenschist to amphibolite facies transition (450 °C and 3.3–4.4 kbar).

At the transition into the KD north of Flin Flon, Jungwirth et al. (2000) mapped isograds for sillimanite-in and migmatite-in in metapelites of the Burntwood group, and calculated metamorphic conditions of 530 °C and 3.6 kbar for sillimanite–garnet–biotite assemblages between the sillimanite-in and migmatite-in isograds. Zwanzig and Bailes (2010) noted that the migmatite front at the transition into the KD north of Flin Flon is characterized by the absence of muscovite and a significant decrease in the abundance of sillimanite.

Evidence for at least two regional metamorphic episodes has been given by Norman et al. (1995) and Ansdell et al. (1995) in the Cleunion Lake area, in the KD northeast of Flin Flon. They concluded that the first episode was a high-temperature (>760 °C) moderate pressure (4.5 kbar) event, which resulted in local partial melting. This event was attributed to underplating of thin crust and an elevated asthenosphere in an intra-arc setting. During the second metamorphic episode, the foliated sillimanite produced during the previous event was folded, and new metamorphic minerals including muscovite, biotite and sillimanite defined a new foliation. According to Norman et al. (1995) this event reached peak conditions of 580–650 °C and 5 kbar. Norman et al. (1995) argued that in the KD, southwesterly directed thrusting became transcurrent and sinistral at the transition into the FD. The authors argued that both the thrusting and the transcurrent movement along the boundary zone are compatible with a general southwesterly transport of the KD over the FD.

Ryan (1998) examined the metamorphism of volcanic rocks in the Cranberry–Iskwasum–Elbow lakes area in the centre of the FD (Figure 5). He interpreted that the rocks to the west of the Elbow–Iskwasum lakes shear zone belong to the greenschist facies, whereas rocks to the east belong to the amphibolite facies. Greenschist facies assemblages are recorded over 30 km from the southern end of Iskwasum Lake to the northern end of Elbow Lake.

Bailes and McRitchie (1978) mapped isograds for staurolite-in, sillimanite-in, staurolite-out and migmatite-in (and cordierite-in at higher grade within the KD) for the sedimentary sequence at File Lake. They noted both muscovite-bearing and muscovite-free assemblages (Figure 5). They also provided evidence of metasomatic cation exchange processes accompanying the transition from the staurolite zone to the sillimanite zone as a prograde metamorphic reaction mechanism. According to these authors, metamorphic peak conditions ranged from 450–500 °C and 3.5–5 kbar at File Lake, to >750 °C and 5.5–7.0 kbar in the centre of the KD. Gordon et al. (1991) estimated metamorphic conditions for the sillimanite-in isograd in the File Lake area to be 540 °C and 3.3 kbar.

Briggs (1990) and Briggs and Foster (1992) studied metapelites in the File Lake and Niblock Lake areas, the latter in the eastern FD (Figure 5). They recognized two metamorphic events by examining relative timing of growth of metamorphic minerals complemented by geothermobarometry. The first episode involved the growth of micas (biotite and muscovite) and did not exceed 475 °C and 3.5 kbar in both areas. The second episode is characterized by the growth of staurolite at about 560 °C and 3.3 kbar and sillimanite at 625 °C and 4.6 kbar at File Lake, and andalusite between 525–625 °C and 2.5–5.0 kbar at Niblock Lake.

Isograds for staurolite-in, sillimanite-in, and staurolite-out were mapped for a series of sedimentary rocks in the Snow Lake area by Froese and Gasparrini (1975). These authors suggested that isograds developed at 525–625 °C and 5–6 kbar. Froese and Moore (1980) recognised two major periods of deformation accompanying regional metamorphism in the Snow Lake area. They mapped the same isograds as Froese and Gasparrini (1975) and showed that the narrow garnet zone, the relatively broad staurolite zone, and the absence of a kyanite zone, are indicative of low–medium pressure conditions (<6 kbar). Furthermore, Froese and Moore (1980) investigated metamorphism of volcanogenic massive-sulphide deposits hosted in volcanic units that show strong pre-metamorphic hydrothermal alteration. They concluded that similar conditions prevailed, even though minerals such as kyanite and anthophyllite were observed in the altered rocks.

Zaleski et al. (1991) estimated metamorphic conditions of the hydrothermally altered rocks of the Linda deposit in Snow Lake to have reached maximum temperatures and pressures of 550 °C and 5 kbar. The temperature was inferred based on the coexistence of Zn-bearing staurolite and quartz, and margarite and quartz, whereas the pressure was obtained from sphalerite
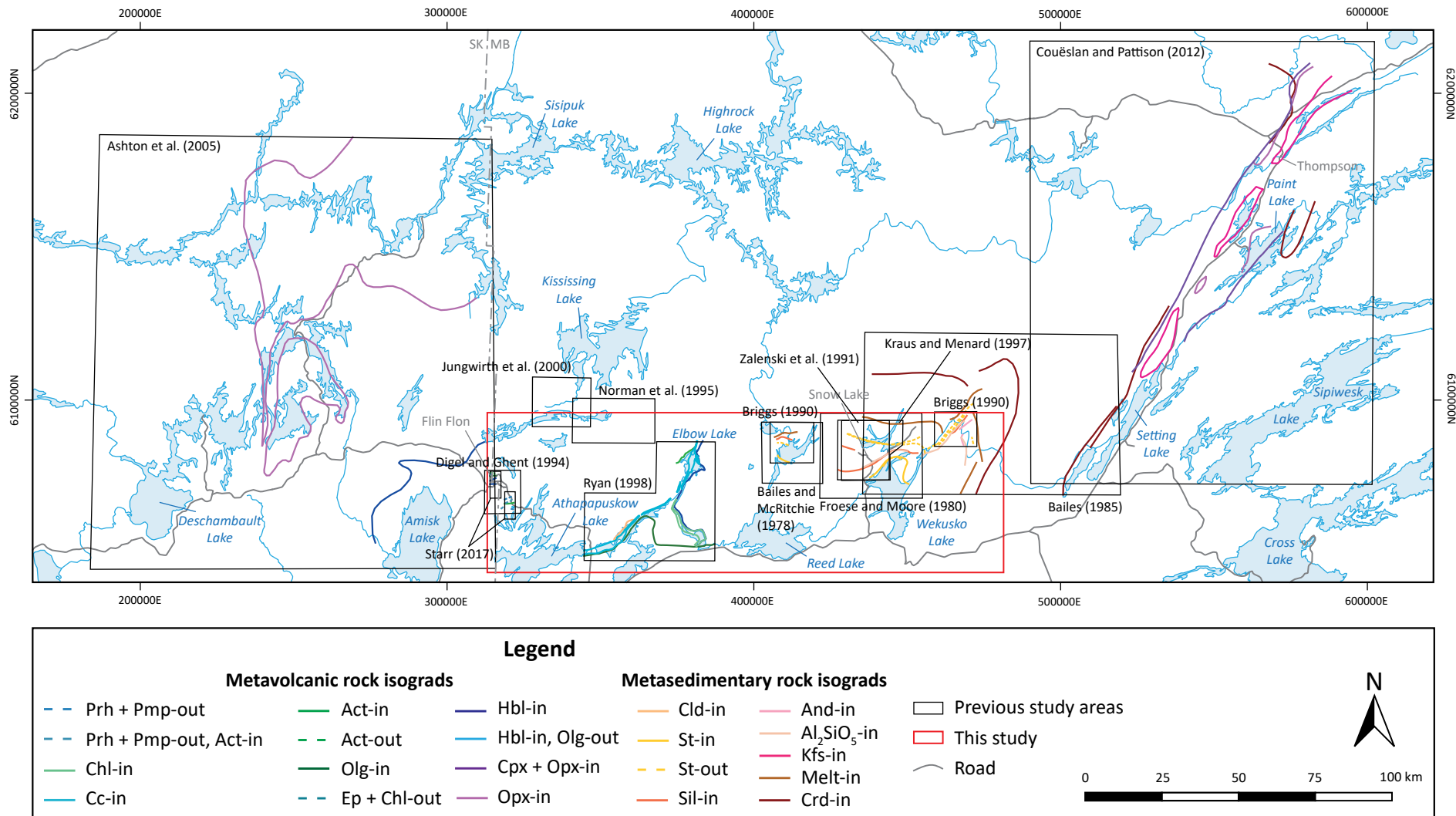
Figure 5: *Map of previous metamorphic projects carried out in the Flin Flon domain. See text for references and summarized description of previous work. Abbreviations: Act, actinolite; And, andalusite; Cc, calcite; Chl, chlorite; Cld, chloritoid; Cpx, clinopyroxene; Crd, cordierite; Ep, epidote; Hbl, hornblende; Kfs, K-feldspar; MB, Manitoba; Olg, oligoclase; Opx, orthopyroxene; Pmp, pumpellyite; Prh, prehnite; Sil, sillimanite; SK, Saskatchewan; St, staurolite. Coordinates are in UTM, zone 14.*

geobarometry for assemblages containing sphalerite and pyrite (no pyrrhotite).

Menard and Gordon (1997) and Kraus and Menard (1997) studied the timing of metamorphic mineral paragenesis with respect to deformational fabrics within the staurolite and sillimanite zones in the Snow Lake area. They suggested a polyphase deformation model (F_1–F_4) characterized by a northerly increase in peak metamorphic conditions from 500–600 °C and 4.5–5.5 kbar for the biotite–staurolite zone at the northern end of Wekusko Lake, to 650–750 °C and 5–7 kbar in the migmatitic domains (cordierite–garnet–sillimanite assemblages) in the southern part of the KD. They also suggested metamorphic chlorite and biotite defining F_2 foliations in the staurolite zone implies that cooling had commenced by the time of F_3, whereas isograds crosscutting large F_3 structures in the sillimanite zone suggests that prograde metamorphism continued until after F_3. According to these studies, folding and associated crustal thickening in the KD was followed by thermal relaxation, which led to peak metamorphism. Samples from the KD show post-F_3 heating and imply that peak metamorphism in the KD occurred later than in the FD where peak conditions were reached prior to the termination of F_3 folding.

In a comparison of petrogenitic grid reactions and the width of mapped metamorphic zones, it was found that above the staurolite-in isograd there is a tighter spacing of isotherms compared to rocks at lower metamorphic grade, this suggests a thermal perturbation centered in the KD (Menard and Gordon, 1997). The resulting high metamorphic field gradient at the interface between the FD and the KD is attributed to the intrusion of plutons. Gordon (1989) calculated that metamorphism in the centre of the KD reached peak metamorphic conditions of 750 °C and 5.5 kbar. White (2005) showed through numerical modelling that tectonic thickening of the sedimentary pile, consistent with present-day thickness estimates and erosional levels, is capable of producing enough crustal heating to cause melt at the base of the sedimentary pile. Heat was advected as the magmas rose to shallower crustal levels and produced the observed P–T conditions without the need of an additional heat source such as the mantle.

Bailes (1985) investigated metamorphism in the Saw Lake–Niblock Lake area, which is situated near the transition from the FD to the Thompson nickel belt (TNB), northeast of Wekusko Lake (Figure 5). Mapped isograds in sedimentary rocks include staurolite-in, andalusite-in, sillimanite-in, staurolite-out and migmatite-in. The author observed a progressive change in the orientation of the isograds from an east trend in the Snow Lake area to a northeast trend in the Niblock Lake area to a southeastern trend east of Niblock Lake. This deflection in isograd orientation was attributed to deformation that occurred during collision with the Superior craton. Temperatures in the Saw Lake area were estimated to increase northward from <450 °C at Wekusko Lake to >700 °C at Wimapedi Lake within the KD with pressures around 4.5 kbar (Bailes, 1985). Temperatures increase to the east, reaching >650 °C at the migmatite-in

isograd at the transition into the TNB (Bailes, 1985; Coueslan and Pattison, 2012). Similarly, in the western part of the TNB the metamorphic grade increases westward from 600 °C at Setting Lake to >650 °C at the migmatite-in isograd at the transition into the FD (Bailes, 1985; Coueslan and Pattison, 2012). The pattern of isograds and the inferred temperatures indicate the presence of a metamorphic high between the FD and the TNB (Figure 5).

Regional metamorphism

Regional metamorphic zones are shown in the accompanying map and in condensed form in Figure 6. In this section the metamorphic mineral assemblages, isograds and zones are described from low to high grade, starting with volcanic rocks and followed by sedimentary rocks. The discussion focuses on five main areas in the FD, with good exposure and abundant samples, which collectively delineate the regional trends (Figure 6). From west to east these are the Flin Flon, Cranberry–Iskwasum–Elbow lakes, Reed Lake–File Lake, Snow Lake and the Saw Lake–Niblock Lake areas. Refer to Appendix 2 for the full list of mineral assemblages.

Volcanic rocks

Prehnite–pumpellyite facies

Prehnite–pumpellyite zone

The prehnite–pumpellyite zone is defined as the area downgrade of the actinolite-in isograd and is characterized by the mineral assemblage prehnite–pumpellyite–albite–chlorite–epidote–quartz (Figure 7a). Typically, prehnite and pumpellyite coexist within samples of this zone, with prehnite being more abundant than pumpellyite. The two minerals are identified in amygdules and as very fine-grained crystals in the matrix intergrown with albite, chlorite, epidote, and rare muscovite. Albite, chlorite, epidote and sericite replace phenocrysts or are found as part of the matrix assemblage. Radial or granular epidote, fibrous chlorite, and quartz also fill amygdules. Rare igneous pyroxene is preserved as partially replaced phenocrysts in samples of this zone. The prehnite–pumpellyite zone is only observed in the Flin Flon area and occurs in outcrops between the North Arm and Inlet Arm of Schist Lake (Figure 6).

Prehnite–pumpellyite to greenschist facies transition

Actinolite–prehnite–pumpellyite zone

The actinolite–prehnite–pumpellyite zone is defined as the area between the actinolite-in isograd and prehnite-out and pumpellyite-out isograds. The key metamorphic mineral assemblage within this zone is actinolite–prehnite–pumpellyite–albite–chlorite–epidote–quartz, including the coexistence of actinolite with either or both of prehnite and pumpellyite (Figure 7b).
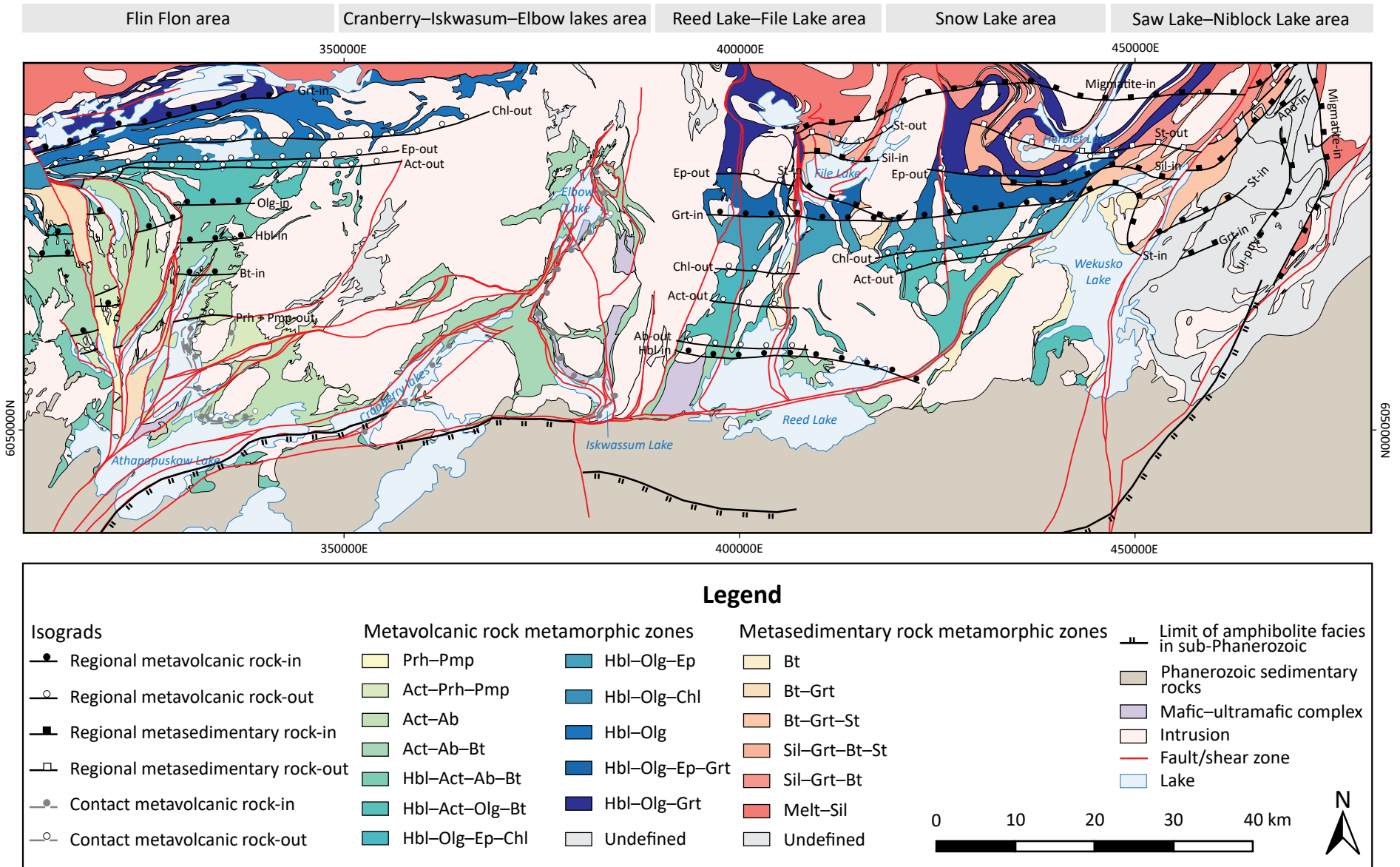
Figure 6: *Simplified map of metamorphic mineral isograds and metamorphic zones of the Flin Flon domain. Refer to text and accompanying map for details. Abbreviations: Ab, albite; Act, actinolite; And, andalusite; Bt, biotite; Chl, chlorite; Ep, epidote; Grt, garnet; Hbl, hornblende; Olg, oligoclase; Prh, prehnite; Pmp; pumpellyite; Sil, sillimanite; St, staurolite.*
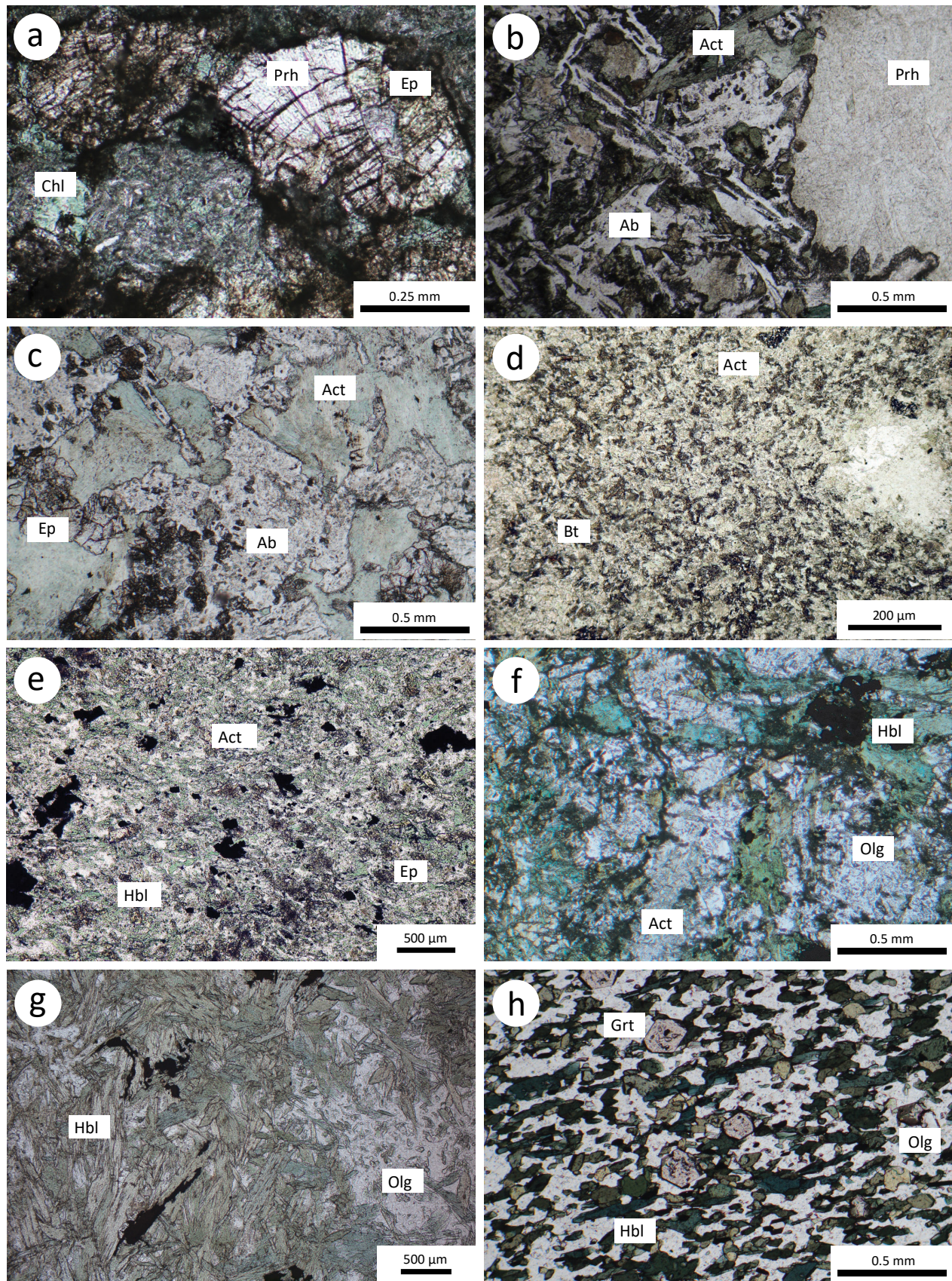
Figure 7: Photomicrographs in plane-polarized light of mafic volcanic rocks: ***a)*** *prehnite, epidote and chlorite in amygdule from the prehnite–pumpell-yite zone;* ***b)*** *prehnite-filled amygdule in contact with actinolite from the actinolite–prehnite–pumpellyite zone;* ***c)*** *actinolite, epidote and albite in sample from the actinolite–albite zone;* ***d)*** *biotite-actinolite schist from the actinolite–albite–biotite zone;* ***e)*** *actinolite-hornblende schist from the hornblende–actinolite–albite–biotite zone;* ***f)*** *hornblende, actinolite and oligoclase in sample from the hornblende–actinolite–oligoclase–biotite zone;* ***g)*** *hornblende schist from the hornblende–oligoclase–epidote–chlorite zone;* ***h)*** *garnet amphibolite from the hornblende–oligoclase–garnet zone. Abbreviations: Ab, albite; Act, actinolite; Bt, biotite; Chl, chlorite; Ep, epidote; Grt, garnet; Hbl, hornblende; Olg, oligoclase; Prh, prehnite.*

Actinolite is the only new mineral in this zone, and it occurs as fine acicular grains intergrown with prehnite and pumpellyite (where present) within the matrix. Mineral assemblages lacking actinolite, such as prehnite–pumpellyite–albite–chlorite–epidote–quartz, and the non-diagnostic assemblage albite–chlorite–epidote, are common in this zone.

The actinolite–prehnite–pumpellyite zone is only defined for the Flin Flon area where it occurs around Schist Lake (north of West Arm, east of North Arm, and a small area on the west shore of Inlet Arm), and at Neso Lake northeast of Athapapuskow Lake. In the Schist Lake area, the zone extends for up to 4 km south to north, whereas around the Neso Lake pluton it is up to 7 km wide (Figure 6).

Greenschist facies

Actinolite–albite zone

The actinolite–albite zone defines the greenschist facies and occupies the area between the prehnite- and pumpellyite-out and the biotite-in isograds. Rocks in this zone contain the assemblage actinolite–albite–epidote–chlorite–quartz (Figure 7c). This zone differs from the previous zone mainly by the lack of prehnite and pumpellyite. Rare muscovite is observed.

The actinolite–albite zone is one of the most widespread metamorphic zones mapped in the western part of the map area. It extends for 3 km south to north in the western part of the Schist Lake area, and covers up to 15 km in the eastern part of the Flin Flon area (from east of Flin Flon to the Northeast Arm of Schist Lake to the North Arm of Athapapuskow Lake). A large actinolite–albite domain occurs in the southern part of the Flin Flon area between the South Athapapuskow shear zone and the Mistik Creek shear zone, reaching as far east as First Cranberry Lake (Figure 6).

Actinolite–albite–biotite zone

The actinolite–albite–biotite zone occurs between the biotite-in and the hornblende-in isograds, and only differs from the actinolite–albite zone by the presence of biotite. Biotite typically occurs as very fine-grained crystals in the matrix of some but not all rocks. Rocks in this zone contain the muscovite-free assemblage actinolite–albite–epidote–biotite–chlorite–quartz (Figure 7d). It has been observed that in several cases the biotite-bearing rocks lack actinolite.

The actinolite–albite–biotite zone has been observed between Schist Lake and the city of Flin Flon (10 km from south to north), at the northern end of North Arm of Athapapuskow Lake (4 km), and around the main body of Reed Lake (exposed for about 10 km). The entire Cranberry–Iskwasum–Elbow lakes area is also part of the actinolite–albite–biotite zone, where it extends from the contact with the Phanerozoic sediments in the south to the northern end of Elbow Lake in the north (Figure 6).

Greenschist to amphibolite facies transition

Hornblende–actinolite–albite–biotite zone

The hornblende–actinolite–albite–biotite zone is defined as the area between the hornblende-in and the oligoclase-in isograds. The zone is characterized by the mineral assemblage hornblende–actinolite–albite–epidote–chlorite–biotite–quartz (Figure 7e). Several different textural relationships between actinolite and hornblende have been identified, including distinct grains, patchy intergrowths and core-rim microstructures (Starr and Pattison, 2019a, b). Some assemblages contain only one of the two minerals. Hornblende occurs as rare, small blebs in samples from the southern part of the zone. The modal amount of hornblende, together with its grain size, increases modestly toward the north. Close to the oligoclase-in isograd, hornblende occurs as tiny dark green needles, aggregates or blades. Brown to green biotite is present as plates or blades of variable size and are often in contact with the hornblende crystals. Actinolite, albite and the matrix assemblage (consisting of fine-grained actinolite, chlorite and quartz) persist throughout the zone as at lower grade.

The hornblende–actinolite–albite–biotite zone has been mapped north of the city of Flin Flon, where it extends for 3 km from south to north. A small hornblende–actinolite–albite–biotite domain occurs along the west shore of White Lake. In the northeastern part of the Flin Flon area, two domains up to 5 km wide are displaced by the Northeast Arm shear zone. In the southwestern part of the Flin Flon area, this zone has been mapped east of the Kaminis Lake pluton and is delimited by the West Arm shear zone to the north and the southern extension of the Ross Lake fault to the east. South of the South Athapapuskow Lake shear zone, the hornblende–actinolite–albite–biotite zone is covered by Phanerozoic sediments, but has been recorded in rocks from drillholes up to 10 km south of the exposed Phanerozoic unconformity (Figure 6; LeClair et al., 1997). In the Reed Lake–File Lake area, it has been mapped as a narrow (2 km wide) zone crossing the northern part of Reed Lake.

Hornblende–actinolite–oligoclase–biotite zone

The hornblende–actinolite–oligoclase–biotite zone is defined as the area between the oligoclase-in and actinolite-out isograds. The typical metamorphic-mineral assemblage is hornblende–actinolite–oligoclase–albite–epidote–chlorite–biotite–quartz (Figure 7f). This zone differs from the hornblende–actinolite–albite zone in that it contains oligoclase as part of the assemblage and a noticeably higher modal abundance of hornblende. Oligoclase occurs as a fine-grained interstitial phase to amphiboles. Where albite and oligoclase coexist, they are commonly found as adjacent individual crystals and in patchy intergrowths and core-rim microstructures, in which an oligoclase-rich rim mantles an albite-rich core. The modal amount of hornblende increases with increasing grade at the expense of actinolite, commonly pseudo-

morphously replacing it. Chlorite, epidote and the matrix assemblage retain the same characteristics as at lower grade.

In the western part of the map area, the hornblende–actinolite–oligoclase–biotite zone occurs north of the city of Flin Flon, where it is overlain by Missi group sedimentary rocks, and surrounding Aimee Lake (up to 5 km wide). In the Reed Lake–File Lake area, it has been mapped around the northern half of Reed Lake adjacent to Burntwood group sedimentary rocks. It occurs to the southwest of Wekusko Lake in the Snow Lake area. In the eastern part of the map area, this zone is considerably wider compared to the western part, extending for up to 15 km from south to north (Figure 6).

Epidote-amphibolite facies

Hornblende–oligoclase–epidote–chlorite zone

A hornblende–oligoclase–epidote–chlorite zone occurs between the actinolite-out and the epidote-out zone. The zone is characterized by the assemblage hornblende–oigoclase–epidote–chlorite–quartz±biotite (Figure 7g). This zone differs from the hornblende–actinolite–oligoclase–biotite zone in that it lacks actinolite. Epidote is fine grained and granular and decreases in modal abundance towards the epidote-out isograd. The mineral abundance of chlorite decreases noticeably within this zone. The hornblende–oligoclase–epidote–chlorite zone has been identified as a 2 km wide zone in the northwestern part of the map, north of Lac Aimée in the Flin Flon area, as a 3 km wide zone north of Reed Lake, and as a 3 km wide zone west of Wekusko Lake (Figure 6).

Hornblende–oligoclase–garnet–epidote zone

The hornblende–oligoclase–garnet–epidote zone is delimited to the south by the garnet-in isograd and to the north by the epidote-out isograd. Mineralogically it is the same as the hornblende–oligoclase–epidote zone with the added presence of garnet. Inclusions in garnet consist mainly of quartz and ilmenite. Epidote is fine grained and granular, and decreases in modal amount towards the epidote-out isograd where it is completely consumed. The hornblende–oligoclase–garnet–epidote zone only occurs in the eastern part of the FD in the Morton Lake–File Lake area (Figure 6). In contrast, the garnet-in isograd occurs upgrade of the epidote-out isograd in the Flin Flon area.

Amphibolite facies

Hornblende–oligoclase–chlorite zone

The zone between the epidote-out and chlorite-out isograd is defined as the hornblende–oligoclase–chlorite zone. The characteristic metamorphic-mineral assemblage for this zone is hornblende–oligoclase–chlorite–quartz±biotite. The zone differs from the hornblende–oligoclase–epidote–chlorite zone in that it lacks epidote. A decrease in the modal amount of chlorite occurs

towards the north. The hornblende–oligoclase–chlorite zone has only been mapped in the Flin Flon area, where it extends for just over 2 km north to south in the vicinity of Wabishkok Lake (Figure 6).

Hornblende–oligoclase zone

The zone north of the chlorite-out and south of the garnet-in isograd is defined as the hornblende-oligoclase zone. This zone is characterized by the classic amphibolite facies, chlorite-free mineral assemblage hornblende–oligoclase–quartz±biotite. The majority of the rock consists of fine-grained oligoclase interstitial to aggregates or blades of dark green hornblende, and platy brown biotite of lesser modal abundance. Ilmenite and Fe-sulphides are the main opaque phases. Similar to the previous zone, the hornblende–oligoclase zone only occurs in the Flin Flon area where, at its widest, it extends 4 km from south to north (Figure 6).

Hornblende–oligoclase–garnet zone

The northernmost zone is found just north of the garnet-in isograd and is defined as the hornblende–oligoclase–garnet zone. The northern boundary of this zone coincides with the disappearance of volcanic rocks at the boundary with the migmatitic sedimentary gneisses of the KD. The characteristic mineral assemblage for this zone is hornblende–oligoclase–biotite–garnet–quartz (Figure 7h). Garnet occurs as porphyroblasts up to 3 mm across that overprint amphibole. Green to blue hornblende grains less than a millimetre to several millimetres long create an interlocking texture. Oligoclase and biotite persist throughout the zone. The hornblende–oligoclase–garnet zone occurs in the northwestern corner of the map area, west of File Lake, and north of the town of Snow Lake, where volcanic rocks occur adjacent to Burntwood group sedimentary rocks (Figure 6).

Sedimentary rocks

Two types of metamorphosed sedimentary rocks have been observed: muscovite-free (low-K bulk composition) and muscovite-bearing (normal-K bulk composition). Muscovite-free rocks are mainly observed in the Reed Lake–File Lake and Snow Lake areas, whereas muscovite-bearing rocks are mainly recognized in the Niblock Lake–Saw Lake area. In the following sections, muscovite has been integrated in the general sequence of metamorphic zones and isograds and details about its occurrence are given where needed.

Greenschist facies

Biotite zone

The biotite zone is exposed between the unconformably overlying units of the Western Canada Sedimentary Basin to the south and the garnet-in isograd to the north. Characteristic metamorphic minerals in this assemblage are plagioclase–

biotite–quartz±chlorite±muscovite±amphibole (Figure 8a). Biotite occurs as tiny, orange-brown-green pleochroic, subhedral to euhedral grains (<50 μm). Biotite crystals define the foliation in areas of high strain. Chlorite is present as tiny laths up to 50 μm long, aligned with biotite where a foliation is observed. Muscovite has been reported in 17 out of 38 samples (45%), most of which come from the shores of Wekusko Lake (13 samples). It occurs as euhedral grains up to 100 μm long and is commonly aligned with the foliation. Plagioclase and quartz make up the majority of the matrix. Minor components in the matrix include opaque minerals and apatite (<100 μm). Subhedral hornblende is present in 12 out of 38 samples in this zone (32%).

The biotite zone has been mapped in the Reed Lake–File Lake area from the northern shore of Reed Lake to the northern end of Morton Lake, and in the Snow Lake area around Wekusko Lake. The zone extends for about 20 km from south to north (Figure 6). Several metamorphic zones and isograds occur in the volcanic rocks over the space of the biotite zone for sedimentary rocks; from low to high grade this includes the hornblende–actinolite–oligoclase–biotite zone, hornblende–oligoclase–epidote–chlorite zone, hornblende–oligoclase–epidote zone and hornblende–oligoclase–epidote–garnet zone. Thus, the biotite zone for sedimentary rocks spans the epidote–amphibolite facies and the lower part of the amphibolite facies for mafic volcanic rocks.

Epidote-amphibolite facies/amphibolite facies

Biotite–garnet zone

The zone between the garnet-in and the staurolite-in isograds is defined as the biotite–garnet zone. The characteristic metamorphic-mineral assemblage in samples from this zone is plagioclase–biotite–garnet–quartz±chlorite±muscovite±amphibole (Figure 8b). This zone differs from the previous by the presence of garnet, which occurs as subhedral to euhedral grains 0.5–3 mm in diameter. Garnet contains μm-scale inclusions of quartz and opaque minerals (ilmenite). Chlorite up to 50 μm in length was observed in 21 out 24 samples (88%). Euhedral muscovite up to 100 μm long occurs in 9 out of 24 samples (38%). Six out of nine muscovite-bearing samples were collected in the Niblock Lake area. Subhedral hornblende crystals were found in six out of eleven muscovite-free samples.

In the Flin Flon area, all sedimentary rock occurrences are part of the biotite–garnet zone. These include the Missi group sedimentary rocks north of the city of Flin Flon and the sliver of metamorphosed sandstone and conglomerate found at Athapapuskow Lake. The biotite–garnet zone occurs as a <2 km wide area between Morton Lake and File Lake, and around Woosey Lake, in the central and eastern parts of the map (Figure 6). In the Reed Lake–File Lake area, the sedimentary rock garnet-in isograd occurs <1 km south of the epidote-out isograd in volcanic rocks, within the hornblende–oligoclase–epidote–garnet zone.

Biotite–garnet–staurolite zone

The biotite–garnet–staurolite zone is defined as the area between the staurolite-in and the sillimanite-in isograds. The zone is characterized by the mineral assemblage plagioclase–biotite–garnet–staurolite–quartz±chlorite±muscovite (Figure 8c). The assemblage records the first appearance of staurolite in the prograde sequence. The staurolite varies in size from 1 mm to 10 cm, is euhedral and has colourless–yellow pleochroism. Grains commonly have an inclusion rich core (mainly quartz, rare ilmenite), and an inclusion poor rim. An increase in the mode and size of staurolite is observed with increasing grade in the biotite–garnet–staurolite zone. Bailes and McRitchie (1978) found that in the lower staurolite–biotite zone, staurolite occurs only in mudstones but toward the upper part of the staurolite–biotite zone it also occurs widely in siltstones and greywackes. Subhedral to euhedral garnet (<0.5 mm) contains quartz inclusions (with minor ilmenite and apatite). Typically, samples that have staurolite contain limited or no garnet in the assemblage and have larger biotite porphyroblasts, compared to rocks with no staurolite. Chlorite and muscovite occur in a number of samples, although in several rocks the chlorite could be secondary. In muscovite-free rocks from the middle of the biotite–staurolite zone, the assemblage chlorite–garnet–hornblende–anthopyllite has been documented (Froese and Moore, 1980). Cordierite has been observed in three samples, together with muscovite and biotite, at slightly higher grades within the biotite–staurolite zone.

The biotite–garnet–staurolite zone is found at Niblock Lake, File Lake and northeast of Wekusko Lake and usually is less than 5 km wide (Figure 6). The isograd marking the incoming of staurolite occurs close to the epidote-out isograd in volcanic rocks, i.e., at the boundary between the lower amphibolite facies and amphibolite facies.

Andalusite–biotite–garnet–staurolite zone

An andalusite-bearing zone occurs only in the Niblock Lake area between the staurolite-in and sillimanite-in isograds in the sedimentary rocks. The characteristic metamorphic mineral assemblage observed in this zone is plagioclase–biotite–garnet–staurolite–andalusite–quartz±chlorite±muscovite. The andalusite poikiloblasts are typically randomly oriented and contain inclusions of micas and quartz.

Sillimanite–biotite–garnet–staurolite zone

Outside of the Niblock Lake area, the region between the sillimanite-in and staurolite-out isograds defines the sillimanite–biotite–garnet–staurolite zone. The characteristic metamorphic mineral assemblage observed in this zone is plagioclase–biotite–garnet–staurolite–sillimanite–quartz±chlorite±muscovite (Figure 8d). The main difference from the previous zone is the presence of sillimanite. Sillimanite fibres commonly surround garnet crystals or share contacts and are occasionally intergrown with biotite. In other instances, sillimanite is present as isolated aggregates up to 4 mm across. Similar to the biotite–garnet–staurolite
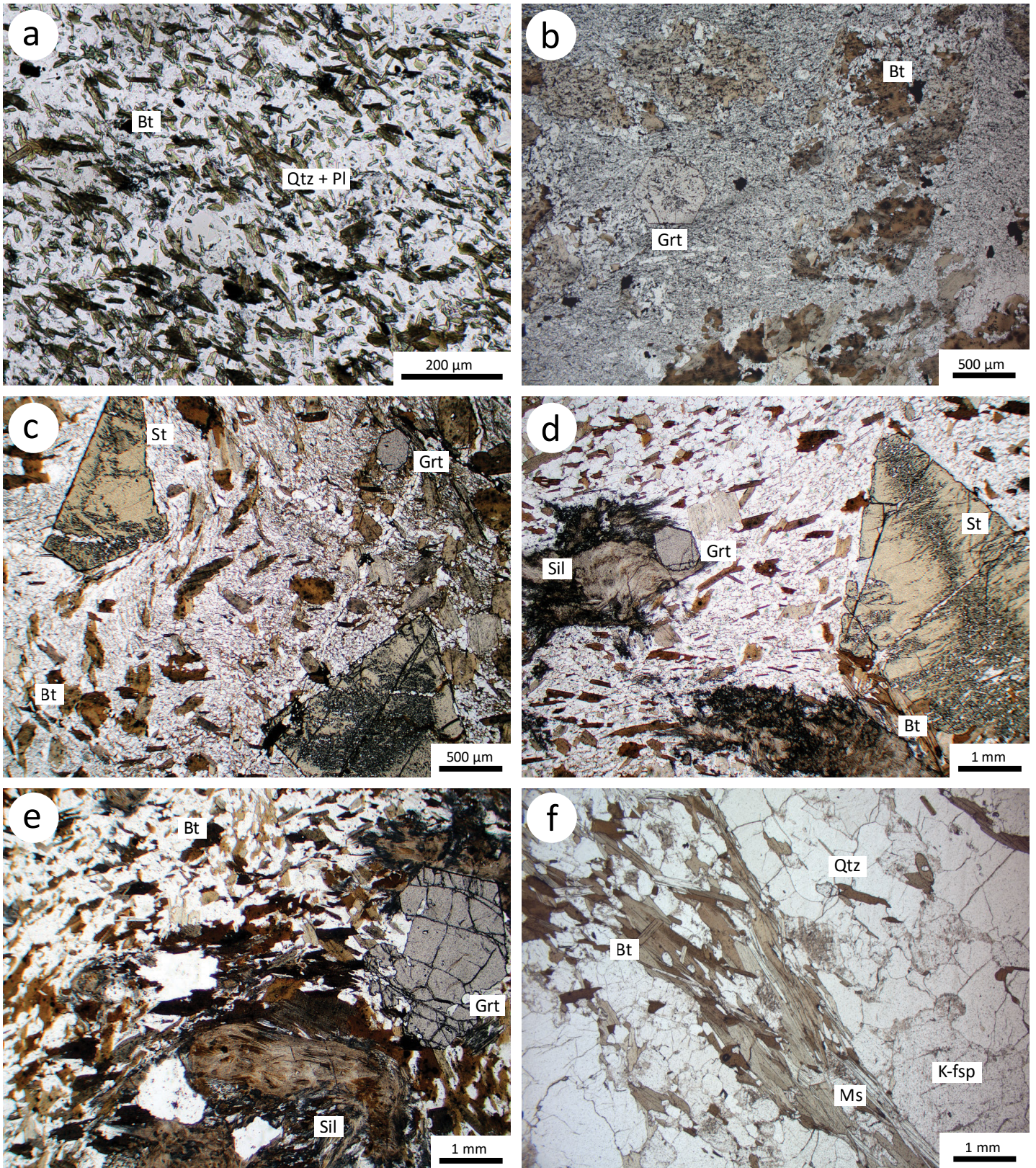
Figure 8: *Photomicrographs in plane-polarized light of sedimentary rocks:* ***a)*** *biotite schist from the biotite zone;* ***b)*** *biotite-garnet schist from the biotite–garnet zone;* ***c)*** *biotite-garnet-staurolite schist from the biotite–garnet–staurolite zone;* ***d)*** *biotite-garnet-sillimanite-staurolite schist from the sillimanite–biotite–garnet–staurolite zone;* ***e)*** *biotite-garnet-sillimanite schist from the sillimanite–biotite–garnet zone;* ***f)*** *mica gneiss from the migmatite–sillimanite zone. Abbreviations: Bt, biotite; Grt, garnet, K-fsp, K-feldspar; Ms, muscovite; Pl, plagioclase; Qtz, quartz; Sil, sillimanite; St, staurolite.*

zone, staurolite forms the largest porphyroblasts, varying in size from sub-millimetre to several centimetres. The modal amount of staurolite decreases up-grade of the sillimanite-in isograd until it is completely consumed at the staurolite-out isograd. Staurolite is rimmed and partially replaced by plagioclase, and coarse, randomly oriented blades of biotite and muscovite (up to 1 mm long). Replacement of staurolite begins as a minor corrosion at the periphery of the staurolite grain and ends as complete pseudomorphs. Tiny chlorite laths are present in many rocks and show the same characteristics as in previous zones, which makes it difficult to differentiate between prograde and retrograde chlorite. Assemblages with cordierite are rare and have only been recorded in 5 out of 62 samples in this zone (8%). Bailes and McRitchie (1978) and Briggs (1990) reported a gradual increase in sillimanite accompanied by the development of cordierite, and a coincident loss of staurolite and chlorite in muscovite-free assemblages.

The sillimanite–biotite–garnet–staurolite zone has been mapped as a continuous 3–5 km wide band from the northern shore of File Lake to the northeastern end of Wekusko Lake, where it bends to a northeasterly trend south of Niblock Lake (Figure 6). Kyanite occurs locally at this grade in the altered rocks in the footwall to the exhalative ore deposits in the Snow Lake area (Froese and Gasparrini, 1975; Bailes, 1980; see discussion below). The first appearance of sillimanite in the Reed Lake–File Lake area occurs up-grade of the epidote-out isograd in volcanic units, whereas in the Snow Lake area the sillimanite-in isograd occurs down-grade of the epidote-out isograd. The sillimanite–biotite–garnet–staurolite zone therefore corresponds to the lower part of the hornblende–oligoclase–garnet zone in mafic volcanic rocks.

Sillimanite–biotite–garnet zone

The zone up-grade of the staurolite-out isograd and down-grade of the migmatite-in isograd is defined as the sillimanite–biotite–garnet zone. The key mineral assemblage observed in rocks from this zone is plagioclase–biotite–garnet–sillimanite–quartz±muscovite (Figure 8e). This zone differs from the previous zone by the absence of staurolite. Sillimanite is typically present as fibrolite except for one sample where discrete sillimanite needles up to 10 mm in length are observed. Biotite shows complex intergrowth textures with fibrolite. Garnet grains are typically anhedral, filled with inclusions (quartz and opaques) and are commonly surrounded by fibrolite. Local euhedral garnet grains contain virtually no inclusions. In the Reed Lake–File Lake and Snow Lake areas, coarse muscovite crystals (up to 1 mm long) are restricted to domains where staurolite crystals were present. Chlorite is present but is probably of retrograde origin. Bailes and McRitchie (1978) suggested that sillimanite developed after staurolite in cordierite-bearing rocks (only documented in three muscovite-free samples).

The sillimanite–biotite–garnet zone occurs as a continuous zone from north of File Lake to Niblock Lake. It is relatively thin at File Lake and Niblock Lake (<2 km) whereas it widens to up to 7 km in between the two areas (Figure 6). It occurs within the amphibolite facies hornblende–oligoclase–garnet zone for mafic volcanic rocks.

Upper-amphibolite facies

Migmatite–sillimanite zone

The zone north of the migmatite-in isograd is defined as the migmatite–sillimanite zone. The characteristic metamorphic-mineral assemblage in samples from this zone is plagioclase–biotite–garnet–sillimanite–quartz±K-feldspar (Figure 8f). Typical for this zone is the presence of migmatitic domains with incoherently folded veins (ptygmatic folds) of leucosome up to 10 cm wide (Figure 3f). The leucosome material consists mainly of plagioclase, quartz, biotite and muscovite, with 27 out of 39 samples (69%) also containing K-feldspar. Grains vary in size from 0.1 mm to 2 mm. Perthitic exsolution lamellae are common in larger K-feldspar grains within the leucosome. Biotite and muscovite occur in blades up to 2 mm long. The host melanosome has similar mineralogy and textures to rocks of the sillimanite–biotite–garnet zone with the addition of muscovite. Sillimanite is mainly found in the form of single needles up to several mm long and occasionally as fibrolite aggregates up to 4 mm in diameter. At higher grade (about 5 km outside the map area), cordierite, together with biotite, garnet and K-feldspar (K-feldspar–cordierite-in isograd), has been recorded by Bailes and McRitchie (1978), Bailes (1985) and Briggs and Foster (1992). The migmatite–sillimanite zone covers virtually the entire northern border of the map area and bends to the southeast in the eastern FD forming a domain between the FD and TNB (Figure 6).

Metagranitoids

Intrusive rocks within the prehnite–pumpellyite facies are characterized by plagioclase variably replaced by albite and epidote; relic pyroxene is commonly present, partially replaced by fine-grained chlorite, prehnite and/or pumpellyite. Intrusive rocks in areas of greenschist facies metamorphism are characterized by albite–oligoclase replacement of Ca-plagioclase and disseminated epidote and chlorite; pyroxene is partially or entirely replaced by fibrous actinolite and chlorite; and magmatic Fe-Ti oxides are partially or totally replaced by hematite and/or titanite. Within amphibolite facies areas, plagioclase is replaced mainly by oligoclase; the main amphibole is hornblende, with minor actinolite; Fe-Ti oxides are replaced by magnetite, hematite and minor titanite.

Contact metamorphism

Contact metamorphism in the FD pre-dates regional metamorphism and is observed mainly around successor-arc plutons. Contact metamorphic aureoles typically extend for up to 2 km outside the margins of the intrusions. Contact aureoles, particularly in the northern part of the map area, are largely overprinted

by subsequent regional metamorphism and are difficult to recognize.

Volcanic rocks

Volcanic rocks in intrusive contact aureoles consist of metamorphosed massive or pillowed basalt and andesite, showing little to no deformation, and are identifiable in the field by dark grey to black weathering. Fresh surfaces are dark green, with some lighter patches of epidotization. Basite isograds identified in pluton contact aureoles comprise a combination of hornblende-in, biotite-in, oligoclase-in, actinolite-out, epidote-out and chlorite-out (see accompanying map). Igneous textures, such as phenocrysts, and pillow or flow structures, are preserved, whereas primary igneous minerals are replaced by metamorphic minerals. Primary pyroxene is replaced by actinolite, and by hornblende (up-grade of the hornblende-in isograd), whereas plagioclase is replaced by albite, and by oligoclase (up-grade of the oligoclase-in isograd). Discrete actinolite grains are intergrown with hornblende where the two amphiboles are present together. Granular epidote, acicular or fibrous chlorite and fine-grained quartz occur as part of the matrix, in veins and in amygdules. Biotite is locally present as small, brown to green, platy grains. Up-grade of the regional hornblende-in isograd, it is difficult to identify contact aureoles in volcanic units because the rocks outside of the aureole contain similar mineral assemblages.

A well-developed contact metamorphic aureole up to 2 km wide surrounds the Lynx Lake pluton and contains isograds for hornblende-in, oligoclase-in and albite-out, and actinolite-out (Lazzarotto et al., 2020). Around the Neso Lake pluton, a contact aureole up to 2 km wide contains isograds for hornblende-in, oligoclase-in, biotite-in and actinolite-out (Lazzarotto et al., 2020).

Sedimentary rocks

Mineral assemblages containing garnet, staurolite, andalusite and sillimanite were observed in some intrusive contact aureoles hosted in sedimentary units (examples listed below). Greywacke, siltstone and mudstone strata adjacent to intrusive bodies are coarsened and granoblastically recrystallized at a microscopic scale, but typically preserve original sedimentary structures such as bedding and grading at a macroscopic scale. Contact aureoles are recognized by the presence of minerals such as garnet, staurolite and andalusite/sillimanite in areas below the regional garnet-in isograd, which are otherwise not present in the regional metamorphic assemblages. At higher grade, it becomes difficult to differentiate between regional and contact metamorphism, mainly because these minerals are also part of the regional metamorphic assemblage.

Burntwood group rocks contain sillimanite adjacent to the Reed Lake pluton and contain andalusite-bearing assemblages up to 1 km from the contact (Bailes, 1980). In the contact aureole of the Reed Lake pluton at Woosey Lake, andalusite has been replaced by a mixture of muscovite and staurolite, and in some cases sillimanite (Bailes, 1980; Zwanzig and Bailes, 2010). The Norris Lake pluton contact aureole in the File Lake area (Bailes, 1980) contains cm-scale porphyroblasts of staurolite and garnet in argillaceous layers.

Discussion of metamorphism

Summary of metamorphic zones and isograds

The five metamorphic areas in the FD defined above include the Flin Flon, Cranberry–Iskwasum–Elbow lakes, File Lake–Reed Lake, Snow Lake and Niblock Lake–Saw Lake areas. The Flin Flon area is characterized by isograds in volcanic rocks spanning prehnite–pumpellyite to amphibolite facies. From south to north, isograds include actinolite-in, prehnite- and pumpellyite-out, biotite-in, hornblende-in, oligoclase-in, actinolite-out, epidote-out, chlorite-out, and garnet-in.

The Cranberry–Iskwasum–Elbow lakes area only contains regional greenschist-facies assemblages in volcanic rocks and is discussed in more detail below. The File Lake–Reed Lake area comprises a sequence of volcanic and sedimentary rocks going from upper greenschist to amphibolite facies. From south to north, isograds in volcanic rocks include hornblende-in, albite-out, actinolite-out, chlorite-out, garnet-in, epidote-out, whereas sedimentary rock isograds were mapped for garnet-in, staurolite-in, sillimanite-in, staurolite-out, and migmatite-in, with sillimanite-in occurring up-grade of epidote-out.

The Snow Lake area contains interlayered volcanic and sedimentary rocks with assemblages comprising the same isograds as found in the File Lake–Reed Lake area, but in a slightly different order (epidote-out occurs up-grade of sillimanite-in). Both chlorite-out and garnet-in occur down-grade of epidote-out in volcanic rocks of the File Lake–Reed Lake and Snow Lake areas. This in contrast to what is observed in the Flin Flon area.

The Niblock Lake–Saw Lake area contains mainly sedimentary rocks. Isograds are similar to the rest of the eastern part of the FD with the addition of an andalusite-in isograd (occurring down-grade of sillimanite-in).

In general, domains of the same metamorphic grade occur further north in the western part of the FD compared to the eastern part. For example, the hornblende-in isograd in the Flin Flon area occurs 12 km further north compared to the File Lake–Reed Lake and Snow Lake areas, and the hornblende–oligoclase–garnet zone in the Flin Flon area begins 10 km north of its start in the File Lake–Reed Lake and Snow Lake areas.

The comparison of the isograd sequence in volcanic and sedimentary rocks going up-grade from prehnite–pumpellyite to amphibolite facies indicates that key reactions in volcanic rocks occur at the transition from prehnite–pumpellyite to greenschist facies and greenschist to amphibolite facies; whereas key reactions in sedimentary rocks, including the appearance of garnet, staurolite and sillimanite, occur in the amphibolite facies. This observation shows that Basites are more suited to study the evolution of metamorphism at low grade, whereas sedimentary

rocks are more sensitive indicators of higher metamorphic grade (e.g., Starr and Pattison, 2019a, b).

Cranberry–Iskwasum–Elbow lakes low grade domain

The Cranberry–Iskwasum–Elbow lakes area is mapped as a large area of greenschist facies assemblages in the centre of the FD (see map). The typical regional metamorphic assemblage includes actinolite–chlorite–epidote, although Ryan (1998) argued that regional amphibolite facies rocks are also present.

Ryan (1998) defined seven metamorphic facies domains (FD-1 to FD-7) in the Elbow Lake area, five of which are within the greenschist facies (FD-1 to FD-5), one in the epidote-amphibolite facies (FD-6) and one in the amphibolite facies (FD-7). Ryan subdivided rocks in the greenschist facies mainly by grain size and texture into five facies domains. Rocks with similar mineralogy but different texture were not separated in this report, and therefore fall in the same metamorphic zone (actinolite–albite–biotite zone). Ryan mapped two chlorite–epidote domains. The first (FD-1) occurs in a large part of the study area and contains what Ryan termed "grungite" (a term used by the author to define unrecognized, fine-grained, crystal aggregates). New evaluation of a number of samples from the Elbow Lake area was performed in the current study, and indicates that prograde actinolite is present in several samples from the FD-1 zone (Figure 6) and was recorded as part of the "grungite" aggregates. The second domain (FD-2, chlorite–epidote domain) only occurs within the Athapapuskow–Cranberry–Elbow lakes and Iskwasum Lake shear zones. According to the interpretations of Ryan (1998), this domain varies from syn- to post-thermal peak metamorphism and is retrograde or fluid-related. Facies domain 3 (FD-3) is characterized by the presence of chloritoid in basites and is only present in a limited area on Cranberry lakes in rocks with locally different bulk composition (possible altered basites; Ryan, 1998).

The area northwest of Elbow Lake is defined as FD-4 and contains actinolite–chlorite assemblages. Investigation of samples from this area by the lead author shows that rocks contain the mineral assemblage actinolite–albite–epidote–biotite–chlorite–quartz, suggesting that these rocks are part of the actinolite–albite–biotite zone as defined here. Ryan (1998) interpreted this area as the result of a combination of increasing metamorphic grade northward, and of contact metamorphism related to the intrusive complex hosted by these rocks.

Facies domains FD-5 and FD-6 are southeast and south of Elbow Lake, east of the Athapapuskow–Cranberry–Elbow lakes and Iskwasum Lake shear zones. Facies domain 5 (FD-5) contains the assemblage actinolite–chlorite–epidote (greenschist facies, comparable to actinolite–albite–biotite zone), whereas rocks of FD-6 contain hornblende–chlorite–epidote (amphibolite facies, hornblende–oligoclase–epidote–chlorite zone). Ryan (1998) interpreted rocks of FD-6 to be of regional metamorphic epidote-amphibolite facies and suggested that they were uplifted along the Cranberry–Elbow lakes and Iskwasum Lake shear zones

because actinolite of FD-4 is the highest-grade amphibole recognized on the west side of the shear zones. Hornblende grains in FD-6 rocks are up to 10 mm long, a much coarser grain size than in domains FD-1 to FD-5 (Ryan, 1998). Because of the relatively high metamorphic grade and close proximity to major intrusions, the present authors interpret the granoblastic assemblages of FD-5 and FD-6 as contact metamorphic in origin, similar to observations of Lazzarotto et al. (2020) in contact aureoles surrounding plutons in the Athapapuskow Lake area.

Domain FD-7 occurs on the southeastern shore of Cranberry lakes and northern shore of Simonhouse Lake and contains rocks comprising hornblende–plagioclase–epidote assemblages. These were interpreted by Ryan (1998) to be contact metamorphic assemblages due to their coarse nature and positioning within 2 km of granodioritic to tonalitic plutons.

The presence of greenschist facies assemblages at the northern end of Elbow Lake, well north of similar assemblages in the Flin Flon sequence to the west and the Reed Lake–File Lake sequence to the east is a puzzle. It raises the question of what controls the distribution of these assemblages. An origin by retrograde metamorphism is considered unlikely. Assemblages related to retrograde alteration are observed exclusively within shear zones and texturally show retrograde minerals (e.g., chlorite) overgrowing prograde foliations (FD-2 of Ryan, 1998).

Alternative possibilities include tectonic displacement of the Elbow Lake block compared to the surrounding areas, synclinal depression arising from fold interference, or it represents a domain that never attained metamorphic conditions higher than greenschist facies. The Elbow Lake block may have been tectonically lowered relative to the Flin Flon area to the west and the Reed Lake–File Lake area to the east or, alternatively, the tectonic offset could be achieved by transcurrent motion as has been observed for blocks in the Flin Flon area (e.g., Syme, 1985; Bailes and Syme, 1989; Ryan, 1998; Syme, 2015; Lazzarotto et al., 2020). Another possibility is that the low-grade domain found in the Cranberry–Iskwasum–Elbow lakes area could be the result of interference of different folding events (i.e., symmetrical synclines that intersect each other) forming a basin structure exposing low grade rocks. The domal structure exposing the high-grade Pelican Window to the northwest of the map area is interpreted to have originated as a sheath fold followed by interference produced by two subsequent phases of folding (Ashton et al., 2005). Further study is needed to address the anomalous grade of the Cranberry–Iskwasum–Elbow lakes domain.

Niblock Lake–Saw Lake low pressure domain

The Niblock Lake–Saw Lake area is the only part of the FD where andalusite is present in the regional metamorphic sequence. According to Bailes (1985), isograds overprint the latest folds and metamorphic minerals overgrow the latest foliation, indicating that the peak of metamorphism in the Niblock Lake–Saw Lake area was reached late in the evolution of the

FD and thus is not due to contact metamorphism. The isograds vary in orientation on a regional scale. The general trend in this area is for metamorphic grade to increase to the west and northwest, although in the southeastern part of the area, east of the Niblock Lake fault, the grade increases in roughly the opposite direction, from west to east (Bailes, 1985; Briggs, 1990). West of the Niblock Lake–Saw Lake area, the isograds trend easterly and northeasterly and define a northerly increase in metamorphic grade over a narrow interval. In the Saw Lake area, the isograds are east-trending north of Wekusko Lake and change to northeast- and north-trending between Wekusko Lake and the quaternary sedimentary cover occupying the area between the FD and the TNB. Bailes (1985) mapped a migmatite-in isograd bending from a northeasterly trend to a southerly trend at the transition into the TNB (Figure 6). The change of orientation of isograds was interpreted by Bailes (1980) as the result of tectonic collision between the FD and the Superior province to the east.

Phase equilibria modelling

Equilibrium phase diagrams were calculated to estimate pressure-temperature conditions at the peak of metamorphism and estimate metamorphic field gradients in different parts of the FD. Five separate equilibrium phase diagrams were calculated for rocks occurring east and west of the Athapapuskow–Cranberry–Elbow lakes shear zone (two for the western part, including the Flin Flon and Elbow Lake areas, and three for the eastern part of the FD, including the File Lake, Snow Lake and Niblock Lake areas; Figures 9, 10, Table 1). Diagrams were created for low-Mg (east-

ern and western part of FD) and high-Mg basaltic rocks (western part of FD); and low-K, muscovite-free (eastern part of FD, i.e., File Lake and Snow Lake areas) and normal-K, muscovite-bearing (eastern part of FD, i.e., Saw Lake–Niblock Lake area) sedimentary rocks. All diagrams were calculated for a temperature range between 400 °C and 700 °C and a pressure range between 1 kbar and 8 kbar. These bulk compositions were chosen because they are representative of the rocks from the different areas, including volcanic-arc and ocean-floor assemblages, and muscovite-bearing and muscovite-free assemblages in sedimentary rocks. Specific bulk compositions used to obtain the diagrams are shown as red stars in the triangular diagrams of Figure 4 (raw data in Table 1). Although representative, small changes in bulk composition can lead to appreciable differences in predicted mineral assemblages and modes (Starr and Pattison, 2019a, b: Lazzarotto et al., 2020; Starr et al., 2020). Therefore, the phase diagrams presented here are unable to account for all of the observed variations in mineral assemblages.

Methods of thermodynamic modelling

Diagrams were calculated using the Gibbs free energy minimization software suite Theriak-Domino (de Capitani and Brown, 1987; de Capitani and Petrakakis, 2010), in combination with the internally consistent thermodynamic dataset of Holland and Powell (1998; updated to version ds5.5). Comparison of the natural sequence with thermodynamic modelling results suggests ds5.5 and associated activity-composition models (a-x models) are generally successful in reproducing the natural observations
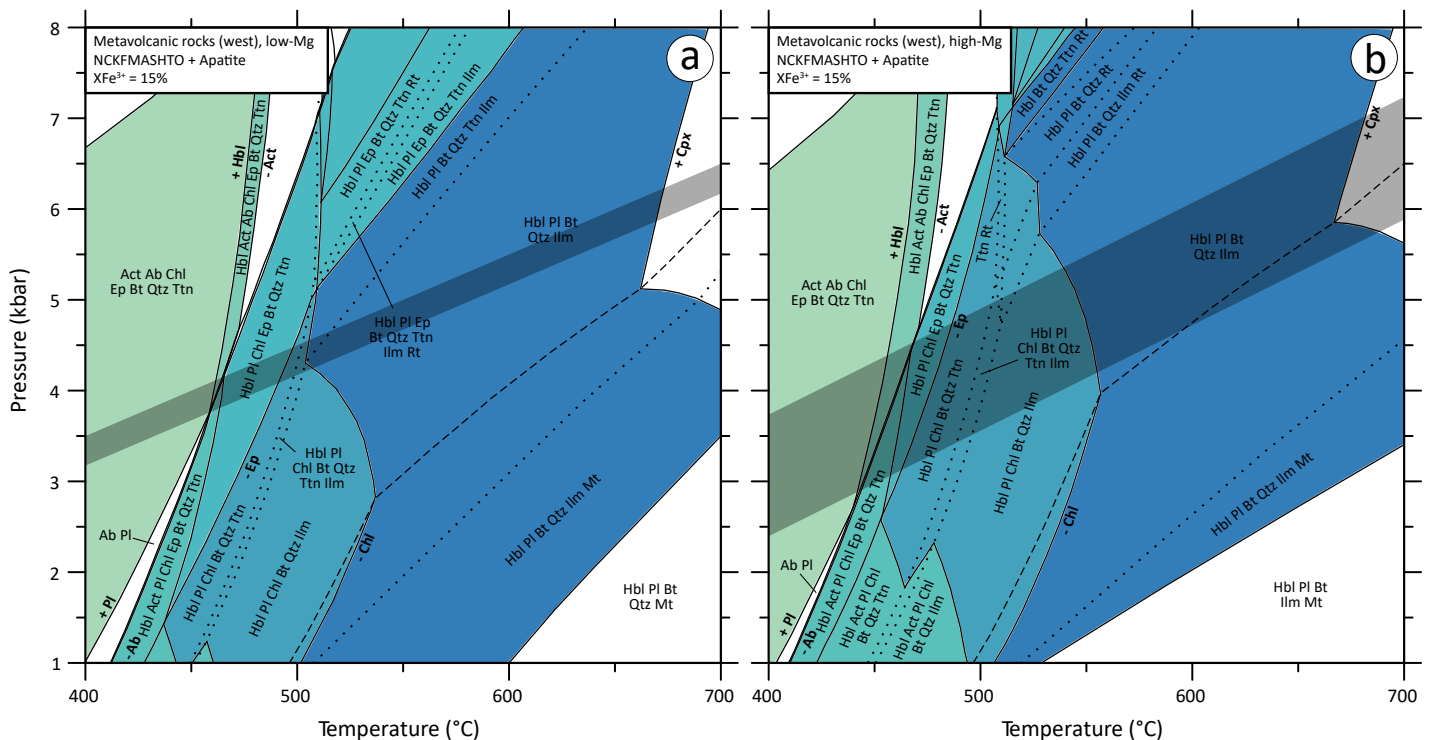
Figure 9: Phase equilibrium diagrams calculated in the NCKFMASHTO system projected from apatite with 15% XFe^{3+} for rocks west of the Athapapuskow–Cranberry–Elbow lakes shear zone: **a)** low-Mg volcanic rock (west) bulk composition; **b)** high-Mg volcanic rock (west) bulk composition. Grey bands show the range of possible metamorphic field gradients. Abbreviations: Ab, albite; Act, actinolite; Bt, biotite; Chl, chlorite; Cpx, clinopyroxene; Ep, epidote; Hbl, hornblende; Ilm, ilmenite; Mt, magnetite; Pl, plagioclase; Qtz, quartz; Rt, rutile; Ttn, titanite.
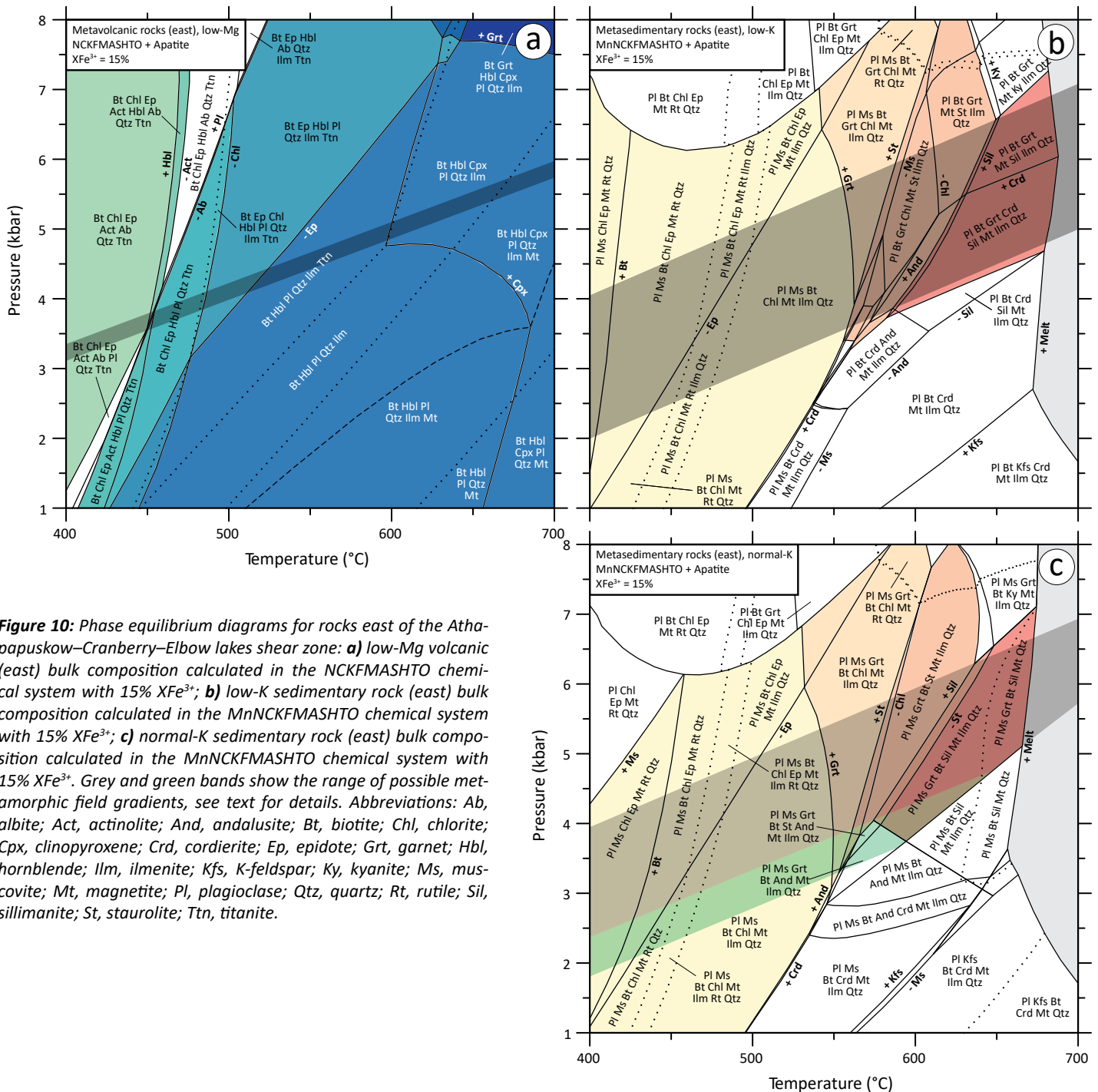
Figure 10: *Phase equilibrium diagrams for rocks east of the Atha-papuskow–Cranberry–Elbow lakes shear zone: **a)** low-Mg volcanic (east) bulk composition calculated in the NCKFMASHTO chemical system with 15% XFe³⁺; **b)** low-K sedimentary rock (east) bulk composition calculated in the MnNCKFMASHTO chemical system with 15% XFe³⁺; **c)** normal-K sedimentary rock (east) bulk composition calculated in the MnNCKFMASHTO chemical system with 15% XFe³⁺. Grey and green bands show the range of possible metamorphic field gradients, see text for details. Abbreviations: Ab, albite; Act, actinolite; And, andalusite; Bt, biotite; Chl, chlorite; Cpx, clinopyroxene; Crd, cordierite; Ep, epidote; Grt, garnet; Hbl, hornblende; Ilm, ilmenite; Kfs, K-feldspar; Ky, kyanite; Ms, muscovite; Mt, magnetite; Pl, plagioclase; Qtz, quartz; Rt, rutile; Sil, sillimanite; St, staurolite; Ttn, titanite.*

from the FD, whereas the more recent thermodynamic dataset (Holland and Powell, 2011; updated to version 6.2) and associated *a-x* models show several differences which are incompatible with the natural observations (Forshaw et al., 2019; Lazzarotto et al., 2020; Starr et al., 2020). The most important difference concerns the relative stability and compositions of amphibole- and plagioclase-group minerals. For example, the appearance of oligoclase and the disappearance of albite are predicted to occur at much higher temperatures than the hornblende-in reaction at moderate pressures, and the predicted field of coexisting albite and oligoclase occupies a much larger area of P–T space (Lazzarotto et al., 2020; Starr et al., 2020). In addition, the predicted

amphibole compositions generated using ds5.5 are closer to the measured compositions, with the amphibole compositions for the ds6.2 modelling containing too little Si (and hence greater tetrahedral Al).

The following *a-x* models were used to model volcanic bulk compositions: clinoamphibole and clinopyroxene (Diener and Powell, 2012), garnet and biotite (White et al., 2007), white mica (Coggon and Holland, 2002), chlorite, epidote, cordierite, staurolite, chloritoid, talc and olivine (Holland and Powell, 1998), orthopyroxene and magnetite-spinel (White et al., 2002), ilmenite-hematite (White et al., 2000), and feldspar (Cbar1 field; Holland and Powell, 2003). The same *a-x* models as above were used

for the thermodynamic modelling of sedimentary rocks except for garnet (Tinkham et al., 2001), biotite (White et al., 2005), melt (White et al., 2007), orthoamphibole (Diener and Powell, 2012) and ilmenite (Tinkham and Ghent, 2005).

Modelling was performed in the Na_2O-CaO-K_2O-FeO-MgO-Al_2O_3-SiO_2-H_2O-TiO_2-Fe_2O_3 (NCKFMASHTO) chemical system. Phase diagrams were calculated for subsolidus mineral assemblages down-grade of the migmatite-in isograd, therefore the systems were oversaturated with H_2O. All P is assumed to be contained in apatite, thus Ca was subtracted from the bulk composition at a molar ratio of 5Ca:3P. Manganese was omitted as a component in calculations for mafic bulk compositions because it results in the predicted stability of garnet in unlikely portions of P–T space (temperature <350 °C).

Ferric iron is an important component in the determination of phase relations of metamorphosed basites because of the high modal proportion of Fe^{3+}-bearing minerals (e.g., Diener and Powell, 2012). Pressure-temperature phase diagrams with different XFe_2O_3 of 0.00, 0.10, 0.15, 0.20, 0.30, (XFe^{3+} of 0.00, 0.09, 0.18, 0.28) and a series of T–XFe_2O_3 diagrams with XFe_2O_3 between 0.00 and 0.30 (XFe^{3+} between 0.00 and 0.28) at 3 to 5 kbar, were calculated. These diagrams were compared with the natural sequence of mineral assemblages to determine the XFe_2O_3 value that best corresponds to the observed sequence of isograds. The calculations suggest that for both bulk compositions, an XFe_2O_3 value of 0.16 (XFe^{3+} of 0.15) best represents the observations (Lazzarotto et al., 2020), similar to the results of Starr and Pattison (2019b) and Starr et al. (2020).

Thermodynamic modelling: western Flin Flon domain

Basaltic rocks

Figure 9 shows the equilibrium phase diagrams for low-Mg and high-Mg basalt bulk compositions. The calculated diagrams for the two bulk compositions show a number of similar features. In both sections, a large field containing the assemblage actinolite–albite–chlorite–epidote–biotite–quartz–sphene is present below 450 °C. Just up-grade of this field are two successive, relatively narrow fields (<20 °C wide) containing coexisting albite and oligoclase, and hornblende and actinolite. The epidote-out reaction transects the fields of hornblende–actinolite–oligoclase and hornblende–oligoclase. The intersection between the actinolite-out and the epidote-out reactions occurs at 430 °C and 1.5 kbar for the low-Mg assemblage, and at 460 °C and 2.5 kbar for the high-Mg assemblage. The chlorite-out reaction is predicted to occur at slightly lower temperatures in the low-Mg assemblage (525 °C), compared to the high-Mg assemblage (550 °C). A relatively large field with the assemblage hornblende–plagioclase–biotite–quartz–ilmenite occurs up-grade of the chlorite-out reaction. Clinopyroxene is predicted to occur at >650 °C and 5 kbar. At relatively low pressures (<3.5 kbar) and high temperatures (>500 °C) magnetite is predicted to be stable. Biotite is stable over the entire calculated P–T range.

The observed sequence of isograds at the transition from greenschist to amphibolite facies is hornblende-in, oligoclase-in, and actinolite-out. Hornblende and actinolite coexist between the hornblende-in and the actinolite-out isograds. Up-grade of the oligoclase-in isograd, albite and oligoclase coexist. The predicted phase equilibria reproduce this sequence of isograds between 3.7–4.2 kbar for the low-Mg basalt, and 2.7–4.4 kbar for the high-Mg basalt. The observed width of domains in the field containing coexisting amphiboles and coexisting plagioclase minerals are significant and do not agree with the narrow fields of coexisting amphiboles (actinolite/hornblende, <20 °C wide at >2.5 kbar) and feldspars (albite/oligoclase, <5 °C wide) predicted by the models. A possible explanation is the metastable persistence of the lower-grade minerals to higher metamorphic grades (Starr and Pattison, 2019a; Lazzarotto et al., 2020).

The observed sequence within the amphibolite facies includes disappearance of epidote followed by the disappearance of chlorite and the appearance of garnet. The garnet-in isograd is observed at the northern limit of the map area, down-grade of the transition into the KD. Most rocks in the amphibolite facies contain ilmenite (rimmed by titanite). Predicted phase equilibria reproduce the observed sequence of isograds at <5 kbar and 475–500 °C for the low-Mg basalt and at <7 kbar and 475–500 °C for the high-Mg basalt. Discrepancies between nature and the models include the prediction of coexisting titanite and ilmenite over only a 10 °C range versus the wide observed range of coexistence, and the calculation of the garnet-in reaction at >680 °C and >8.8 kbar, conditions that are too restricted (too high pressure and temperature) to be reasonable when compared to the other P–T constraints. The most likely explanation for the predicted restriction in garnet stability is omission of Mn as a component (see above), and the uncertainties in thermodynamic properties and *a-x* models for minerals in metamorphosed basites (e.g., Forshaw et al., 2019; Santos et al., 2019; Starr et al., 2020).

Thermodynamic modelling: eastern Flin Flon domain

Basaltic rocks

Figure 10a shows the calculated NCKFMASHTO phase equilibrium diagram for the low-Mg (east) bulk composition. The predicted epidote-out reaction occurs up-temperature of the albite-out (and actinolite-out) reaction. It delimits an area where hornblende and epidote coexist in the assemblage hornblende–plagioclase–biotite–epidote–quartz–sphene±chlorite±ilmenite and defines the epidote-amphibolite facies. Down-temperature of the chlorite-out reaction (approximately 450 °C) and below 3 kbar is a field with coexisting plagioclase, hornblende and chlorite, with no epidote. The clinopyroxene-in reaction is predicted to occur at 600 °C above 5 kbar and at 650 °C below 5 kbar. Garnet is predicted to be stable at >600 °C and >7.5 kbar.

Similar to the western side, the calculated phase equilibria for the eastern side reproduce the observed sequence of isograds within the greenschist facies between 3.5–4.0 kbar. The main discrepancy between the model and nature is the observed

spacing of isograds in the field compared to the narrow temperature range calculated in the model for coexisting amphiboles (actinolite/hornblende, <20 °C wide at >2.5 kbar) and feldspars (albite/oligoclase, <5 °C wide). Within the amphibolite facies, the observed sequence of isograds consists of chlorite-out, followed by garnet-in and epidote-out. The calculated model predicts the disappearance of chlorite before epidote at >3 kbar and 475 °C, consistent with the observations. As noted above with the phase diagrams for the western FD, the predicted garnet and clinopyroxene stabilities are considered to be unreliable.

Sedimentary rocks

Figure 10b shows the MnNCKFMASHTO phase equilibrium diagram for the low-K mudstone bulk composition. The biotite-in reaction occurs at approximately 400 °C and is followed up-temperature by an epidote-out reaction, which delimits the lower limit of a relatively large field containing the assemblage plagioclase–muscovite–biotite–chlorite–quartz–magnetite±sphene±rutile±ilmenite. The predicted upper temperature limit of this field is defined, from high to low pressure, by the garnet-in, staurolite-in, andalusite-in and cordierite-in reactions. Staurolite-in, andalusite-in and cordierite-in are followed closely by the loss of muscovite in rocks that still contain chlorite. Andalusite is limited to a narrow field from 525 to 575 °C and pressures between 2.5 and 3.5 kbar, whereas staurolite is stable from 530 to 630 °C in the pressure range 3–8 kbar. The chlorite-out reaction occurs within the staurolite stability field. The first development of sillimanite is predicted to coincide with the staurolite-out reaction in chlorite-free rocks. Cordierite is predicted to be stable in the high temperature–low pressure part of the diagram, above 500 °C and below 4–6 kbar. Garnet is stable at >500 °C and >3 kbar. The solidus is calculated at 650–700 °C.

The dominant sequence of isograds observed in the sedimentary rock sequence in all areas except the Niblock Lake–Saw Lake area consists of garnet-in followed by staurolite-in, sillimanite-in, staurolite-out, and migmatite-in. This sequence is developed mainly in muscovite-free assemblages down-grade of the staurolite-in isograd in the File Lake and Snow Lake areas (Bailes and McRitchie, 1978; Froese and Moore, 1980; Briggs and Foster, 1992; this study). The prediction of stable muscovite in Figure 10b does not agree with the observed mineral assemblages in these samples. In the phase diagram of Figure 10b, the chlorite-out reaction is predicted between the staurolite-in and the sillimanite-in reactions. Isograds for chlorite-out have not been identified in the field because of difficulties in differentiating prograde from retrograde chlorite (Bailes, 1985).

Cordierite is reported in 11 samples, which contain the muscovite-free assemblage biotite–garnet–cordierite ±staurolite±Al$_2$SiO$_5$ in the File Lake–Reed Lake and Niblock Lake–Saw Lake areas (e.g., Bailes, 1980; Bailes, 1985; Briggs, 1990), and is predicted at >550 °C and 4–6 kbar. Bulk compositional data suggests cordierite-bearing rocks are slightly more Mg-rich (see Appendices A and B). Hornblende and anthophyllite was

observed down-grade of the sillimanite-in isograd by several authors (e.g., Froese and Gasparrini, 1975; Bailes and McRitchie, 1978; Briggs, 1990; this study) but are not predicted anywhere in the calculated phase diagram. This suggests that the bulk composition of the phase diagram in Figure 10b might not match the bulk composition of the rocks containing these minerals, or that there are deficiencies in the thermodynamic modelling. The migmatite-in isograd is calculated at about 700 °C in agreement with the temperatures that were calculated for similar rocks in the KD (Kraus and Menard, 1997; Bailes and McRitchie, 1978; Gordon, 1989; Gordon et al., 1994).

Figure 10c shows the MnNCKFMASHTO phase-equilibrium diagram for the "normal"-K mudstone bulk composition in which muscovite is common. This more pelitic bulk composition is seen mainly in the Niblock Lake–Saw Lake area. Down-grade of the cordierite-in, Al$_2$SiO$_5$-in and staurolite-in reactions, the phase diagram section is similar to the phase diagram for muscovite-free rocks. Staurolite-in is followed closely by chlorite-out at 550–600 °C above 3.5 kbar, with muscovite-out occurring up-grade of the solidus above 3.5 kbar, and down-grade of the solidus below 3.5 kbar in the temperature range 600–700 °C. A field containing the mineral assemblage muscovite–biotite–garnet–staurolite–andalusite is predicted at 550–560 °C and 3.5-4.0 kbar, and is equivalent to the assemblage observed in the Niblock Lake–Saw Lake area. Andalusite is replaced by sillimanite up-grade of this field, and shortly after staurolite is consumed. Garnet is limited to the upper right quadrant of the diagram above 550 °C and 3 kbar. The sequence of isograds mapped in the Niblock Lake–Saw Lake area matches the predictions. The possible range of metamorphic field gradients consistent with the sequence of isograds is shown in green in Figure 10c.

Metamorphic pressure–temperature conditions

Previous thermodynamic-modelled phase equilibria in volcanic rocks from the Flin Flon area indicate that the sequence of isograds observed for the prehnite–pumpellyite to greenschist facies transition in the southern part of the FD near Schist Lake correspond to peak metamorphic conditions of 250–300 °C and 2.3–3.2 kbar (Starr et al., 2020). In comparison, pressure–temperature conditions at the greenschist to amphibolite facies transition were 450 °C and 3.3–4.4 kbar in the northern part of the Flin Flon area (Starr et al., 2020; Lazzarotto et al., 2020). These estimates are in agreement with the observed isograds and thermodynamic modelling performed in this study (Figure 9).

The typical regional metamorphic assemblage in basaltic rocks from the Elbow Lake area is actinolite–albite–chlorite–epidote. Thermodynamic modelling of rocks with similar bulk composition (low-Mg basalt) indicate albite + actinolite coexist below ~470 °C (Figure 9b), which provides a maximum temperature for peak conditions in the Elbow Lake area.

The garnet-in isograd occurs at lower temperatures compared to epidote-out for volcanic rocks of the File Lake–Reed

Lake and Snow Lake areas. In contrast, garnet-in occurs up-grade of epidote-out in the Flin Flon area. Assuming similar bulk compositions, this suggests higher pressures in the File Lake–Reed Lake and Snow Lake areas compared to the Flin Flon area; however, the sequence of reactions predicted in thermodynamic phase equilibria models suggests that this is not the case. The different sequence of isograds could be caused by differences in bulk composition between the areas east and west of the Athapapuskow–Cranberry–Elbow lakes shear zone. As noted in the discussion of bulk compositions, rocks in the eastern part of the FD have higher bulk compositional FeO content compared to the rocks from the west, which could partly explain why garnet occurs at lower grade in the File Lake–Reed Lake and Snow Lake areas.

In the File Lake–Reed Lake area, basaltic rock reactions downgrade of the hornblende-in isograd were metamorphosed below 400 °C and 3 kbar in the northern Reed Lake area. The garnet-in isograd for sedimentary rocks indicates 530 °C and 4.5 kbar at the northern end of Morton Lake. The migmatite isograd indicates 650 °C and 5.5 kbar north of File Lake. Froese and Moore (1980) suggested that peak pressure conditions were close to the kyanite–sillimanite reaction boundary (between 5 and 6 kbar) in the Snow Lake area based on the presence of anthophyllite, sillimanite and local kyanite. Phase-equilbria modelling indicates conditions of 450 °C and 3.5–4 kbar at the actinolite-out isograd in volcanic rocks in the Woosey Lake and Wekusko Lake areas south of Snow Lake, and 550–600 °C and 4.5–5.5 kbar at the sillimanite-in isograd in sedimentary rocks around the town of Snow Lake (Figure 10). Kyanite has been observed in the alteration zone of the footwall of volcanogenic massive-sulphide deposits in the Snow Lake area (e.g., Hutcheon, 1978; Zaleski et al., 1991; Caté, 2016). These assemblages are interpreted to be the result of prograde metamorphism affecting rocks that where hydrothermally altered prior to metamorphism.

The presence of both andalusite and sillimanite within the prograde sequence of the Niblock Lake–Saw Lake area led Briggs and Foster (1992) to suggest pressures below the aluminosilicate triple point at 2.5 to 4 kbar, about 1 kbar lower than estimates for the Snow Lake area (Figure 10c). The presence of both cordierite and andalusite at Niblock Lake–Saw Lake (Briggs, 1990) is further evidence of lower pressure. Temperatures are inferred to increase from ~450 °C in the biotite zone at Wekusko Lake, to over 700 °C at the migmatite-in isograd north of Niblock Lake. A cordierite-in isograd was mapped by Bailes (1985) and was suggested to correspond to about 650 °C east of the study area near Setting Lake. Thermodynamic modelling performed in this study indicates that andalusite-in followed by sillimanite-in at Niblock Lake occurred at 550–600 °C and 3–3.5 kbar, whereas partial melting is predicted to start at 650 °C and >4.5 kbar (Figure 10c). Late faults disrupt the sequence of isograds in the Saw Lake–Niblock Lake area, similar to observations in the Flin Flon area. Fault-related displacement of isograds has not been observed in the File Lake and Snow Lake areas.

Metamorphic field gradients

Metamorphic field gradients were determined by comparing the metamorphic mineral assemblages and prograde sequence of isograds observed in the field with the calculated sequence of reactions in phase-equilibrium diagrams. Special emphasis is placed on mineral-in isograds because it has been shown that minerals can persist as metastable phases to higher temperatures (e.g., Starr and Pattison, 2019a). Different sequences of isograds mapped in the five areas of the FD are used to assess variations in metamorphic field gradient across the belt.

Mineral assemblage sequences in the low-Mg basalt and the high-Mg basalt suggest a similar metamorphic field gradient for the Flin Flon area (Figure 9, grey bands). This is also observed across block-bounding faults that displace isograd sequences (Figure 6; Bailes and Syme, 1989; Lazzarotto et al., 2020). Three main constraints are used to determine the metamorphic field gradient: 1) the 250–300 °C and 1.5–2.3 kbar estimate of the P–T conditions suggested by Starr et al. (2020) for the prehnite–pumpellyite to greenschist facies transition at Schist Lake; 2) the sequence of isograds including hornblende-in, oligoclase-in, albite-out, actinolite-out occurring at 430–460 °C and 2.5–4 kbar around the city of Flin Flon and north of Athapapuskow Lake; and 3) the mapped sequence of chlorite-out up-grade of epidote-out, at Wabishkok Lake (Figure 6). This results in a metamorphic field gradient of approximately 100 °C/kbar for the Flin Flon area.

The similarity in the isograd sequence of the Reed Lake–File Lake and Snow Lake areas suggests a similar metamorphic field gradient (Figure 10a). Estimation of the metamorphic field gradient in the Reed Lake–File Lake and Snow Lake areas benefits from the close proximity of prograde sequences in volcanic and sedimentary rocks, which allows for the comparison of two distinctly different bulk compositions with differing mineral assemblage paragenesis. Four constraints are used to determine the metamorphic field gradient for the area: 1) the observed series of isograds comprising hornblende-in followed by albite-out and actinolite-out at 450 °C and 3.5–4 kbar at Reed Lake and west of Wekusko Lake; 2) the mapped isograd sequence of epidote-out occurring up-grade of chlorite-out at Morton Lake (450–500 °C, 4 kbar); 3) the similarity in sequence and spacing of basaltic rock isograds in the Reed Lake–File Lake and Snow Lake areas compared to the Flin Flon area; and 4) the slope of the metamorphic field gradient, which is assumed to be similar to the Flin Flon area, due to similar spacing of the mapped isograds in volcanic rocks for all areas of the FD. The metamorphic field gradient for the muscovite-free (low-K) sedimentary rocks in the Reed Lake–File Lake and Snow Lake areas (Figure 10b) is constrained by the sequence of isograds for garnet-in, staurolite-in, sillimanite-in and staurolite-out occurring between 550–650 °C and 4.0–6.6 kbar. The pressure is constrained by the appearance of garnet downgrade of the first appearance of staurolite, and the presence of sillimanite rather than kyanite in the mineral assemblage. Combining the results from the two different bulk compositions, the result is a metamorphic field gradient of approximately 100 °C/kbar.

An andalusite-in isograd was identified in the Niblock Lake–Saw Lake area, which contrasts with the Reed Lake–File Lake and Snow Lake areas and implies a lower-pressure metamorphic field gradient (Figure 6). The metamorphic field gradient for the muscovite-bearing (normal-K) sedimentary rocks in the Niblock Lake–Saw Lake area (Figure 10c, green band) is constrained by the sequence of isograds for garnet-in, staurolite-in, andalusite-in, sillimanite-in, and staurolite-out. The Niblock Lake–Saw Lake area field gradient defines a similar slope as the low-K sedimentary rocks in the File Lake–Reed Lake and Snow Lake areas (Figure 10c, grey band), but at pressures between 3.0 and 4.0 kbar.

Extrapolation of the metamorphic field gradients from the FD to higher grades in the KD is in agreement with geothermobarometric calculations of peak metamorphic conditions in the KD (650–700 °C and 5.5–7 kbar; Bailes and McRitchie, 1978; Gordon, 1989; Gordon et al., 1994; Kraus and Menard, 1997). Menard and Gordon (1997) suggested that rocks further north in the KD were heated an additional 100 °C, up to a maximum temperature of 750 °C (with no effect on pressure), noting that the timing of this heat pulse may have post-dated regional metamorphism in the FD.

Relating metamorphism in the Flin Flon domain with adjacent areas

A number of authors have mapped metamorphic sequences in areas adjacent to the Flin Flon domain of Manitoba (Figures 5, 6). The FD extends west into Saskatchewan where Ashton et al. (2005) mapped two isograds defined as "greenschist/amphibolite facies" and "amphibolite/upper amphibolite-granulite facies" with increasing grade towards the Pelican Window, a high-grade domain interpreted as a window into deeper crustal units. Ashton et al. (2005) reported similar greenschist and amphibolite facies mineral assemblages as presented in this study for both volcanic and sedimentary rock sequences, including actinolite–epidote–plagioclase below the "greenschist/amphibolite facies" isograd and hornblende–plagioclase between the "greenschist/amphibolite and amphibolite/granulite facies" isograd. Reported higher grade assemblages include hornblende–plagioclase–clinopyroxene above the "amphibolite/granulite facies" isograd of Ashton et al. (2005).

Metamorphic work in the TNB was conducted by Couëslan et al. (2011, 2013) and Couëslan and Pattison (2012). These authors mapped isograds within pelitic rocks (andalusite + staurolite-out, sillimanite + K-feldspar–in and migmatite-in), basaltic rocks (hornblende-in, orthopyroxene-in and clinopyroxene-in), and iron formation (orthopyroxene-in from the breakdown of Fe-Mg amphibole). Isograds for basaltic and sedimentary rocks are similar to those identified in the FD, but extend to higher metamorphic grade. The isograd pattern in the TNB comprises an elongate northeast-trending relatively low-grade core (amphibolite facies, with staurolite + andalusite-bearing mineral assemblages occurring at the lowest grade) that increases in grade to granulite facies to the east and west. Metamorphism in the TNB is interpreted to be related to the collision of the Superior craton

with the KD at ca. 1840–1800 Ma, which overlaps in time with metamorphism in the FD (Ansdell, 2005).

Mapping by Bailes (1985) included the Saw Lake area and part of the southwestern TNB (Figure 5). He recognized a change in orientation of the isograds in the FD from east- to northeast- to north-trending close to the TNB (Figure 5). The result is a 30 km wide high-grade (migmatitic) domain of rocks between the FD and the TNB (Reid, 2018). Reactions proposed to occur in sedimentary rocks in this high-grade domain include muscovite + plagioclase + quartz + H_2O = sillimanite + melt and biotite + sillimanite + plagioclase + quartz + H_2O = cordierite + garnet + melt.

One study reports orthopyroxene as part of the migmatitic assemblages within the KD about 20 km north of Snow Lake (Growdon, 2010), but no isograds are presented. No isograds for pyroxene are present in the FD of Manitoba; however, the presence of these minerals at higher grade further into the KD agrees with the metamorphic field gradient observed through the FD and into the KD.

Amphibolite facies mineral assemblages were reported in drillcore from beneath the Phanerozoic sedimentary cover south of the exposed FD (e.g., Leclair et al., 1997; Simard et al., 2010; Gagné, 2016; Reid, 2018). This indicates a general increase in metamorphic grade to the south and southeast (Figure 6). Leclair et al. (1997) reported greenschist facies assemblages (actinolite–chlorite–epidote–plagioclase) in the sub-Phanerozoic units of the Snow Lake assemblage 5 km south of the shield margin, and reported hornblende–garnet assemblages in volcanic rocks 10 km south of the shield margin. This suggests an increase from greenschist facies to amphibolite facies towards the south and southeast, and is supported by biotite–garnet–sillimanite assemblages they observed in sedimentary rocks 16 km south of the shield margin. Upper-amphibolite facies assemblages (hornblende–garnet–plagioclase) are documented in the sub-Phanerozoic Namew gneiss complex 20 km south of the shield margin and just east of the Manitoba–Saskatchewan border (Simard et al., 2010). Drillcore data from Gagné (2016) indicate a transition from greenschist facies assemblages (actinolite–chlorite–epidote–plagioclase) to amphibolite-facies assemblages (containing hornblende and garnet) in basaltic rocks 10 km south of Reed Lake. Mineral assemblages in sedimentary rocks progress from biotite and biotite–garnet assemblages to rocks containing sillimanite, anthophyllite, cordierite and staurolite with increasing grade towards the south. Reid (2018) documented garnet amphibolite in volcanic rocks and rare sillimanite in sedimentary rocks from beneath the Phanerozoic sediments 25 km southeast of Wekusko Lake and suggested an increase in metamorphic grade to the southeast.

Summary of metamorphic patterns in the exposed and sub-Phanerozoic Flin Flon domain

In summary, combining the new metamorphic map and the above results, the overall pattern of metamorphism in the FD comprises an elongate, east-trending domain (prehnite–pumpellyite facies to greenschist facies) of up to 10 km in width bounded

by parallel east-trending domains of increasing metamorphic grade to the north and south. The metamorphic grade increases to the north from greenschist facies (4 to 20 km width), amphibolite facies (5 to 15 km width), upper-amphibolite facies (6 to 10 km width) to granulite facies (in the KD). In the sub-Phanerozoic FD, the grade increases toward the south and southeast to amphibolite facies.

Economic considerations

Base metal deposits

The FD is one of the most productive Proterozoic base metal mineral regions in the world. It is host to several VMS deposits, which formed by seafloor venting of metalliferous hydrothermal fluids in active volcanic settings (e.g., Galley et al., 2007). More than 320 million tonnes of Cu-Zn ore have been discovered to date from 29 deposits (Pehrsson et al., 2016). All deposits discovered to date occur in an island-arc setting, within tholeiitic, back-arc, ocean-floor and shoshonitic assemblages dominated by basalt and basaltic andesite (e.g., Syme and Bailes, 1993). These deposits, which formed early in the tectonic evolution of the FD, are overprinted by the metamorphic and deformation processes described in this report. Recognizing the effects of metamorphism on these deposits and their associated alteration is important for mineral exploration and mining (e.g., Ames et al., 2016; Bailes et al., 2016).

Studies of metamorphosed VMS deposits have documented the distinct mineral assemblages associated with the hydrothermally altered rocks of the footwall and hangingwall zones of VMS deposits (e.g., Bonnet and Corriveau, 2007). Alteration minerals in unmetamorphosed VMS deposits typically include quartz, sericite, illite, chlorite, serpentine, albite, epidote, pyrite, carbonates, talc, clay minerals, sulfates, and Fe-oxides (Galley et al., 2007). These minerals react during metamorphism to form a wide variety of metamorphic minerals including andalusite, corundum, topaz, sillimanite, kyanite, cordierite, garnet, phlogopite, pyroxene and Fe-Mg amphibole, which are useful indicators for domains of hydrothermal alteration and potentially mineralization (Bonnet and Corriveau, 2007). Recognizing the changes in metamorphic mineral assemblages between the country rock and the hangingwall and footwall of the deposits can be used as a "vector" to mineralisation. The location and associated mineral assemblages of FD VMS deposits with respect to regional metamorphic grade are summarized in Table 2.

Metamorphic mineral assemblages within the various deposit have been investigated by several authors (e.g., Trout Lake deposit, Ordóñez-Calderón et al., 2016; Schist Lake, Mandy and Centennial deposits, Bailes and Syme, 1989; Flin Flon, Callinan and 777 deposits, Koo and Mossman, 1975; Syme and Bailes, 1993; Ames et al., 2016; Schetselaar et al., 2018; Wim deposit, Gale, 1983; Sherridon deposit, Gale, 1983; Tinkham and Karlapalem, 2009; Reed Lake, Moose, Sylvia, Limestone, Rail and Talbot deposits, Simard et al., 2010; Kofman deposit, Ferreira et al., 1996, Simard et al., 2010; Anderson deposit, Galley,

1993; Bailes et al., 2016; Linda deposit, Zaleski et al., 1991, Bailes et al., 2016; Chisel and Lalor deposits, Bailes et al., 2016, Caté, 2016; Osborne deposit, Gale, 1983, Bristol and Froese, 1989; see Table 2 for details). All known deposits were metamorphosed to greenschist facies or higher. No known deposits exist within the prehnite–pumpellyite facies and prehnite–pumpellyite facies to greenschist facies transition. The characteristic metamorphic mineral assemblages found in the altered rocks associated with VMS deposits are separated in the following sections into two types: hangingwall mineral assemblages and footwall mineral assemblages.

Volcanogenic massive-sulphide deposits in the greenschist facies include the Trout Lake, Reed Lake, Moose, Kofman, Schist Lake, Mandy, and Centennial deposits (Table 2). The hangingwalls to these deposits are commonly characterized by strong silica and sericite alteration, locally with high modal amounts of chlorite and epidote (Bailes and Syme, 1989; Simard et al., 2010; Ordóñez-Calderón et al., 2016). The more highly altered footwall assemblage generally consists of actinolite (up to 30%) and chlorite (up to 50%) with sections of strongly foliated and chloritized mafic and felsic volcaniclastics. The mineralization of the deposits is characterized by fine-grained chalcopyrite, pyrite and sphalerite.

The Flin Flon, 777, Callinan and Sylvia deposits lie within the greenschist facies to amphibolite facies transition (Table 2). Similar to the greenschist facies deposits, the hangingwall assemblages consist of chlorite (20%), biotite (10%), and epidote (20%) with the addition of hornblende (30%; Koo and Mossman, 1975; Ames et al., 2016). Footwall rocks show moderate to strong silicification, chloritization and carbonatization, with assemblages characterized by anomalous concentration of chlorite (25%), biotite (15%), hornblende, sericite, garnet, talc, and Fe-Mg carbonates (Syme and Bailes, 1993; Pearson et al., 2012; Ames et al., 2016). Strongly chloritized rocks in the Flin Flon, Callinan and 777 deposits are interpreted as the footwall alteration pipe, with hydrothermally altered basalt and volcanic tuff units observed in more distal parts of the deposits (Koo and Mossman, 1975; Syme and Bailes, 1993; Pearson et al., 2012; Ames et al., 2016). The mineralized lenses of the deposits consist of fine-grained massive sulphide including varying concentrations of pyrrhotite, pyrite, and chalcopyrite with local sphalerite, arsenopyrite and chalcocite.

The Limestone and Rail deposits occur within the regional epidote-amphibolite facies zone (Table 2). The hangingwall zones are characterized by moderate to intense silicification and chloritization with assemblages containing large amounts of chlorite, biotite, epidote, and hornblende (Simard et al., 2010). The footwall assemblage is similar to that of the hangingwall (high modal percentages of chlorite and biotite) with the addition of large porphyroblasts of hornblende, garnet and staurolite (Simard et al., 2010). Sulphide mineralization is coarser grained compared to lower grade deposits and includes chalcopyrite, sphalerite, pyrrhotite and pyrite (Simard et al., 2010).

Table 2: Summary of location and associated mineral assemblages of VMS deposits in the Flin Flon domain with respect to regional metamorphic grade. Mineral abbreviations after Kretz (1983).

Regional metamorphic sequence	Metamorphism of VMS deposits
Prehnite–pumpellyite facies	
Metavolcanic rocks: • Prh–Pmp–Ab–Chl–Ep • Fine-grained Prh and Pmp in amygdales; fine-grained matrix	No known deposits
Prehnite–pumpellyite facies to greenschist facies transition	
Metavolcanic rocks: • Act–Prh–Pmp–Ab–Chl–Ep • Fine acicular Act (up to 2 mm); fine-grained matrix	No known deposits
Greenschist facies	
Metavolcanic rocks: • Act–Ab–Ep–Bt–Chl • Fine-grained Bt; acicular Act (up to 2 mm); fine-grained matrix Metasedimentary rocks: • Bt–Chl–Ms–Amp • Subhedral to euhedral Bt (1 mm); subhedral Amp (up to 1 mm); fine-grained matrix	Trout Lake deposit: • Footwall: acicular Act (10 mm, up to 30%); Cc–Bt–Ep; intense chloritization (Ordóñez-Calderón et al., 2016) • Ore minerals: chalcopyrite–pyrite–sphalerite Reed Lake deposit: • Chl–Ep–Ser; intense silicification and sericitization (Simard et al., 2010) • Ore minerals: chalcopyrite–pyrite–sphalerite Moose deposit: • Chl–Ser–Cc; silicification, intense carbonatization (Simard et al., 2010) • Ore minerals: pyrite–pyrrhotite–sphalerite–chalcopyrite Kofman deposit: • Chl–Ser; intense silicification (Ferreira et al., 1996; Simard et al., 2010) • Ore minerals: pyrite–pyrrhotite–chalcopyrite–sphalerite Schist Lake–Mandy deposit: • Chl–Ser–Cc; intense silicification and chloritization (Bailes and Syme, 1989) • Ore minerals: chalcopyrite–sphalerite–pyrite Centennial deposit: • Footwall: Chl–Cc; chloritization and carbonatization (Bailes and Syme, 1989) • Ore minerals: chalcopyrite–sphalerite–pyrite
Greenschist facies to amphibolite facies transition	
Metavolcanic rocks: • Hbl–Act–Olg–Ab–Ep–Chl–Bt • Coexisting Hbl and Act • Coexisting Ab and Olg • Fine-grained Hbl and Act, sometimes acicular (up to 1 mm); increase in modal amount of Hbl with increasing metamorphic grade; fine-grained matrix Metasedimentary rocks: • Bt–Chl–Ms–Amp • Subhedral to euhedral Bt (up to 1 mm); subhedral Amp (up to 1 mm); fine-grained matrix	Flin Flon–777 deposit: • Footwall: Chl-rich (up to 30%), Bt (up to 20%), Ser, Tc, Cc; zones of intense silicification (Syme and Bailes, 1993; Schetselaar et al., 2018) • Hangingwall: Chl-rich (up to 30%), Bt (up to 20%), Ep (up to 30%), Act, Hbl (up to 50%), Ab; moderate silicification (Koo and Mossman, 1975; Ames et al., 2016) • Ore minerals: chalcopyrite–pyrrhotite–sphalerite Callinan deposit: • Footwall: Intense Czo–Act–Grt–Cc; zones of intense silicification (Koo and Mossman, 1975; Syme and Bailes, 1993) • Hangingwall: Chl-rich (up to 30%), Bt (up to 20%), Ep (up to 30%), Act, Hbl, Ab; moderate silicification (Koo and Mossman, 1975; Ames et al., 2016) • Ore minerals: fine-grained chalcopyrite–pyrrhotite–sphalerite–pyrite; minor arsenopyrite, galena Sylvia deposit: • Chl–Bt–Hbl–Ser–Cc; intense chloritization and sericitization (Simard et al., 2010) • Ore minerals: pyrite–pyrrhotite–chalcopyrite–sphalerite–galena

Abbreviations: Ab, albite; Act, actinolite; Amp, amphibole; Anth, anthophyllite; Bt, biotite; Cc, calcite; Chl, chlorite; Crd, cordierite; Czo, clinozoisite; Ep, epidote; Ged, gedrite; Grt, garnet; Hbl, hornblende; Kfs, K-feldspar; Ky, kyanite; Ms, muscovite; Olg, oligoclase; Pmp, pumpellyite; Prh, prehnite; Ser, sericite; Sil, sillimanite; St, staurolite; Tc, talc.

Table 2 (continued): Summary of location and associated mineral assemblages of VMS deposits in the Flin Flon domain with respect to regional metamorphic grade. Mineral abbreviations after Kretz (1983).

Regional metamorphic sequence	Metamorphism of VMS deposits
Epidote amphibolite facies	
Metavolcanic rocks: • Hbl–Olg–Ep–Chl–Bt–Grt • Fine-grained Ep decreases in modal amount with increasing metamorphic grade • Blades of Hbl (up to 5 mm); subhedral to euhedral Grt (up to 3 mm); fine-grained matrix Metasedimentary rocks: • Bt–Grt–St–Al_2SiO_5–Chl–Ms • Bt porphyroblasts (up to 1 mm); subhedral to euhedral Grt (up to 5 mm); increase in mode and size of St (up to 10 cm) with increasing metamorphic grade; Sil as fibrolite	Limestone deposit: • Footwall (?): Chl–Bt–Grt–St–Ser–Hbl (Simard et al., 2010) • Ore minerals: pyrrhotite–pyrite–chalcopyrite, minor sphalerite Rail deposit: • Bt–Hbl–Grt–Ep–Chl (Simard et al., 2010) • Ore minerals: chalcopyrite–sphalerite–pyrrhotite–pyrite
Amphibolite facies	
Metavolcanic rocks: • Hbl–Olg–Bt–Grt–Chl • Disappearance of Chl with increasing metamorphic grade • Blades of Hbl (up to 10 mm); fine-grained matrix Metasedimentary rocks: • Bt–Grt–Sil–Ms–Kfs • Partial melting up-grade of the migmatite-in isograd • Sil as fibrolite and as euhedral grains; anhedral to subhedral Grt	Anderson deposit: • Hangingwall: Ep–Chl–Olg–Hbl–Grt (Galley, 1993) • Footwall: Chl (up to 30%), Bt (up to 30%), Ser, Grt (up to 2 cm), St (up to 2 cm), Ky (up to 2 cm), Hbl, Ep; zones of intense silicification (Bailes et al., 2016) • Ore minerals: sphalerite–chalcopyrite–pyrrhotite–pyrite Linda deposit: • Hangingwall: Ms–Chl–Bt–St (Zaleski et al., 1991) • Footwall: Bt–Chl–St–Grt–Ky; calc-silicate zone with Ep and Hbl (Zaleski et al., 1991; Bailes et al., 2016) • Ore minerals: pyrite, minor sphalerite, chalcopyrite, pyrrhotite Chisel–Lalor deposit: • Footwall: St–Grt–Amp–Ky–Crd–Anth; fine-grained Chl–Bt–Ms–Ep in matrix (Bailes et al., 2016; Caté, 2016) • Ore minerals: pyrite–sphalerite, minor chalcopyrite, pyrrhotite Talbot Lake deposit: • Bt (up to 70%), Grt; calcsilicate alteration (Simard et al., 2010) • Ore minerals: pyrite–chalcopyrite–sphalerite–pyrrhotite Wim deposit: • Bt–Grt–Hbl–Crd–Anth–Sil (Gale, 1983) • Ore minerals: pyrite–chalcopyrite–pyrrhotite, minor sphalerite Sherridon deposit: • Bt–Ms–Hbl–Grt–Crd (Gale, 1983; Tinkham and Karlapalem, 2009) • Ore minerals: pyrite–chalcopyrite–pyrrhotite, minor sphalerite Osborne deposit: • Hangingwall: Bt–Ms–Chl (Gale, 1983; Bristol and Froese, 1989) • Footwall: Bt–Chl–Grt–Hbl–St–Anth–Crd–Ged (Gale, 1983; Bristol and Froese, 1989) • Ore minerals: pyrite–chalcopyrite–pyrrhotite, minor sphalerite

Abbreviations: Ab, albite; Act, actinolite; Amp, amphibole; Anth, anthophyllite; Bt, biotite; Cc, calcite; Chl, chlorite; Crd, cordierite; Czo, clinozoisite; Ep, epidote; Ged, gedrite; Grt, garnet; Hbl, hornblende; Kfs, K-feldspar; Ky, kyanite; Ms, muscovite; Olg, oligoclase; Pmp, pumpellyite; Prh, prehnite; Ser, sericite; Sil, sillimanite; St, staurolite; Tc, talc.

The Anderson, Linda, Chisel, Lalor, Talbot, Wim, Sherridon, and Osborne deposits are located in the regional amphibolite facies domain (Table 2). Hangingwall assemblages contain epidote, chlorite, biotite, hornblende, garnet, muscovite, staurolite, kyanite and sillimanite (Bailes et al., 2016). The more highly altered footwall rocks contain assemblages of chlorite, biotite and minor muscovite with porphyroblasts of staurolite (up to 10 cm long), garnet (up to 5 cm), kyanite, sillimanite, cordierite, hornblende and minor anthophyllite, gedrite and gahnite. Sub-concordant footwall alteration zones are located immediately below the mineral deposits. They are characterized by chlorite–garnet–biotite-rich rocks with varying amount of staurolite and amphibole and are interpreted as metamorphosed chlorite–sericite alteration zones (Galley, 1993; Bailes et al., 2016; Caté,

2016). Metamorphosed feeder pipes to the VMS systems occur as discordant alteration zones characterized by assemblages with kyanite, gahnite, garnet and tourmaline (Galley, 1993; Bailes et al., 2016; Caté, 2016). Metamorphosed rocks from deeper, more extensive regional semi-conformable alteration zones include silicified plagioclase-epidote-amphibole rocks containing muscovite, biotite and sillimanite knots. These zones are interpreted as distal quartz–sericite alteration haloes (Galley, 1993; Bailes et al., 2016; Caté, 2016). Large amounts of Zn and Mn in some parts of the alteration zones allowed for the stabilization of staurolite and garnet, respectively, at lower than expected metamorphic grades (Zaleski et al., 1991). Sulphide mineralization consists of pyrite and pyrrhotite with coarse-grained sphalerite and locally abundant chalcopyrite and chalcocite.

Gold deposits

Gold mineralization in the FD can be divided into three main types: epithermal Au deposits (e.g., Laurel Lake; Ansdell and Kyser, 1990), mesothermal Au deposits (e.g., Rio, Tartan Lake, Graham; Ansdell and Kyser, 1992), and Au associated with VMS deposits (e.g., Lalor and Flin Flon; Galley et al., 2007; Caté, 2016). Pre-metamorphic epithermal gold deposits in the FD occur in quartz-carbonate veins and were emplaced at relatively high temperatures (>250 °C; Ansdell and Kyser, 1990, 1992). Mesothermal gold deposits occur along crustal-scale shear zones and are interpreted to have formed late in the tectonometamorphic evolution of the greenstone belt (post-dating regional deformation, magmatism and metamorphism) at temperatures above 300 °C (Galley et al., 1986, 1989; Ansdell and Kyser, 1990, 1992; Schledewitz, 1997; Syme et al., 1998). These deposits are interpreted to be associated with the migration of fluids derived from metamorphic dehydration reactions with some igneous contribution (Ansdell and Kyser, 1992). Dehydration reactions in metamorphosed basites at the transition from greenschist to amphibolite facies are interpreted to provide fluids for the transport of gold (e.g., Phillips and Powell, 1993). In addition, crustal-scale shear zones can create pathways and/or traps for the transport and deposition of gold in solution (e.g., Dubé et al., 2007). Starr and Pattison (2019b) suggested that the fluids released from volcanic rocks at the greenschist to amphibolite facies transitions in the Flin Flon area were unlikely to have had the appropriate composition to be a source for orogenic gold formation. Their observations indicate that the devolatilization reactions did not involve carbonate and pyrite/pyrrhotite, which are thought to be important for generating fluids associated with orogenic gold deposits. On the other hand, Ridley and Diamond (2000) argued that the composition of ore-forming fluids may not be reflective of the source, because of precipitation and dissolution processes that occur along the transport pathway. The new metamorphic map and well-constrained metamorphic zones presented in this study make the Flin Flon belt an ideal location for the further study of the relationships between orogenic gold deposits and metamorphism, devolatilization and deformation.

Recommendations for future study

Minimal work has been done on the contact aureoles within the FD. A number of contact aureoles were reported in volcanic and sedimentary rocks surrounding pre-metamorphic plutons (e.g., Bailes, 1980; Ryan, 1998; Syme and Whalen, 2012; Syme, 2015) but to our knowledge only a few have been investigated in detail (Lazzarotto et al., 2020). Contact aureoles allow the depth of pluton emplacement to be estimated, which combined with the age of emplacement, allows the establishment of P–T-time "pins" in the evolution of the crust prior to peak regional metamorphism.

About half of the exposed rocks of the FD consists of metamorphosed intrusive rocks, which were not investigated in this study. A number of these are mafic intrusive rocks and have similar mineralogy to the volcanic rocks. Investigation of petrographic and geochemical compositions, and thermodynamic modelling of these mafic rocks might allow for the definition of new metamorphic isograds and zones specific to these bulk compositions. A metamorphic study of mafic plutons could help understand the link between the low-grade Cranberry–Iskwasum–Elbow lakes area and the surrounding higher-grade zones.

More samples from both the volcanic and sedimentary units are needed to better define and position the isograds east of Wekusko Lake. A better understanding of metamorphism in that area could allow for better linking of isograds and metamorphic zones with the work of Couëslan et al. (2011, 2013) and Couëslan and Pattison (2012) in the TNB.

Whereas this study focused mainly on the Manitoba portion of the FD, the greenstone belt extends west into Saskatchewan. Ashton et al. (2005) defined two general isograds at the transition from greenschist to amphibolite facies and from amphibolite to granulite facies. Several authors have demonstrated that facies transitions in the FD comprise multiple reactions and occur over several kilometres (e.g., Starr and Pattison, 2019a, b; Lazzarotto et al., 2020). Additional study could entail a more detailed evaluation of the metamorphic assemblages and isograds used to define the facies transitions of Ashton et al. (2005), and to link these isograds across the provincial boundary into Manitoba.

Starr and Pattison (2019b) showed that the mineral reactions involved in the greenschist to amphibolite facies transition in the Flin Flon area were unlikely to release fluids conducive to the formation of orogenic gold deposits. The newly presented map reveals that the sequence of isograds, and therefore the sequence of mineral reactions, occurring in the eastern part of the FD differs from what is observed in the western part (Starr and Pattison, 2019a, b; Lazzarotto et al., 2020). Further investigation of reactions in the eastern FD would reveal more about the composition of the released fluids and their capability to transport precious metals.

References

Ague, J.J. 1991: Evidence for major mass transfer and volume strain during regional metamorphism of pelites; Geology, v. 19, p. 855–858.

Ames, D.E., Galley, A.G., Kjarsgaard, I.M., Tardif, N. and Taylor, B.T. 2016: Hanging-wall vectoring for buried volcanogenic massive sulfide deposits, Paleoproterozoic Flin Flon mining camp, Manitoba, Canada; Economic Geology, v. 111, p. 963–1000.

Ames, D.E., Tardif, N., MacLachlan, K. and Gibson, H.L. 2002: Geology and hydrothermal alteration of the hanging wall stratigraphy to the Flin Flon–777–Callinan volcanogenic massive sulphide horizon (NTS 63K12NW and 13SW), Flin Flon area, Manitoba; in Report of Activities 2002, Manitoba Industry, Trade and Mines, Manitoba Geological Survey, p. 20–34, URL <https://manitoba.ca/iem/geo/field/roa02pdfs/GS-02.pdf> [April 2022].

Ansdell, K.M. 1993: U-Pb zircon constraints on the timing and provenance of fluvial sedimentary rocks in the Flin Flon and Athapapuskow basins, Flin Flon Domain, Trans-Hudson Orogen, Manitoba and Saskatchewan; in Radiogenic Age and Isotopic Studies: Report 7, Geological Survey of Canada, Paper 93-2, p. 49–57.

Ansdell, K.M. 2005: Tectonic evolution of the Manitoba–Saskatchewan segment of the Paleoproterozoic Trans-Hudson orogen, Canada; Canadian Journal of Earth Sciences, v. 42, p. 741–759.

Ansdell, K.M. and Kyser, T.K. 1990: Epigenetic gold mineralization in the Flin Flon domain: fluid characteristics; in Modern Exploration Techniques, L.S. Beck and C.T. Harper (ed.), Saskatchewan Geological Society, Special Publication 10, p. 219–234.

Ansdell, K.M. and Kyser, T.K. 1992: Mesothermal gold mineralization in a Proterozoic greenstone belt; western Flin Flon Domain, Saskatchewan, Canada; Economic Geology, v. 87, p. 1496–1524.

Ansdell, K.M., Connors, K.A., Stern, R.A. and Lucas, S.B. 1999: Coeval sedimentation, magmatism, and fold-thrust belt development in the Trans-Hudson Orogen: geochronological evidence from the Wekusko Lake area, Manitoba, Canada; Canadian Journal of Earth Sciences, v. 36, p. 293–312.

Ansdell, K.M., Kyser, T.K., Stauffer, M.R. and Edwards, G. 1992: Age and source of detrital zircons from the Missi Formation: a Proterozoic molasse deposit, Trans-Hudson Orogen, Canada; Canadian Journal of Earth Sciences, v. 29, p. 2583–2594.

Ansdell, K.M., Lucas, S.B., Connors, K. and Stern, R.A. 1995: Kisseynew metasedimentary gneiss belt, Trans-Hudson orogen (Canada): back-arc origin and collisional inversion; Geology, v. 23, p. 1039–1043.

Ashton, K.E., Lewry, J.F., Heaman, L.M., Hartlaub, R.P., Stauffer, M.R. and Tran, H.T. 2005: The Pelican Thrust Zone: basal detachment between the Archean Sask Craton and Paleoproterozoic Flin Flon - Glennie Complex, western Trans-Hudson Orogen; Canadian Journal of Earth Sciences, v. 42, p. 685–706.

Bailes, A.H. 1979: Sedimentology and metamorphism of a Proterozoic volcaniclastic turbidite suite that crosses the boundary between the Flin Flon and Kisseynew belts, File Lake, Manitoba, Canada; Ph.D. thesis, University of Manitoba, Winnipeg, Manitoba, 154 p.

Bailes A.H. 1980: Geology of the File Lake area; Manitoba Energy and Mines, Mineral Resources Division, Geological Report 78–1, 134 p., 1 map at 1:25 000 scale, URL <https://manitoba.ca/iem/info/libmin/GR78-1.zip> [April 2022].

Bailes, A.H. 1985: Geology of the Saw Lake area; Manitoba Energy and Mines, Geological Services, Geological Report 83-2, 47 p., 1 map at 1:25 000 scale, URL <https://manitoba.ca/iem/info/libmin/GR83-2.zip> [April 2022].

Bailes, A.H. and McRitchie, W.D. 1978: The transition from low to high grade metamorphism in the Kisseynew sedimentary gneiss belt, Manitoba; in Metamorphism in the Canadian Shield, J.A. Fraser and W.W. Heywood (ed.), Geological Survey of Canada, Paper 78-10, p. 155–178.

Bailes, A.H. and Syme, E.C. 1989: Geology of the Flin Flon-White Lake area; Manitoba Energy and Mines, Geological Services, Geological Report GR 87-1, 313 p., 2 maps at 1:20 000 scale, URL <https://manitoba.ca/iem/info/libmin/GR87-1.zip> [April 2022].

Bailes, A.H., Galley, A.G., Paradis, S. and Taylor, B.E. 2016: Variations in large synvolcanic alteration zones at Snow Lake, Manitoba, Canada, with proximity to associated volcanogenic massive sulfide deposits; Economic Geology, v. 111, p. 933–962.

Bailes, A.H., Syme, E.C., Galley, A.G., Skirrow, R.G. and Ziehlke, D.V. 1987: Early Proterozoic volcanism, hydrothermal activity, and associated ore deposits at Flin Flon and Snow Lake, Manitoba; Geological Association of Canada–Mineralogical Association of Canada, Joint Annual Meeting, May 19–24, 1987, Saskatoon, Saskatchewan, Field Trip Guidebook No. 1, 95 p.

Bleeker, W. 1990: New structural-metamorphic constraints on early Proterozoic oblique collision along the Thompson nickel belt, Manitoba, Canada; in The Early Proterozoic Trans-Hudson Orogen of North America, J.F. Lewry and M.R. Stauffer (ed.), Geological Association of Canada, Special Paper 37, p. 57–73.

Bonnet, A.-L. and Corriveau, L. 2007: Alteration vectors to metamorphosed hydrothermal systems in gneissic terranes; in Mineral Deposits of Canada: a synthesis of major deposit-types, district metallogeny, the evolution of geological provinces, and exploration methods, W.D. Goodfellow (ed.), Geological Association of Canada, Mineral Deposits Division, Special Publication 5, p. 1035–1049.

Briggs, W.D. 1990: Pressure-temperature conditions and staurolite to aluminum silicate reaction mechanisms in metapelites near File Lake and Niblock Lake, Manitoba, Canada; M.Sc. thesis, University of Iowa, Iowa City, Iowa, 317 p.

Briggs, W.D. and Foster, C.T. 1992: Pressure–temperature conditions of early Proterozoic metamorphism during the Trans-Hudson Orogen as determined from rocks straddling the Flin Flon – Kisseynew boundary at Niblock and File lakes, Manitoba; Canadian Journal of Earth Sciences, v. 29, p. 2497–2507.

Bristol, C.C. and Froese, E. 1989: Highly metamorphosed altered rocks associated with the Osborne Lake volcanogenic massive sulfide deposit, Snow Lake area, Manitoba; The Canadian Mineralogist, v. 27, p. 593–600.

Caté, A. 2016: Geology of the Paleoproterozoic Zn-Cu-Au Lalor volcanogenic massive sulphide deposit and its gold-rich lenses, Snow Lake, Manitoba/Géologie du gisement de sulfures massifs volcanogène Paléoprotérozoique à Zn-Cu-Au de Lalor et de ses lentilles riches en or, Snow Lake, Manitoba; Ph.D. thesis, Université du Québec, Québec, Quebec, 430 p.

Clowes, R., Cook, F., Hajnal, Z., Hall, J., Lewry, J., Lucas, S. and Wardle, R. 1999: Canada's LITHOPROBE project (collaborative multidisciplinary geoscience research leads to new understanding of continental evolution); Episodes, v. 22, p. 3–20.

Coggon, R. and Holland, T.J.B. 2002: Mixing properties of phengitic micas and revised garnet-phengite thermobarometers; Journal of Metamorphic Geology, v. 20, p. 683–696.

Connors, K.A. and Ansdell, K. M. 1994: Revision of stratigraphy and structural history in the Wekusko Lake area, eastern Trans-Hudson Orogen; in Report of Activities 1994, Manitoba Energy and Mines, Minerals Division, p. 104–107, URL <https://manitoba.ca/iem/geo/field/roa94.pdf> [April 2022].

Couëslan, C.G. and Martins, T. 2014: Geological scoping study of the Sherridon structure, northern margin of the Flin Flon domain, western Manitoba (parts of NTS 63N2, 3); *in* Report of Activities 2014, Manitoba Mineral Resources, Manitoba Geological Survey, p. 125–130, URL <https://manitoba.ca/iem/geo/field/roa14pdfs/GS-10.pdf> [April 2022].

Couëslan, C.G. and Pattison, D.R.M. 2012: Low-pressure regional amphibolite-facies to granulite-facies metamorphism of the Paleoproterozoic Thompson Nickel Belt, Manitoba; Canadian Journal of Earth Sciences, v. 49, p. 1117–1153.

Couëslan, C.G., Pattison, D.R.M. and Dufrane, S.A. 2013: Paleoproterozoic metamorphic and deformation history of the Thompson Nickel Belt, Superior Boundary Zone, Canada, from in situ U–Pb analysis of monazite; Precambrian Research, v. 237, p. 13–35.

Couëslan, C.G., Pattison, D.R.M. and Tinkham, D.K. 2011: Regional low-pressure amphibolite-facies metamorphism at the Pipe II mine, Thompson nickel belt, Manitoba, and comparison of metamorphic isograds in metapelites and meta-iron formations; The Canadian Mineralogist, v. 49, p. 721–747.

David, J., Bailes, A.H. and Machado, N. 1996: Evolution of the Snow Lake portion of the Palaeoproterozoic Flin Flon and Kisseynew belts, Trans-Hudson Orogen, Manitoba, Canada; Precambrian Research, v. 80, p. 107–124.

de Capitani, C. and Brown, T.H. 1987: The computation of chemical equilibrium in complex systems containing non-ideal solutions; Geochimica et Cosmochimica Acta, v. 51, p. 2639–2652.

de Capitani, C. and Petrakakis, K. 2010: The computation of equilibrium assemblage diagrams with Theriak/Domino software; American Mineralogist, v. 95, p. 1006–1016.

Diener, J.F.A. and Powell, R. 2012: Revised activity–composition models for clinopyroxene and amphibole; Journal of Metamorphic Geology, v. 30, p. 131–142.

Digel, S. and Ghent, E.D. 1994: Fluid-mineral equilibria in prehnite-pumpellyite to greenschist facies metabasites near Flin Flon, Manitoba, Canada: implications for petrogenetic grids; Journal of Metamorphic Geology, v. 12, p. 467–477.

Digel, S. and Gordon, T.M. 1993: Quantitative estimates of pressure-temperature-fluid composition in metabasites from prehnite-pumpellyite to amphibolite facies near Flin Flon; Report of Third Transect Meeting, April 1–2, 1993, Regina, Saskatchewan, LITHO-PROBE Secretariat, University of British Columbia, Vancouver, British Columbia, Report 34, p. 139–156.

Digel, S.G. and Gordon, T.M. 1995: Phase relations in metabasites and pressure-temperature conditions at the prehnite-pumpellyite to greenschist facies transition, Flin Flon, Manitoba Canada; *in* Low-Grade Metamorphism of Mafic Rocks, P. Schiffman and H.W. Day (ed.), Geological Society of America, Special Paper, v. 296, p. 67–80.

Dubé, B., Gosselin, P., Mercier-Langevin, P., Hannington, M. and Galley, A. 2007: Gold-rich volcanogenic massive sulphide deposits; *in* Mineral Deposits of Canada: a synthesis of major deposit-types, district metallogeny, the evolution of geological provinces, and exploration methods, W.D. Goodfellow (ed.), Geological Association of Canada, Mineral Deposits Division, Special Publication 5, p. 75–94.

Ellis, S., Beaumont, C. and Pfiffner, O.A. 1999: Geodynamic models of crustal-scale episodic tectonic accretion and underplating in subduction zones; Journal of Geophysical Research: Solid Earth, v. 104, p. 15169–15190.

Fedorowich, J.S., Kerrich, R. and Stauffer, M.R. 1995: Geodynamic evolution and thermal history of the central Flin Flon Domain, Trans-Hudson Orogen: constraints from structural development, $^{40}Ar/^{39}Ar$, and stable isotope geothermometry; Tectonics, v. 14, p. 472–503.

Ferreira, J.B., Mitchell, J. and Gula, D. 1996: Mineral deposits and occurrences in the south half of the Cormorant Lake area, (NTS 63K/1 to 63K/8); Manitoba Energy and Mines, Geological Services, Mineral Deposit Series Report No. 33, 150 p., 8 maps at 1:50 000 scale.

Forshaw, J.B., Waters, D.J., Pattison, D.R.M., Palin, R.M. and Gopon, P. 2019: A comparison of observed and thermodynamically predicted phase equilibria and mineral compositions in mafic granulites; Journal of Metamorphic Geology, v. 37, p. 153–179.

Froese, E. 1969: Metamorphic rocks from the Coronation Mine and surrounding area; *in* Symposium on the Geology of Coronation Mine, Saskatchewan, A.R. Byers (ed.), Geological Survey of Canada, Paper 68-5, p. 55–77.

Froese, E. and Gasparrini, E. 1975: Metamorphic zones in the Snow Lake area, Manitoba; The Canadian Mineralogist, v. 13, p. 162–167.

Froese, E. and Moore, J. 1980: Metamorphism in the Snow Lake area, Manitoba; Geological Survey of Canada, Paper 78-27, 21 p., 1 map at 1:50 000 scale.

Gagné, S. 2016: Examination of exploration drillcore from the Reed Lake area, Flin Flon belt, west-central Manitoba (parts of NTS 63K7, 8, 9, 10); *in* Report of Activities 2016, Manitoba Growth, Enterprise, and Trade, Manitoba Geological Survey, p. 63–73, URL <https://manitoba.ca/iem/geo/field/roa16pdfs/GS-6.pdf> [April 2022].

Gale, D.F., Lucas, S.B. and Dixon, J.M. 1999: Structural relations between the polydeformed Flin Flon arc assemblage and Missi Group sedimentary rocks, Flin Flon area, Manitoba and Saskatchewan; Canadian Journal of Earth Sciences, v. 36, p. 1901–1915.

Gale, G.H. 1983: Proterozoic exhalative massive sulphide deposits; *in* Proterozoic Geology: selected papers from an international proterozoic symposium, L.G. Medaris Jr., C.W. Byers, D.M. Mickelson and W.C. Shanks (ed.), Geological Society of America, Memoir 161, p. 191–207.

Galley, A.G. 1993: Characteristics of semi-conformable alteration zones associated with volcanogenic massive sulphide districts; Journal of Geochemical Exploration, v. 48, p. 175–200.

Galley, A.G., Ames, D.E. and Franklin, J.M. 1989: Results of studies on gold metallogeny of the Flin Flon belt; *in* Investigations by the Geological Survey of Canada in Manitoba and Saskatchewan during the 1984–1989 Mineral Development Agreements, A.G. Galley (ed.), Geological Survey of Canada, Open File 2133, p. 25–32.

Galley, A.G., Hannington, M.D. and Jonasson, I.R. 2007: Volcanogenic massive sulphide deposits; *in* Mineral Deposits of Canada: a Synthesis of Major Deposit-Types, District Metallogeny, the Evolution of Geological Provinces, and Exploration Methods, W.D. Goodfellow (ed.), Geological Association of Canada, Mineral Deposits Division, Special Publication No. 5, p. 141–161.

Galley, A.G., Ziehlke, D.V, Franklin, J.M., Ames, D.E. and Gordon, T.M. 1986: Gold mineralization in the Snow Lake–Wekusko Lake region, Manitoba; *in* Gold in the Western Shield, L.A. Clark (ed.), Canadian Institute of Mining and Metallurgy, Special Volume 38, p. 379–398.

Gilbert, H.P. 2012: Geology and geochemistry of arc and ocean-floor volcanic rocks in the northern Flin Flon Belt, Embury–Wabishkok–Naosap lakes area, Manitoba (parts of NTS 63K13, 14); Manitoba Innovation, Energy and Mines, Manitoba Geological Survey, Geoscientific Report GR2011-1, 46 p., 1 DVD, URL <https://manitoba.ca/iem/info/libmin/GR2011-1.zip> [April 2022].

Gordon, T.M. 1989: Thermal evolution of the Kisseynew sedimentary gneiss belt, Manitoba: metamorphism at an early Proterozoic accretionary margin; *in* Evolution of metamorphic belts, J.S. Daly, R.A. Cliff and B.W.D. Yardley (ed.), Geological Society of London, Special Publication, no. 43, p. 233–243.

Gordon, T.M., Aranovich, L.Y. and Fed'kin, V.V. 1994: Exploratory data analysis in thermobarometry: an example from the Kisseynew sedimentary gneiss belt, Manitoba, Canada; American Mineralogist, v. 79, p. 973–982.

Gordon, T.M., Ghent, E.D. and Stout, M.Z. 1991: Algebraic analysis of the biotite-sillimanite isograd in the File Lake area, Manitoba; The Canadian Mineralogist, v. 29, p. 673–686.

Gordon, T.M., Hunt, P.A., Bailes, A.H. and Syme, E.C. 1990: U-Pb ages from the Flin Flon and Kisseynew belts, Manitoba: chronology of crust formation at an early Proterozoic accretionary margin; *in* The Early Proterozoic Trans-Hudson Orogen of North America, J.F. Lewry and M.R. Stauffer (ed.), Geological Association of Canada, Special Paper 37, p. 177–199.

Growdon, M.L. 2010: Crustal development and deformation of Laurentia during the Trans-Hudson and Alleghenian orogenies; Ph.D. thesis, Indiana University, Bloomington, Indiana, 221 p.

Heaman, L.M., Kamo, S.L., Ashton, K.E., Reilly, B.A., Slimmon, W.L. and Thomas, D.J. 1992: U–Pb geochronological investigations in the Trans-Hudson Orogen, Saskatchewan; *in* Summary of Investigations 1992, Saskatchewan Geological Survey, Saskatchewan Energy and Mines, Miscellaneous Report 92-4, p. 120–123.

Hoffman, P.F. 1988: United plates of America, the birth of a craton: early Proterozoic assembly and growth of Laurentia; Annual Review of Earth and Planetary Sciences, v. 16, p. 543–603.

Holland, T. and Blundy, J. 1994: Non-ideal interactions in calcic amphiboles and their bearing on amphibole-plagioclase thermometry; Contributions to Mineralogy and Petrology, v. 116, p. 433–447.

Holland, T. and Powell, R. 2003: Activity–composition relations for phases in petrological calculations: an asymmetric multicomponent formulation; Contributions to Mineralogy and Petrology, v. 145, p. 492–501.

Holland, T.J.B. and Powell, R. 1998: An internally consistent thermodynamic data set for phases of petrological interest; Journal of Metamorphic Geology, v. 16, p. 309–343.

Holland, T.J.B. and Powell, R. 2011: An improved and extended internally consistent thermodynamic dataset for phases of petrological interest, involving a new equation of state for solids; Journal of Metamorphic Geology, v. 29, p. 333–383.

Hutcheon, I. 1978: Calculation of metamorphic pressure using the sphalerite-pyrrhotite-pyrite equilibrium; American Mineralogist, v. 63, p. 87–95.

Jungwirth, T., Gordon, T.M. and Froese, E. 2000: Metamorphism of the Burntwood group in the Duval Lake area, Manitoba, Canada; The Canadian Mineralogist, v. 38, p. 435–442.

Koo, J. and Mossman, D.J. 1975: Origin and metamorphism of the Flin Flon stratabound Cu-Zn sulfide deposit, Saskatchewan and Manitoba; Economic Geology, v. 70, p. 48–62.

Kraus, J. and Menard, T. 1997: A thermal gradient at constant pressure; implications for low-to medium-pressure metamorphism in a compressional tectonic setting, Flin Flon and Kisseynew domains, Trans-Hudson Orogen, central Canada; The Canadian Mineralogist, v. 35, p. 1117–1136.

Kraus, J. and Williams, P.F. 1998: Relationships between foliation development, porphyroblast growth and large-scale folding in a metaturbidite suite, Snow Lake, Canada; Journal of Structural Geology, v. 20, p. 61–76.

Kretz, R. 1983: Symbols for rock-forming minerals; American Mineralogist, v. 68, p. 277–279.

Lafrance, B., Gibson, H.L., Pehrsson, S., Schetselaar, E., DeWolfe, Y.M. and Lewis, D. 2016: Structural reconstruction of the Flin Flon volcanogenic massive sulfide mining district, Saskatchewan and Manitoba, Canada; Economic Geology, v. 111, p. 849–875.

Lazzarotto, M., Pattison, D.R.M., Gagné, S. and Starr, P.G. 2020: Metamorphic and structural evolution of the Flin Flon – Athapapuskow Lake area, west-central Manitoba; Canadian Journal of Earth Sciences, v. 57, p. 1269–1288.

Leclair, A.D., Lucas, S.B., Broome, H.J., Viljoen, D.W. and Weber, W. 1997: Regional mapping of Precambrian basement beneath Phanerozoic cover in southeastern Trans-Hudson Orogen, Manitoba and Saskatchewan; Canadian Journal of Earth Sciences, v. 34, p. 618–634.

Lewry, J.F., Hajnal, Z., Green, A., Lucas, S.B., White, D., Stauffer, M.R., Ashton, K.E., Weber, W. and Clowes, R. 1994: Structure of a Paleoproterozoic continent-continent collision zone: a LITHOPROBE seismic reflection profile across the Trans-Hudson Orogen, Canada; Tectonophysics, v. 232, p. 143–160.

Lucas, S.B., Stern, R.A., Syme, E.C., Reilly, B.A. and Thomas, D.J. 1996: Intraoceanic tectonics and the development of continental crust: 1.92–1.84 Ga evolution of the Flin Flon Belt, Canada; Geological Society of America Bulletin, v. 108, p. 602–629.

Menard, T. and Gordon, T.M. 1997: Metamorphic P-T paths from the eastern Flin Flon belt and Kisseynew domain, Snow Lake, Manitoba; The Canadian Mineralogist, v. 35, p. 1093–1116.

NATMAP Shield Margin Project Working Group 1998: Geology, NATMAP Shield Margin Project area, Flin Flon Belt, Manitoba/Saskatchewan; Geological Survey of Canada, "A" Series Map 1968A, Manitoba Energy and Mines, Geological Map A-98-2 and Saskatchewan Energy and Mines, Map 258A, scale 1:100 000, with accompanying notes, 54 p.

Norman, A.R., Williams, P.F. and Ansdell, K.M. 1995: Early Proterozoic deformation along the southern margin of the Kisseynew gneiss belt, Trans-Hudson Orogen: a 30 Ma progressive deformation cycle; Canadian Journal of Earth Sciences, v. 32, p. 875–894.

Norquay, L.I. 1997: Structural and metamorphic evolution of North Star Lake area, Manitoba; M.Sc. thesis, University of Manitoba, Winnipeg, Manitoba, 244 p.

Ordóñez-Calderón, J.C., Lafrance, B., Gibson, H.L., Schwartz, T., Pehrsson, S.J. and Rayner, N.M. 2016: Petrogenesis and geodynamic evolution of the Paleoproterozoic (~1878 Ma) Trout Lake volcanogenic massive sulfide deposit, Flin Flon, Manitoba, Canada; Economic Geology, v. 111, p. 817–847.

Pattison, D.R.M. and Spear, F.S. 2018: Kinetic control of staurolite–Al_2SiO_5 mineral assemblages: implications for Barrovian and Buchan metamorphism; Journal of Metamorphic Geology, v. 36, p. 667–690.

Pearson B., Lyhkun D., Spence C., West S. and Carter R. 2012: Technical Report 777 Mine Flin Flon, Manitoba, Canada; HudBay Minerals Inc., NI 43-101 technical report, 220 p.

Pehrsson, S., Gibson, H.L. and Gilmore, K. 2016: A special issue on volcanogenic massive sulfide deposits of the Trans-Hudson Orogen: preface; Economic Geology, v. 111, p. 803–816.

Phillips, G.N. and Powell, R. 1993: Link between gold provinces; Economic Geology, v. 88, p. 1084–1098.

Reid, K.D. 2018: Sub-Phanerozoic basement geology from drillcore observations in the Watts, Mitishto and Hargrave rivers area, eastern Flin Flon belt, west-central Manitoba (parts of NTS 63J5, 6, 11, 12, 13, 14); *in* Report of Activities 2018, Manitoba Growth, Enterprise and Trade, Manitoba Geological Survey, p. 37–47.

Ridley, J.R. and Diamond, L.W. 2000: Fluid geochemistry of orogenic gold lode deposits and implications for genetic models; *in* Gold in 2000, S.G. Hagemann and P.E. Brown (ed.), Society of Economic Geologists, Reviews in Economic Geology, v. 13, p. 141–162.

Ryan, J.J. 1998: Structural analysis of the Elbow–Cranberry–Iskwasum lakes area: a multiply reactivated deformation corridor in the Trans-Hudson orogen of Manitoba; Ph.D. thesis, University of New Brunswick, Fredericton, New Brunswick, 361 p.

Ryan, J.J. and Williams, P.F. 1999: Structural evolution of the eastern Amisk collage, Trans-Hudson orogen, Manitoba; Canadian Journal of Earth Sciences, v. 36, p. 251–273.

Santos, C.A., Moraes, R. and Szabó, G.A.J. 2019: A comparison between phase diagram modelling of metamafic rocks and experimental and independent thermobarometric data; Lithos, v. 340–341, p. 108–123.

Schetselaar, E., Ames, D. and Grunsky, E. 2018: Integrated 3D geological modeling to gain insight in the effects of hydrothermal alteration on post-ore deformation style and strain localization in the Flin Flon volcanogenic massive sulfide ore system; Minerals, v. 8, URL <https://doi.org/10.3390/min8010003>.

Schledewitz, D.C.P. 1997: Squall Lake project: geology and gold mineralization north of Snow Lake (NTS 63K/16NE); *in* Report of Activities 1997, Manitoba Energy and Mines, Minerals Division, p. 79–83, URL <https://manitoba.ca/iem/geo/field/roa97.zip> [April 2022].

Schneider, D.A., Heizler, M.T., Bickford, M.E., Wortman, G.L., Condie, K.C. and Perilli, S. 2007: Timing constraints of orogeny to cratonization: thermochronology of the Paleoproterozoic Trans-Hudson orogen, Manitoba and Saskatchewan, Canada; Precambrian Research, v. 153, p. 65–95.

Schumacher, J.C. 1997: Appendix 2: the estimation of ferric iron in electron microprobe analysis of amphiboles; Mineralogical Magazine, v. 61, p. 312–321.

Simard, R.-L., McGregor, C.R., Rayner, N. and Creaser, R.A. 2010: New geological mapping, geochemical, Sm-Nd isotopic and U-Pb age data for the eastern sub-Phanerozoic Flin Flon belt, Manitoba (part of NTS 63J3–6, 11, 12, 14, and 63K1, 2, 7–10); *in* Report of Activities 2010, Manitoba Innovation, Energy and Mines, Manitoba Geological Survey, p. 69–87, URL <https://manitoba.ca/iem/geo/field/roa10pdfs/GS-6.pdf> [April 2022].

Starr, P.G. 2017: Sub-greenschist to lower amphibolite gacies metamorphism of basalts: examples from Flin Flon, Manitoba and Rossland, British Columbia; Ph.D. thesis, University of Calgary, Calgary, Alberta, 495 p.

Starr, P.G. and Pattison, D.R.M. 2019a: Equilibrium and disequilibrium processes across the greenschist–amphibolite transition zone in metabasites; Contributions to Mineralogy and Petrology, v. 174, no. 18, URL <https://doi.org/10.1007/s00410-019-1553-y>.

Starr, P.G. and Pattison, D.R.M. 2019b: Metamorphic devolatilization of basalts across the greenschist-amphibolite facies transition zone: insights from isograd mapping, petrography and thermodynamic modelling; Lithos, v. 342, p. 295–314.

Starr, P.G., Pattison, D.R.M. and Ames, D.E. 2020: Mineral assemblages and phase equilibria of metabasites from the prehnite–pumpellyite to amphibolite facies, with the Flin Flon greenstone belt (Manitoba) as a type example; Journal of Metamorphic Geology, v. 38, p. 71–102.

Stauffer, M.R. 1990: The Missi Formation: an Aphebian molasse deposit in the Reindeer Lake zone of the Trans-Hudson orogen, Canada; *in* The Early Proterozoic Trans-Hudson Orogen of North America, J.F. Lewry and M.R. Stauffer (ed.), Geological Association of Canada, Special Paper 37, p. 121–142.

Stauffer, M.R. and Mukherjee, A. 1971: Superimposed deformations in the Missi meta-sedimentary rocks near Flin Flon, Manitoba; Canadian Journal of Earth Sciences, v. 8, p. 217–242.

Stern, R.A., Syme, E.C. and Lucas, S.B. 1995a: Geochemistry of 1.9 Ga MORB- and OIB-like basalts from the Amisk collage, Flin Flon belt, Canada: evidence for an intra-oceanic origin; Geochimica et Cosmochimica Acta, v. 59, p. 3131–3154.

Stern, R.A., Syme, E.C., Bailes, A.H. and Lucas, S.B. 1995b: Paleoproterozoic (1.90–1.86 Ga) arc volcanism in the Flin Flon belt, Trans-Hudson Orogen, Canada; Contributions to Mineralogy and Petrology, v. 119, p. 117–141.

Stern, R.A., Machado, N., Syme, E.C., Lucas, S.B. and David, J. 1999: Chronology of crustal growth and recycling in the Paleoproterozoic Amisk collage (Flin Flon belt), Trans-Hudson orogen, Canada; Canadian Journal of Earth Sciences, v. 36, p. 1807–1827.

Syme, E.C. 2015: Geology of the Athapapuskow Lake area, western Flin Flon belt, Manitoba (part of NTS 63K12); Manitoba Mineral Resources, Manitoba Geological Survey, Geoscientific Report GR2014-1, 210 p., URL <https://manitoba.ca/iem/info/libmin/GR2014-1.zip> [April 2022].

Syme, E.C. and Bailes, A.H. 1993: Stratigraphic and tectonic setting of early Proterozoic volcanogenic massive sulfide deposits, Flin Flon, Manitoba; Economic Geology, v. 88, p. 566–589.

Syme, E.C. and Whalen, J.B. 2012: Geology of the Elbow Lake area, central Flin Flon belt, Manitoba (part of NTS 63K15W); Manitoba Innovation, Energy and Mines, Manitoba Geological Survey, Geoscientific Report GR2012-1, 100 p., 1 DVD, URL <https://manitoba.ca/iem/info/libmin/GR2012-1.zip> [April 2022].

Syme, E.C., Lucas, S.B., Bailes, A.H. and Stern, R.A. 1999: Contrasting arc and MORB-like assemblages in the Paleoproterozoic Flin Flon belt, Manitoba, and the role of intra-arc extension in localizing volcanic-hosted massive sulphide deposits; Canadian Journal of Earth Sciences, v. 36, p. 1767–1788.

Syme, E.C., Lucas, S.B., Zwanzig, H.V., Bailes, A.H., Ashton, K.E. and Haidl, F.M. 1998: Geology, NATMAP shield margin project area, Flin Flon belt, Manitoba/Saskatchewan, accompanying notes; Geological Survey of Canada, Map 1968A, Manitoba Energy and Mines, Map A-98-2 and Saskatchewan Energy and Mines, Map 258A, 54 p.

Thomas, D.J. 1991: Revision bedrock geological mapping: Bootleg Lake–Birch Lake area (parts of NTS 63K-12 and 63L-9); *in* Summary of Investigations 1991, Saskatchewan Geological Survey, Saskatchewan Energy and Mines, Miscellaneous Report 91-4, p. 2–8.

Thomas, D.J. 1992: Highlights of investigations around the Flin Flon mine: reassessment of the structural history; *in* Summary of Investigations 1992, Saskatchewan Energy and Mines, Saskatchewan Geological Survey, Miscellaneous Report 92-4, p. 3–15.

Tinkham, D.K. and Ghent, E.D. 2005: Estimating P-T conditions of garnet growth with isochemical phase-diagram sections and the problem of effective bulk-composition; The Canadian Mineralogist, v. 43, p. 35–50.

Tinkham, D.K. and Karlapalem, N. 2009: Hydrothermal alteration and metamorphism of the Sherridon structure, Sherridon area, Manitoba (part of NTS 63N3); *in* Report of Activities 2008, Manitoba Science, Technology, Energy and Mines, Manitoba Geological Survey, p. 79–86.

Tinkham, D.K., Zuluaga, C.A. and Stowell, H.H. 2001: Metapelite phase equilibria modeling in MnNCKFMASH: the effect of variable Al_2O_3 and $MgO/(MgO+FeO)$ on mineral stability; Geological Materials Research, v. 3, p. 1–42.

Whalen, J.B., Syme, E.C. and Stern, R.A. 1999: Geochemical and Nd isotopic evolution of Paleoproterozoic arc-type granitoid magmatism in the Flin Flon belt, Trans-Hudson orogen, Canada; Canadian Journal of Earth Sciences, v. 36, p. 227–250.

White, D.J. 2005: High-temperature, low-pressure metamorphism in the Kisseynew domain, Trans-Hudson orogen: crustal anatexis due to tectonic thickening?; Canadian Journal of Earth Sciences, v. 42, p. 707–721.

White, D.J., Lucas, S.B., Hajnal, Z., Green, A.G., Lewry, J.F., Weber, W., Bailes, A.H., Syme, E.C. and Ashton, K. 1994: Paleo-Proterozoic thick-skinned tectonics: lithoprobe seismic reflection results from the eastern Trans-Hudson Orogen; Canadian Journal of Earth Sciences, v. 31, p. 458–469.

White, R.W., Pomroy, N.E. and Powell, R. 2005: An *in situ* metatexite-diatexite transition in upper amphibolite facies rocks from Broken Hill, Australia; Journal of Metamorphic Geology, v. 23, p. 579–602.

White, R.W., Powell, R. and Clarke, G.L. 2002: The interpretation of reaction textures in Fe-rich metapelitic granulites of the Musgrave Block, central Australia: constraints from mineral equilibria calculations in the system $K_2O–FeO–MgO–Al_2O_3 SiO_2 H_2O–TiO_2 Fe_2O_3$; Journal of Metamorphic Geology, v. 20, p. 41–55.

White, R.W., Powell, R. and Holland, T.J.B. 2007: Progress relating to calculation of partial melting equilibria for metapelites; Journal of Metamorphic Geology, v. 25, p. 511–527.

White, R.W., Powell, R., Holland, T.J.B. and Worley, B.A. 2000: The effect of TiO_2 and Fe_2O_3 on metapelitic assemblages at greenschist and amphibolite facies conditions: mineral equilibria calculations in the system $K_2O–FeO–MgO–Al_2O_3–SiO_2–H_2O–TiO_2–Fe_2O_3$; Journal of Metamorphic Geology, v. 18, p. 497–511.

Zaleski, E., Froese, E. and Gordon, T.M. 1991: Metamorphic petrology of Fe-Zn-Mg-Al alteration at the Linda volcanogenic massive sulfide deposit, Snow Lake, Manitoba; The Canadian Mineralogist, v. 29, p. 995–1017.

Zwanzig, H.V. 1990: Kisseynew gneiss belt in Manitoba: stratigraphy, structure, and tectonic evolution; in The Early Proterozoic Trans-Hudson Orogen of North America, J.F. Lewry and M.R. Stauffer (ed.), Geological Association of Canada, Special Paper 37, p. 95–120.

Zwanzig, H.V. 2000: Structure and stratigraphy of the south flank of the Kisseynew Domain in the Trans-Hudson Orogen, Manitoba: implications for 1.845–1.77 Ga collision tectonics; Canadian Journal of Earth Sciences, v. 36, p.1859–1880.

Zwanzig, H.V. and Bailes, A.H. 2010: Geology and geochemical evolution of the northern Flin Flon and southern Kisseynew domains, Kississing–File lakes area, Manitoba (parts of NTS 63K, N); Manitoba Innovation, Energy and Mines, Manitoba Geological Survey, Geoscientific Report GR2010-1, 135 p.